



*A National Center of Excellence in Advanced Technology Applications*

ISSN 1520-295X

---

# Sliding Fragility of Unrestrained Equipment in Critical Facilities

by

W.H. Chong and T.T. Soong

University at Buffalo, State University of New York  
Department of Civil, Structural and Environmental Engineering  
Buffalo, NY 14260

Technical Report MCEER-00-0005

July 5, 2000

This research was conducted at the University at Buffalo, State University of New York, and was supported primarily by the Earthquake Engineering Research Centers Program of the National Science Foundation under award number EEC-9701471.

## NOTICE

This report was prepared by the University at Buffalo, State University of New York, as a result of research sponsored by the Multidisciplinary Center for Earthquake Engineering Research (MCEER) through a grant from the Earthquake Engineering Research Centers Program of the National Science Foundation and other sponsors. Neither MCEER, associates of MCEER, its sponsors, the University at Buffalo, State University of New York, nor any person acting on their behalf:

- a. makes any warranty, express or implied, with respect to the use of any information, apparatus, method, or process disclosed in this report or that such use may not infringe upon privately owned rights; or
- b. assumes any liabilities of whatsoever kind with respect to the use of, or the damage resulting from the use of, any information, apparatus, method, or process disclosed in this report.

Any opinions, findings, and conclusions or recommendations expressed in this publication are those of the author(s) and do not necessarily reflect the views of MCEER, the National Science Foundation, or other sponsors.



---

## Sliding Fragility of Unrestrained Equipment in Critical Facilities

by

W.H. Chong<sup>1</sup> and T.T. Soong<sup>2</sup>

Publication Date: July 5, 2000

Submittal Date: January 20, 2000

Technical Report MCEER-00-0005

Task Numbers 99-1504 and 99-2401

NSF Master Contract Number EEC 9701471

- 1 Graduate Assistant, Department of Civil, Structural and Environmental Engineering, University at Buffalo, State University of New York; Currently with Watson Bowman ACME Corporation
- 2 Samuel P. Capen Professor, Department of Civil, Structural and Environmental Engineering, University at Buffalo, State University of New York

MULTIDISCIPLINARY CENTER FOR EARTHQUAKE ENGINEERING RESEARCH  
University at Buffalo, State University of New York  
Red Jacket Quadrangle, Buffalo, NY 14261

---

## Preface

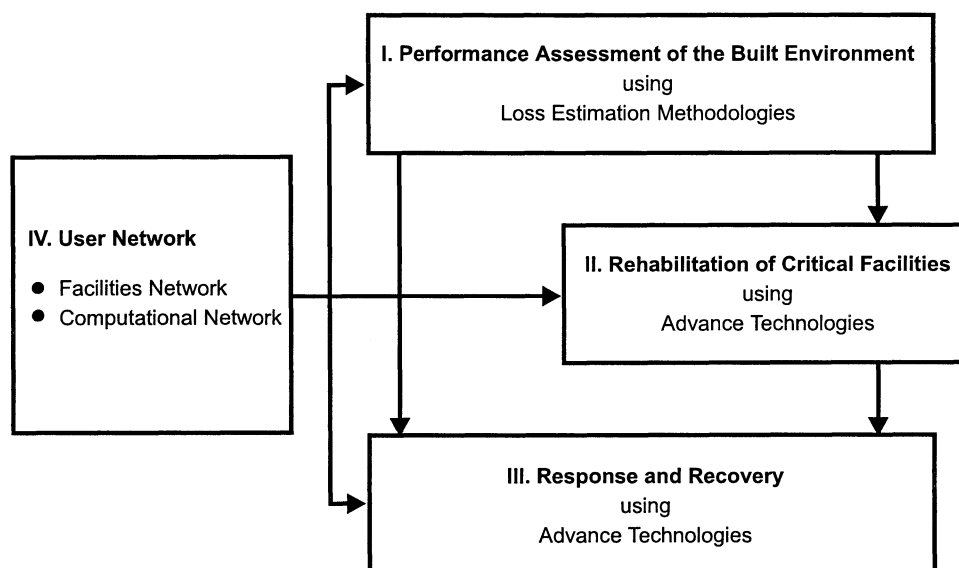
The Multidisciplinary Center for Earthquake Engineering Research (MCEER) is a national center of excellence in advanced technology applications that is dedicated to the reduction of earthquake losses nationwide. Headquartered at the University at Buffalo, State University of New York, the Center was originally established by the National Science Foundation in 1986, as the National Center for Earthquake Engineering Research (NCEER).

Comprising a consortium of researchers from numerous disciplines and institutions throughout the United States, the Center's mission is to reduce earthquake losses through research and the application of advanced technologies that improve engineering, pre-earthquake planning and post-earthquake recovery strategies. Toward this end, the Center coordinates a nationwide program of multidisciplinary team research, education and outreach activities.

MCEER's research is conducted under the sponsorship of two major federal agencies: the National Science Foundation (NSF) and the Federal Highway Administration (FHWA), and the State of New York. Significant support is derived from the Federal Emergency Management Agency (FEMA), other state governments, academic institutions, foreign governments and private industry.

The Center's NSF-sponsored research is focused around four major thrusts, as shown in the figure below:

- quantifying building and lifeline performance in future earthquake through the estimation of expected losses;
- developing cost-effective, performance based, rehabilitation technologies for critical facilities;
- improving response and recovery through strategic planning and crisis management;
- establishing two user networks, one in experimental facilities and computing environments and the other in computational and analytical resources.





*The objective of this research is to develop fragility information and rehabilitation strategies for nonstructural components in critical facilities. The research concentrates on experimental and analytical studies of the sliding response of freestanding rigid objects subjected to base excitation. Analytical and experimental techniques are combined to allow determination of fragility curves for freestanding rigid equipment under seismic excitations for further improvement of seismic mitigation measures.*

*A discrete system model, an analytical model for two-dimensional sliding under two-dimensional excitation, is developed and analyzed for specific base motions. Shaking table testing with a range of excitations and system parameters is used to define stability bounds for pure sliding motion. A comparison of the analytical and experimental results is then performed to further verify the validity of the analytical model. Future improvements and discrepancies in the model assumptions are also discussed in this report.*

## ABSTRACT

Through the years, seismic design of buildings has been well developed and is continually updated and improved. Yet, nonstructural components housed in buildings are rarely designed with the same degree of consideration as buildings. As a result, buildings that remain structurally sound after a strong earthquake often lose their operational capabilities due to damage to their nonstructural components, such as piping systems, communication equipment and other types of components. The recent 1994 Northridge, 1995 Kobe, and 1999 Turkey and Taiwan earthquakes further demonstrate the importance of controlling damage to nonstructural components, particularly in critical facilities, such as hospitals, in order to ensure their functionality during and after a major earthquake.

Earthquake vulnerability of nonstructural components is usually reduced by fastening or bracing individual objects. However, there are some nonstructural components in buildings which often cannot be restrained for protection from earthquake shaking. The response of these objects will consist of sliding, rocking, or jumping. Understanding these response types will allow estimation of vulnerability to earthquake damage and will assist in the design of appropriate mitigation measures.

This research concentrates on experimental and analytical studies of the sliding response of freestanding rigid objects subjected to base excitation. Analytical and experimental techniques are combined to allow determination of fragility curves for free-standing rigid equipment under seismic excitations for further improvement of seismic mitigation measures.

A discrete system model, an analytical model for two-dimensional sliding under two-dimensional excitation, is developed and analyzed for specific base motions. Shaking table testing with a range of excitations and system parameters is used to define stability bounds for pure sliding motion. A comparison of the analytical and experimental results is then performed to further verify the validity of the analytical model. Discrepancies in the model assumptions and future improvements of the nonstructural model are also discussed in this report.

## ACKNOWLEDGEMENTS

This work was supported in part by the Multidisciplinary Center for Earthquake Engineering Research, Buffalo, NY under Grant Nos. MCEER-991504 and MCEER-992401. This support is gratefully acknowledged.

The authors would also like to thank M. Pitman, D. Walch, and their co-workers in the SUNY/Buffalo Structural Engineering Laboratory for their help in the experimental portion of this research.

## TABLE OF CONTENTS

SECTION	TITLE	PAGE
<b>1</b>	<b>INTRODUCTION</b>	1
1.1	Background	2
1.2	Types of Rigid Block Motion During Earthquake	2
1.3	Objectives of Study	5
1.4	Approach of Research	6
	Organization	6
<b>2</b>	<b>SLIDING PROBLEM FORMULATION</b>	9
2.1	Conditions for Sliding	9
2.2	Graphical Representation of Motion Types	9
2.3	Equation of Sliding Motion	11
2.4	Generation of Acceleration Time History Inputs	14
2.4.1	SIMQKE : An Artificial Motion Generation Program	14
2.4.2	Response Spectrum based on 1997 NEHRP Guidelines	14
2.5	Summary of Analytical Results	17
2.5.1	Sliding Performance of Free-Standing Rigid Block	17
2.5.2	Analytical Fragility Curves	17
2.5.3	Discussion of Results	31
<b>3</b>	<b>EXPERIMENTS FOR SLIDING PROBLEM</b>	41
3.1	Test Set-Up	41
3.1.1	The Shaking Table	41
3.1.2	The Sliding Surfaces	41
3.1.3	Instrumentation	45
3.1.4	Acceleration Time History Inputs	45
3.2	Determination of Static Coefficient of Friction	55
3.2.1	The Pulling Test	55
3.2.2	The Tilting Test	55
3.2.3	Average Static Coefficient of Friction	59
3.3	Summary of Experimental Results	59
3.3.1	Sliding Performance of Free-Standing Rigid Block	59
3.3.2	Experimental Fragility Curves	59
3.3.3	Discussion of Results	68
3.4	Comparison of Analytical and Experimental Results	68
<b>4</b>	<b>CONCLUSION</b>	77
4.1	Conclusion	77
4.2	Recommendations for Future Research	77
4.2.1	Sliding-Rocking Motion Type and Jumping Motion Type	77
4.2.2	Deviation from Horizontal Supporting Base	78
4.2.3	Experimental Estimation of Dynamic Friction Coefficient	78

**TABLE OF CONTENTS (continued)**

<b>SECTION</b>	<b>TITLE</b>	<b>PAGE</b>
<b>5</b>	<b>REFERENCES</b>	<b>79</b>
	<b>APPENDIX A – NUMERICAL METHOD FOR SLIDING PROBLEM</b>	<b>81</b>
	<b>APPENDIX B – SIMQKE PROGRAM</b>	<b>85</b>
	<b>APPENDIX C – TABLE FOR STATIC AND DYNAMIC FRICTION COEFFICIENTS</b>	<b>103</b>

## LIST OF FIGURES

FIGURE	TITLE	PAGE
1.1	Effects of Earthquake on Nonstructural Components (FEMA 74, 1994)	3
1.2	Free-Standing Rigid Block under Seismic Excitation	4
2.1	Graphical Representation of Motion Types when $\ddot{y}_g > 0$ or $\ddot{y}_g < 0$	12
2.2	Graphical Representation of Motion Types when $\ddot{y}_g = 0$ (Gates and Scawthorn, 1982)	13
2.3	General Procedure Response Spectrum (NEHRP, 1997)	21
2.4	Generated Response Spectrum	21
2.5	Generated Time History Input I : HPGA = 0.7g	22
2.6	Generated Time History Input II : HPGA = 0.7g	23
2.7	Generated Time History Input III : HPGA = 0.7g	24
2.8	Generated Time History Input IV : HPGA = 0.7g	25
2.9	Analytical Solution I	26
2.10	Analytical Solution II	27
2.11	Analytical Solution III	28
2.12	Analytical Solution IV	29
2.13	Analytical Solution V	30
2.14	Effect of Dynamic Friction Coefficient on the Acceleration-at-which-Threshold-Displacement-Occur	36
2.15	Fragility Curves for $\mu_d = 0.1$ ; Failure Threshold = 1 inch	37
2.16	Fragility Curves for $\mu_d = 0.1$ ; Failure Threshold = 2 inches	37
2.17	Fragility Curves for $\mu_d = 0.2$ ; Failure Threshold = 1 inch	38
2.18	Fragility Curves for $\mu_d = 0.2$ ; Failure Threshold = 2 inches	38
2.19	Fragility Curves for $\mu_d = 0.3$ ; Failure Threshold = 1 inch	39
2.20	Fragility Curves for $\mu_d = 0.3$ ; Failure Threshold = 2 inches	39
2.21	Fragility Curves for $\mu_d = 0.4$ ; Failure Threshold = 1 inch	40
2.22	Fragility Curves for $\mu_d = 0.4$ ; Failure Threshold = 2 inches	40
3.1	Shaking Table and Experimental Set-up	42
3.2	Schematic Sketch of Shaking Table System (Kosar, et al., 1993)	43
3.3	Steel Bars to Constrain Sliding Performance	44
3.4(a)	Locations of Horizontal and Vertical Accelerometers	46
3.4(b)	Locations of Horizontal Accelerometers	47
3.4(c)	Locations of Vertical Accelerometers	47
3.5(a)	Locations of Horizontal LVDT and Markers	48
3.5(b)	Front View of Rigid Block with LVDT attached	49
3.5(c)	Side View of Rigid Block with LVDT attached	49
3.5(d)	Side View of LVDT	50
3.5(e)	Front View of LVDT	50
3.6	Locations of Permanent Markers	51
3.7	Scaled El Centro Earthquake Time History	52

## LIST OF FIGURES (continued)

FIGURE	TITLE	PAGE
3.8	Scaled Pacoima Earthquake Time History	52
3.9	Scaled Kobe Earthquake Time History	53
3.10	Scaled Northridge Earthquake Time History	53
3.11	Scaled Taft Earthquake Time History	54
3.12	The Pulling Test Assembly	56
3.13	The Tilting Test Assembly	56
3.14	The Tilting Test Procedure	57
3.15	Instrument for Angle Measurement	58
3.16	Typical Experimental Result from El Centro Earthquake Input	61
3.17	Typical Experimental Result from Kobe Earthquake Input	62
3.18	Typical Experimental Result from Pacoima Earthquake Input	63
3.19	Typical Experimental Result from Northridge Earthquake Input	64
3.20	Typical Experimental Result from Taft Earthquake Input	65
3.21	Experimental Fragility Curves for Failure Threshold = 1 inch	66
3.22	Experimental Fragility Curves for Failure Threshold = 2 inches	67
3.23	Comparison of Experimental and Analytical Fragility Curves with $\mu_d = 0.3$ , Failure Threshold = 1 inch	72
3.24	Comparison of Experimental and Analytical Fragility Curves with $\mu_d = 0.3$ , Failure Threshold = 2 inches	73
3.25	Comparison of Experimental and Analytical Fragility Curves with $\mu_d = 0.21$ , Failure Threshold = 1 inch	74
3.26	Comparison of Experimental and Analytical Fragility Curves with $\mu_d = 0.21$ , Failure Threshold = 2 inches	75

## LIST OF TABLES

TABLE	TITLE	PAGE
1.1	Conditions for Different Types of Initiated Response during Earthquake	5
2.1	Values of $F_a$ as a Function of Site Class and Mapped Short-Period Maximum Considered Earthquake Spectral Acceleration (NEHRP, 1997)	16
2.2	Values of $F_v$ as a Function of Site Class and Mapped 1 Second Period Maximum Considered Earthquake Spectral Acceleration (NEHRP, 1997)	16
2.3	Number of Time History Inputs for Each Dynamic Friction Coefficient	18
2.4	Summary of Analytical Solution for $\mu_d = 0.1$	19
2.5	Summary of Analytical Solution for $\mu_d = 0.2$	19
2.6	Summary of Analytical Solution for $\mu_d = 0.3$	20
2.7	Summary of Analytical Solution for $\mu_d = 0.4$	20
2.8	Analytical Probabilities of Failure for $\mu_d = 0.1$	32
2.9	Analytical Probabilities of Failure for $\mu_d = 0.2$	33
2.10	Analytical Probabilities of Failure for $\mu_d = 0.3$	34
2.11	Analytical Probabilities of Failure for $\mu_d = 0.4$	35
3.1	Number of Runs for Each Combination of HPGA and VPGA in Experiments	45
3.2	Summary of Experimental Results	60
3.3	Summary of Analytical Solution for $\mu_d = 0.21$	60
3.4	Experimental Probabilities of Failure	70
3.5	Analytical Probabilities of Failure for $\mu_d = 0.21$	71
C1	Coefficients of Friction for Selected Engineering Materials	103



## SECTION 1 INTRODUCTION

### 1.1 Background

Nonstructural components are, basically, all components of a building other than those considered to perform primary structural functions. They include mechanical and electrical equipment, architectural elements, and building contents. Technically, they are sufficiently strong and rigid to remain in place, but are wholly unintegrated with the primary structure as the structural load-bearing system. In other words, they can affect structural behavior only through inertial forces; they add no stiffness to the primary structure; and are infrequently designed to resist seismic forces. On the other hand, secondary components, which are sometimes confused with nonstructural components, can affect the seismic behavior of a primary structure.

Through the years, earthquakes have earned a growing reputation for their consistent propensity to find the 'weak link' in a complex system and lead that system into a progressive failure mode. As a result of this ability to locate and strike the weakest point of an assembly, nonstructural components have always been the 'victims' of earthquakes.

The bottom line in evaluating a well-constructed building is found in its success in providing safety and comfort for its occupants. In most structural designs, engineers tend to emphasize structural damage in earthquakes. However, in certain situations, damage to nonstructural components can pose a more dangerous threat to life safety than structural damage. This can be revealed from an evaluation of various veterans hospitals following the San Fernando earthquake in 1971. Many facilities, which still structurally intact, were no longer functional because of loss of essential equipment and supplies. More importantly, it has also been recognized that survival after the occurrence of a strong earthquake of nonstructural components may be vital in terms of providing emergency services, as in the case of equipment in power stations, hospitals, or communication facilities.

In addition to safety threat resulted from the failure of nonstructural components, economic loss from nonstructural component damage has also received special attention by engineers. In fact, in some cases, damage to nonstructural components will greatly exceed the cost of structural damage. For example, of \$143,000 in total damage of a building caused by the San Fernando earthquake, in 1972-value dollars, only \$2,000 was structural damage while the remaining 98.56% was nonstructural. Moreover, costly damage to nonstructural components could occur in earthquakes of moderate intensities, which would cause little or no structural damage.

In accordance with such a concern for human safety as well as economic considerations, effort should be made to reduce the potential for damage to nonstructural components of structures as part of the effort to reduce the overall seismic hazard to structures. Thus, it is very important for structural engineers to not underestimate the performance of nonstructural components during earthquakes. In view of this, understanding the vulnerability of nonstructural components to earthquake excitation is critical to protection from future damage.

## 1.2 Types of Rigid Block Motion During Earthquake

Nonstructural components are subject to damage during an earthquake either directly due to ground shaking or indirectly due to movement of buildings. Earthquake ground shaking has three primary effects on nonstructural components in buildings. These are inertial or shaking effects on the nonstructural components themselves, distortions imposed on nonstructural components when the building structure vibrates, and separation or pounding at the interface between adjacent structures. These three effects are shown in Figure 1.1 ( FEMA, 1994).

Evaluating the seismic performance of nonstructural components which are subjected to damage caused by inertial or shaking effects ( first case in Figure 1.1) is of concern in this research. Figure 1.2 shows a free-standing rigid block resting on a supporting base subjected to base excitation due to an earthquake. There are basically four types of response which could occur. The block could either be at rest, or sliding, or rocking, or jumping or having a kind of motion which is a combination of these motion types.

In accordance with the four types of response mentioned above, there are basically three kinds of motion equilibrium equations that dictate the motion of the free-standing rigid block under a seismic excitation :

1. Vertical Equilibrium : Gravity force equals the vertical component of the input excitation:

$$mg + m\ddot{y}_g = 0 \quad (1.1)$$

2. Horizontal Equilibrium : Horizontal component of the input excitation equals the friction force:

$$\left| m\ddot{x}_g \right| = \mu_s m(g + \ddot{y}_g) \quad ; \quad g + \ddot{y}_g \geq 0 \quad (1.2)$$

3. Moment Equilibrium : Moment induced by the input excitation equals the restoring moment:

$$h \left| m\ddot{x}_g \right| = bm(g + \ddot{y}_g) \quad ; \quad g + \ddot{y}_g \geq 0 \quad (1.3)$$

in which,

- $m$  is the mass of the free-standing rigid block
- $g$  is the gravitational acceleration, which is  $9.81 \text{ m/sec}^2$  ( $32.2 \text{ ft/sec}^2$ )
- $\ddot{x}_g$  is the horizontal acceleration within an acceleration time history (positive to left)
- $\ddot{y}_g$  is the vertical acceleration within an acceleration time history (positive downward)
- $\mu_s$  is the coefficient of static friction between sliding surfaces
- $h$  is one-half of the block height
- $b$  is one-half of the block width

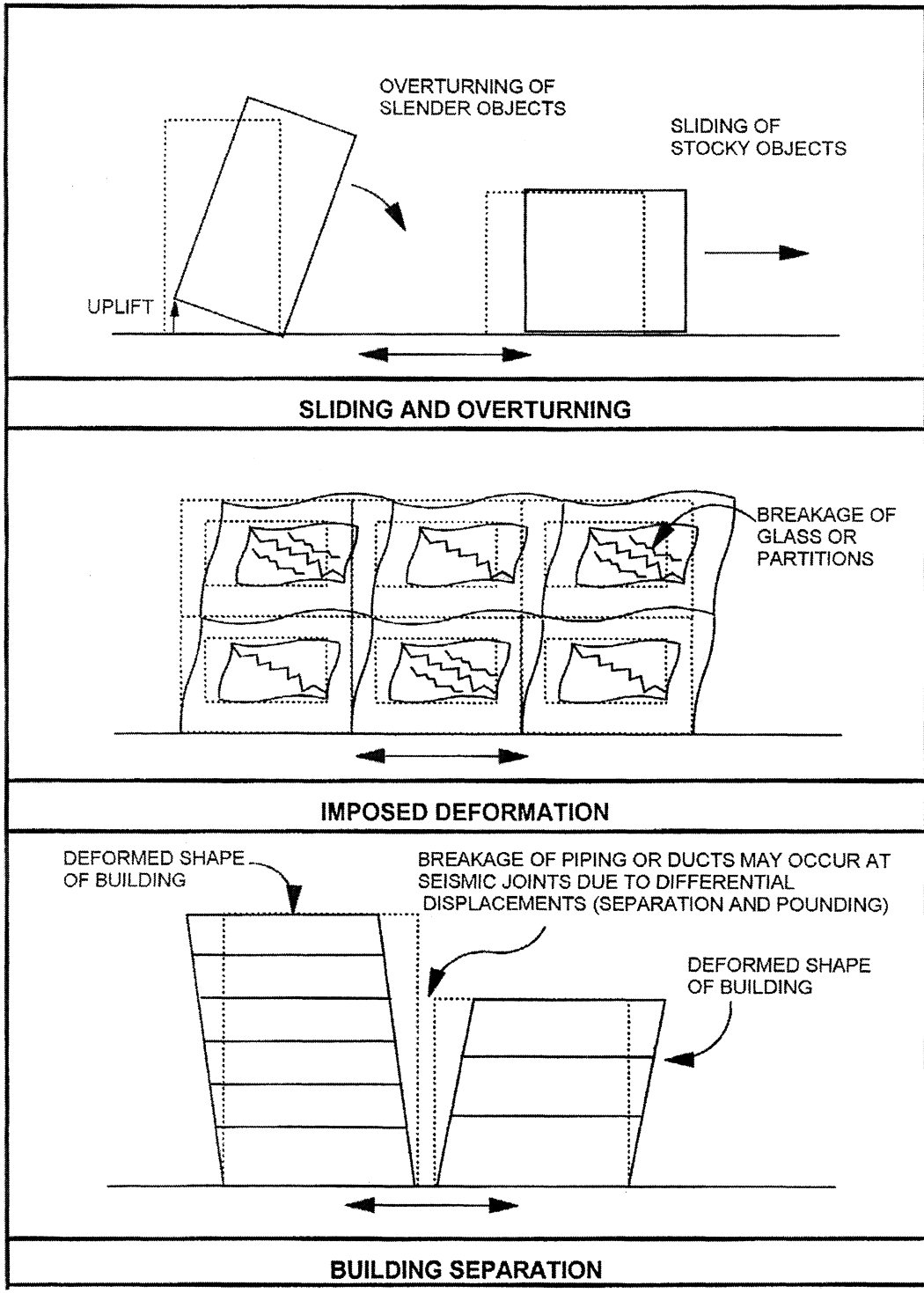


Figure 1.1 Effects of Earthquake on Nonstructural Components (FEMA 74, 1994)

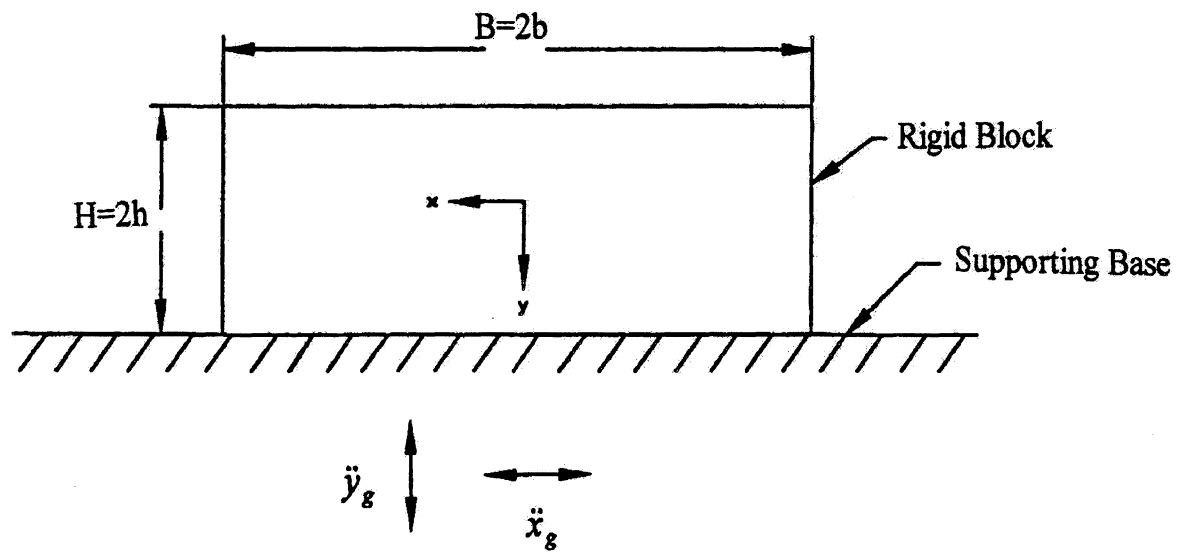


Figure 1.2 Free-Standing Rigid Block Under Base Excitation

If one of the forces exceeds the other in each of the equilibrium equation mentioned above, different types of motions could be initiated. The conditions for initiating these four types of motion are illustrated below in Table 1.1 :

Table 1.1 Conditions for Different Types of Initiated Response during Earthquake

Motion Types	Vertical Inequality	Horizontal Inequality	Moment Inequality
<b>At Rest</b>	$(g + \ddot{y}_g) \geq 0$	$ \ddot{x}_g  \leq \mu_s (g + \ddot{y}_g)$	$ \ddot{x}_g  \leq \frac{b}{h} (g + \ddot{y}_g)$
<b>Jumping</b>	$(g + \ddot{y}_g) \leq 0$	–	–
<b>Rocking</b>	$(g + \ddot{y}_g) \geq 0$	$ \ddot{x}_g  \leq \mu_s (g + \ddot{y}_g)$	$ \ddot{x}_g  \geq \frac{b}{h} (g + \ddot{y}_g)$
<b>Sliding</b>	$(g + \ddot{y}_g) \geq 0$	$ \ddot{x}_g  \geq \mu_s (g + \ddot{y}_g)$	$ \ddot{x}_g  \leq \frac{b}{h} (g + \ddot{y}_g)$

As noticed from Table 1.1,  $(g + \ddot{y}_g) \geq 0$  is the pre-requisite for the at rest, sliding and rocking motion. In addition, the prerequisite for the initiation of a sliding motion is  $\frac{b}{h} > \mu_s$ . On the other hand,  $\frac{b}{h} < \mu_s$  is the prerequisite to initiate rocking motion.

### 1.3 Objectives of Study

Clearly, sliding is an important failure mode for free-standing block-type equipment subjected to strong earthquakes. If an unrestrained rigid object does not rock during earthquake shaking, then it may slide across its mounting surface. Sliding itself is not objectionable. In fact, sliding can be effectively used as a means of horizontal base isolation. However, excessive sliding clearly can damage the object or cause damage to other objects if the sliding displacement is large enough to allow impact with other objects. Failure criteria will therefore depend on the allowable relative displacement as well as the combination of the allowable relative displacement and the absolute acceleration at which allowable relative displacement occurs.

The major objective of this research is to construct fragility curves for different peak ground accelerations (PGA), both horizontal and vertical, as well as different coefficients of friction based on certain sliding failure thresholds as mentioned above. Since base accelerations are random in nature, a statistical method is necessary for both analytical modeling and experimental measurements of sliding response.

With these failure curves constructed, their sensitivity to some important response parameters, which are the coefficient of friction for the sliding surfaces, the peak ground accelerations of excitation, both horizontal and vertical, for pure sliding response could be determined for evaluation of the seismic performance as well as for the design of free-standing block-type equipment.

## **1.4 Approach of Research**

In order to construct the fragility curves for sliding failure mode, the conditions for sliding to be initiated are important in this research. With the determined conditions for pure sliding motion, (excluding rocking and jumping), the equation of sliding motion of a free-standing rigid block could be formed base on the assumptions made for pure sliding motion. This equation of motion can then be solved using a numerical method.

In order to obtain the probability of failure, many varieties of excitation should be included as the inputs in solving the differential equation of motion. In this work, SIMQKE will be used in randomly generating the excitation inputs and fragility results will be obtained through Monte Carlo simulation.

With the solutions solved numerically with given input excitation at discrete points, different failure thresholds could be set to obtain the probability of failure based on three distinct parameters in this research, namely, the coefficient of dynamic friction of the sliding surfaces as well as the horizontal and vertical peak ground accelerations. The probabilities of failure obtained from different sets of combinations of the three parameters can then be plotted in graphs based on different failure thresholds.

Experiments were performed to verify the validity of the analytical solutions described above. The experiments involved putting a free-standing rigid block on a shaking table to simulate the sliding motion during an earthquake and measuring the relative displacement and absolute acceleration time histories of the sliding block, as the results obtained analytically. Fragility curves constructed from these experimental results were compared with the analytical fragility curves. With this comparison performed, discussion and conclusion could be made in accordance with the objectives set previously.

## **1.5 Organization**

In this research, investigations are carried out, analytically and experimentally, to determine the vulnerability of a free-standing rigid block, under the sliding failure mode, and subjected to earthquake excitations. Emphasis is given to constructing the fragility curves based on different failure thresholds, specifically on both sliding and impact thresholds.

In Section 1, background on the nonstructural components and their damageability during and after an earthquake are addressed. Different types of possible response of nonstructural components under base excitations are presented, followed by the objectives and approach of this research.

In Section 2, conditions for sliding are addressed, and reemphasized by a graphical representation. Equation of sliding motion is then developed based upon these sliding conditions. Due to the fact that the performance of nonstructural components under base excitations is stochastic and nonlinear, a Monte Carlo procedure, which will be illustrated throughout Sections

2.4 and 2.5, is used in constructing the analytical sliding fragility curves. Discussion of these analytical results concludes this section.

In Section 3, concentration is placed on seismic simulation testing procedure. In addition, determination of coefficient of static friction of the tested sliding surfaces is presented in order to relate experimental results with the analytical results. A comparison of these two results concludes this section.

In Section 4, conclusions obtained from this research are presented. Moreover, in Section 4.2, the validity of assumptions used in this research such as classical impact model and perfectly horizontal supporting base will be addressed. The idea of determining the dynamic friction coefficient by experimental means concludes this section.

## SECTION 2 SLIDING PROBLEM FORMULATION

### 2.1 Conditions for Sliding

Sliding of a free-standing rigid body occurs when the horizontal seismic load acting on the rigid body exceeds the friction force between the rigid body and its supporting base. Moreover, sliding of a equipment which is bolted to the floor could also occur when bolts fail due to the excessive seismic load. In this research, only free-standing equipment with low centers of gravity is considered, so that the possibility of overturning and rocking of the equipment is ignored.

Theoretically, a free-standing rigid block, under a seismic excitation, as shown in Figure 1.2, will start to slide, but not rock nor jump, when the following conditions are valid :

$$(g + \ddot{y}_g) \geq 0 \quad \text{Vertical Force Inequality} \quad (2.1)$$

$$|\ddot{x}_g| \geq \mu_s (g + \ddot{y}_g) \quad \text{Horizontal Force Inequality} \quad (2.2)$$

$$|\ddot{x}_g| \leq \frac{b}{h} (g + \ddot{y}_g) \quad \text{Moment Inequality} \quad (2.3)$$

Equation (2.1) is the vertical force inequality. It ensures that resultant of the vertical gravity force and the vertical input excitation is always in the direction of the gravity force. In other words, the block does not lose its weight so that the jumping condition will not be initiated.

Equation (2.2) is the horizontal force inequality. The maximum horizontal inertia force, within the excitation period, must be larger than the maximum friction force that exists to initiate a sliding motion.

Equation (2.3) is the moment inequality about the free-standing rigid block corner point O, shown in Figure 1.2. The maximum toppling moment caused by base excitation must be smaller than the restoring moment in order to ensure that no overturning motion of the rigid block could occur.

The three equations described above are based on the following assumptions:

1. Only in-plane motions are considered.
2. The block and the supporting base are assumed rigid.
3. The surface of the supporting base is horizontal.

### 2.2 Graphical Representation of Motion Types

Due to many uncertainties in estimating the vertical excitation level during an earthquake, the vertical acceleration is assumed to be proportional to the horizontal acceleration. Thus,  $\ddot{y}_g$  will be represented as  $k\ddot{x}_g$  in this study, in which  $k$  is the proportional constant, which varies from 0 to 1.



Let us do some mathematical manipulations of  $|\ddot{x}_g|$  and  $(g + \ddot{y}_g)$  as the following:

$$1. \text{ Divide } |\ddot{x}_g| \text{ by } (g + \ddot{y}_g) \quad \Rightarrow \quad \frac{|\ddot{x}_g|}{g + \ddot{y}_g} = \frac{|\ddot{x}_g|}{g + k\ddot{x}_g} \quad (2.4)$$

$$\text{or} \quad \frac{1}{\frac{g}{|\ddot{x}_g|} + k \frac{\ddot{x}_g}{|\ddot{x}_g|}} \quad (2.5)$$

which can be expressed as :

$$\frac{1}{\frac{g}{|\ddot{x}_g|} + k \operatorname{sgn}(\ddot{y}_g)} \quad (2.6)$$

in which  $\ddot{y}_g$  is the vertical ground acceleration and  $\operatorname{sgn}(\ddot{y}_g)$  is the Signum function defined by :

$$\operatorname{sgn}(\ddot{y}_g) = +1 \quad \text{for } \ddot{y}_g > 0 \quad ; \quad \operatorname{sgn}(\ddot{y}_g) = -1 \quad \text{for } \ddot{y}_g < 0$$

2. Equation (2.6) can be broken down into two values which are expressed as two constants,  $a$  and  $c$ , as follows :

$$a = \frac{1}{\frac{g}{|\ddot{x}_g|} + k} \quad , \text{ when } \ddot{y}_g > 0 \quad (2.7)$$

$$c = \frac{1}{\frac{g}{|\ddot{x}_g|} - k} \quad , \text{ when } \ddot{y}_g < 0 \quad (2.8)$$

With the constants  $a$  and  $c$  determined from equation (2.7) and (2.8), one can relate these two constants, the coefficient of static friction, and the rigid block aspect ratio,  $b/h$ , with the two possible motions of the rigid block, sliding and rocking, by comparing equations (2.7) and (2.8) with the conditions for sliding and rocking in Table 1.1. The final result of this comparison is shown in Figure 2.1, which is based on the following: For a sliding motion,

1. From Table 1.1, the conditions for sliding could be simplified as follows:

$$\mu_s (g + \ddot{y}_g) \leq |\ddot{x}_g| \leq \frac{b}{h} (g + \ddot{y}_g) \Rightarrow \mu_s \leq \frac{|\ddot{x}_g|}{(g + \ddot{y}_g)} \leq \frac{b}{h} \quad (2.9)$$

2. From equation (2.9), the prerequisite for a pure sliding motion is therefore

$$\mu_s \leq \frac{b}{h} \quad , \quad (\text{shown in the squared area in Figure 2.1}) \quad (2.10)$$

3. Combining (2.7), (2.8) and (2.9), we have the following:

$$\mu_s \leq a \leq \frac{b}{h}, \quad \text{when } \ddot{y}_g > 0 \quad (2.11)$$

$$\mu_s \leq c \leq \frac{b}{h}, \quad \text{when } \ddot{y}_g < 0 \quad (2.12)$$

Thus, we obtained the hatched area, shown in Figure 2.1, for a pure sliding motion region. The rocking motion region could be obtained using the same analysis method as for sliding motion region.

As for the region where both  $\mu_s$  and  $\frac{b}{h}$  are smaller than  $a$ , the horizontal inertia force exceeds the static friction force while creating a toppling moment to overcome the restoring moment. Thus, a combination of sliding and rocking motion may occur. On the other hand, when both  $\mu_s$  and  $\frac{b}{h}$  are larger than  $c$ , the horizontal inertia force is restricted by the static force while the toppling moment is restricted by the restoring moment at the same time and thus the free-standing rigid block will be at rest under the input seismic loading.

As  $\ddot{y}_g = 0$ , where  $a$  and  $c$  vanish, we could obtain a graph as shown in Figure 2.2 (Gates and Scawthorn, 1982).

### 2.3 Equation of Sliding Motion

As shown in Figure 1.2, the free-standing rigid block, which is undergoing a sliding motion caused by both horizontal and vertical excitations of its supporting base, is a simplified analytical model for an unrestrained block type equipment under seismic loading. The excitations of the supporting base may represent a strong earthquake motion.

The equation of sliding motion that will be established in this section is based on the assumption that the restoring moment is large enough to resist the toppling moment,  $b/h > c$ , so that rocking will not occur, neither does jumping motion. In other words, pure sliding motion occurs while the block is experiencing earthquake excitations.

With the above assumption established, the equation of sliding motion of rigid block can be expressed as the following :

$$m(\ddot{x} + \ddot{x}_g) + \mu_d(mg + m\ddot{y}_g) \text{sgn}(\dot{x}) = 0 \quad (2.13)$$

which is valid when sliding conditions shown in Table 1.1 are satisfied. By eliminating  $m$ , equation (2.9) can be simplified as :

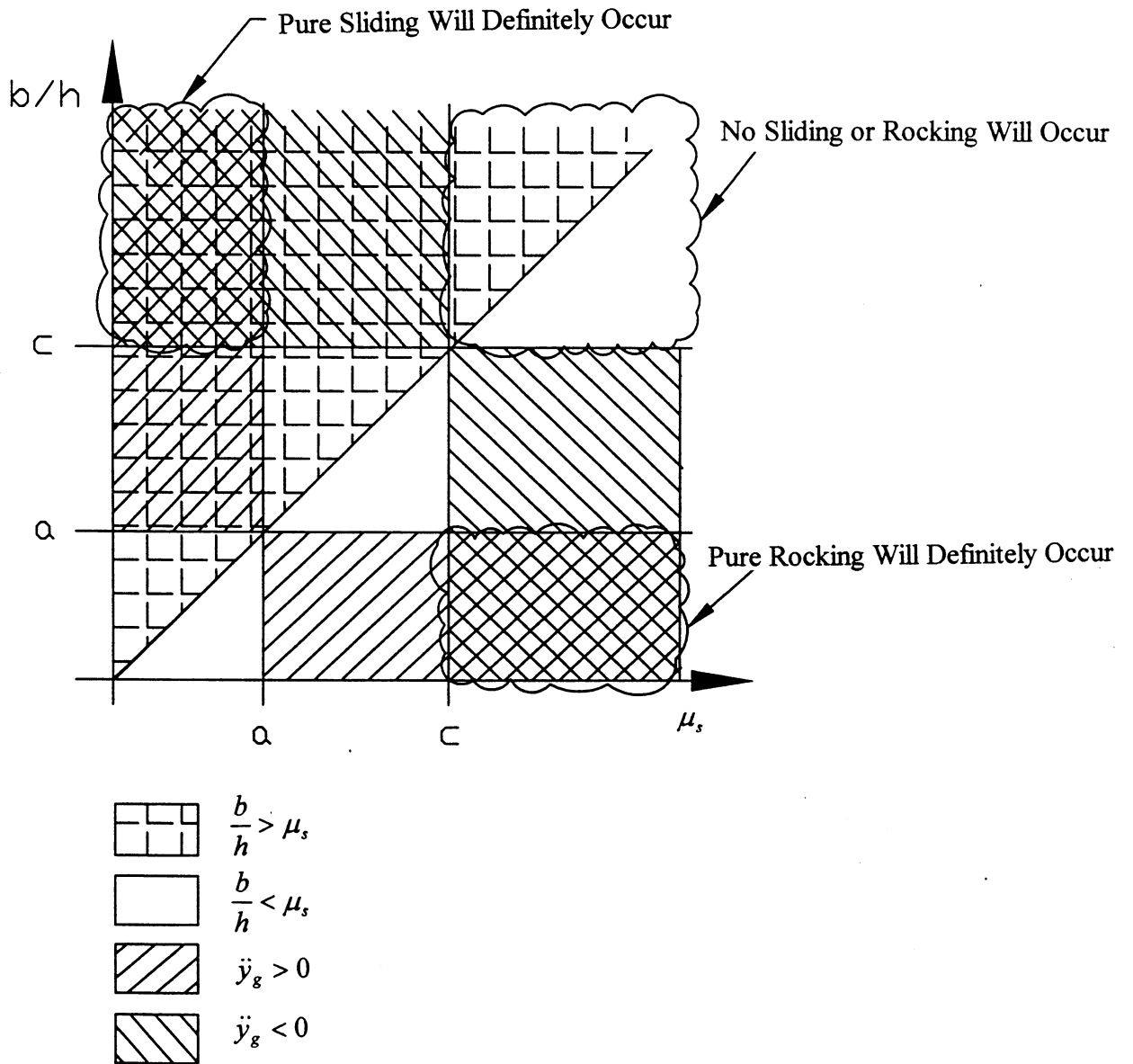


Figure 2.1 Graphical Representation of Motion Types when  $\ddot{y}_g > 0$  or  $\ddot{y}_g < 0$

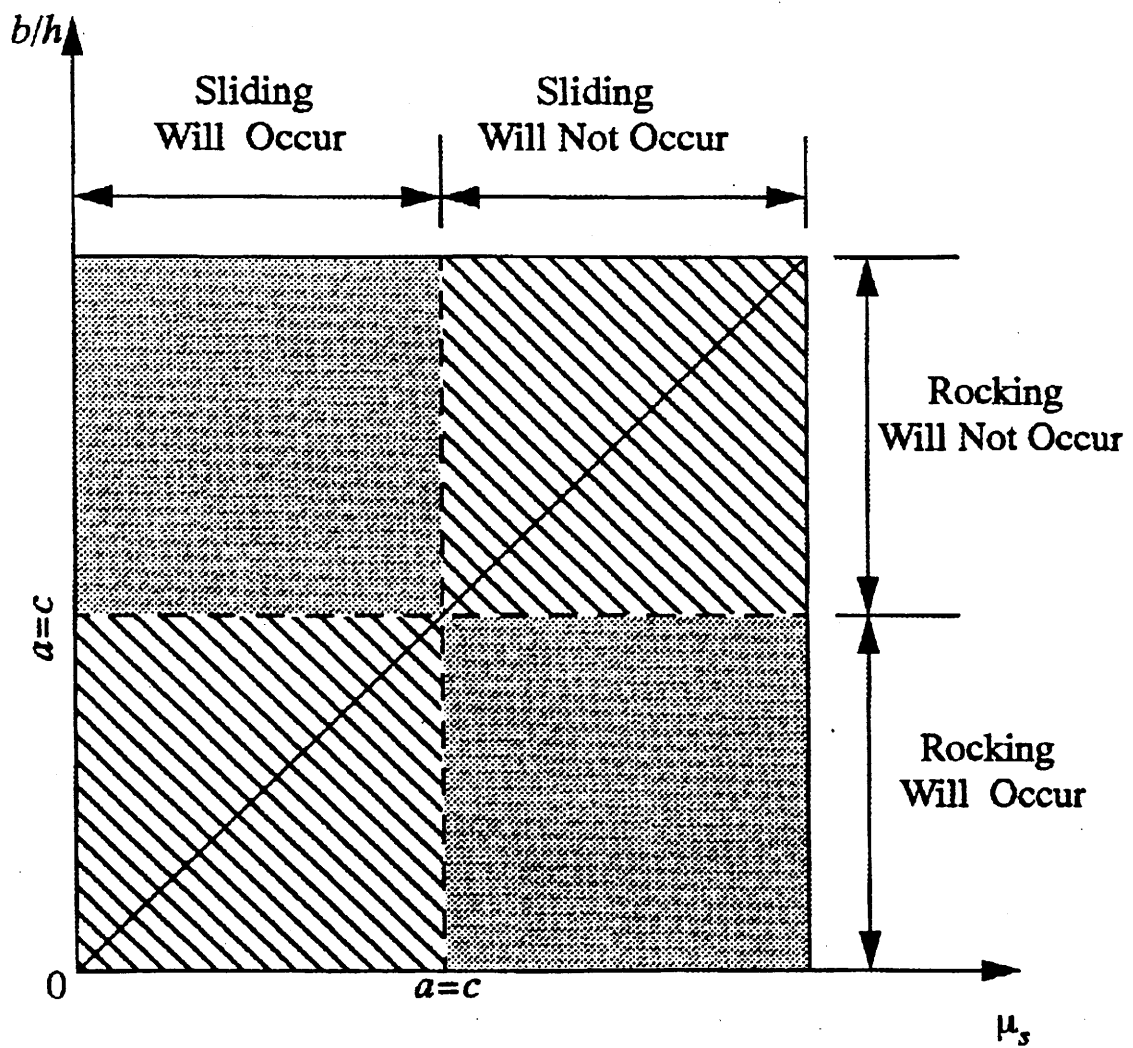


Figure 2.2 Graphical Representation of Motion Types when  $\ddot{y}_g = 0$  (Gates and Scawthorn, 1982)

$$(\ddot{x} + \ddot{x}_g) + \mu_d(g + \ddot{y}_g) \text{sgn}(\dot{x}) = 0 \quad (2.14)$$

which is valid when sliding conditions shown in Table 1.1 are satisfied. In the above,  $\ddot{x}$  is the block relative acceleration at any instance within a time history and  $\mu_d$  is the coefficient of dynamic friction.

With equation (2.14) determined to describe the sliding motion of the free-standing rigid block, discrete system solution is performed, as shown in Appendix A, to obtain the analytical solutions shown in Section 2.5. Ninety excitation inputs were generated, as described in Section 2.4. These excitation inputs were scaled down to different horizontal and vertical excitations as the excitation inputs in the discrete system solution. In addition, five dynamic friction coefficients were used as an input parameter in this theoretical solution procedure.

## 2.4 Generation of Acceleration Time History Inputs

Ninety acceleration time history inputs were generated using SIMQKE, an artificial motion generation program, by inputting a response spectrum, which was generated based on 1997 NEHRP Recommended Provisions for Seismic Regulations for New Buildings and other Structures (NEHRP, 1997), into the SIMQKE program. An introduction of the SIMQKE program will be presented in Section 2.4.1, followed by an illustration on generating the response spectrum using the guidelines specified by NEHRP in Section 2.4.2. Finally, some typical acceleration time history inputs, for a horizontal peak ground acceleration (HPGA) of 0.7g, generated by SIMQKE will be presented at the end of this section, as Figures 2.5~2.8.

### 2.4.1 SIMQKE : An Artificial Motion Generation Program

SIMQKE (Vanmarcke et al., 1976 ) is a program, written in FORTRAN 77 language, for artificial earthquake motion generation. It has the capabilities of computing a power spectral density function from a specified smooth response spectrum and generating statistically independent artificial acceleration time histories and trying, by iteration, to match the specified response spectrum. The resultant acceleration time history inputs are heavily depend on the response spectrum input to the program. The user's guidelines manual and the SIMQKE program are shown in Appendix B.

### 2.4.2 Response Spectrum based on 1997 NEHRP Guidelines

The input response spectrum in SIMQKE was generated based on the guidelines in Chapter 4, Ground Motion, of NEHRP Provisions (NEHRP, 1997). According to the 1997 NEHRP, either the general procedure specified in Sec.4.1.2, of 1997 NEHRP, or the site-specific procedure specified in Sec.4.1.3, of 1997 NEHRP, can be used in generating response spectra. In this research, the general procedure was used.

**Parameter Determination.** In order to generate a response spectrum, two spectra response acceleration parameters need to be determined. They are the Maximum Considered Earthquake (MCE) spectral response acceleration for short periods,  $S_{MS}$ , and at one second,  $S_{M1}$ , which are

adjusted for site class effects to include local site effects. These two parameters are determined according to the following equations to adjust for site class effects :

$$S_{MS} = F_a S_s \quad (2.15)$$

$$S_{M1} = F_v S_1 \quad (2.16)$$

in which  $F_a$ ,  $F_v$ ,  $S_s$  and  $S_1$  are parameters determined according to Tables 2.1 and 2.2.

Due to the fact that the soil properties are not known in sufficient detail to determine the Site Class, Site Class D in Sec. 4.1.2.1 of 1997 NEHRP is used. The value of  $S_s$  is taken to be three and the value of  $S_1$  is taken to be one for the purpose of making the  $S_{DS}$  to be 2.0g by referring to equation (2.17), which will be illustrated later in this section.  $S_s$  and  $S_1$  can be chosen randomly to create a  $S_{DS}$  of 2.0g because they are independent.

After taken into account the site class effect,  $S_{MS}$  and  $S_{M1}$  are scaled to design values according to the equations below :

$$S_{DS} = \frac{2}{3} S_{MS} \quad (2.17)$$

$$S_{D1} = \frac{2}{3} S_{M1} \quad (2.18)$$

where  $S_{DS}$  is the design spectral response acceleration at short periods, and  $S_{D1}$  is the design spectral response acceleration at one second period.

**General Procedure Response Spectrum.** With all the above parameters determined, a design response spectrum curve can be developed as indicated in Figure 2.3 (NEHRP, 1997), which is explained in details as follows :

1. For periods less than or equal to  $T_o$ , the design spectral response acceleration,  $S_a$ , is given by the following equation :

$$S_a = 0.6 \frac{S_{DS}}{T_o} T + 0.4 S_{DS} \quad (2.19)$$

2. For periods greater than or equal to  $T_o$  ( $T_o = 0.2 S_{D1} / S_{DS}$ ) and less than or equal to  $T_s$  ( $T_s = S_{D1} / S_{DS}$ ), the design spectral response acceleration,  $S_a$ , is taken as equal to  $S_{DS}$ .
3. For periods greater than  $T_s$ , the design spectral response acceleration,  $S_a$ , is taken as given by the following equation :

Table 2.1 Values of  $F_a$  as a Function of Site Class and Mapped Short-Period Maximum Considered Earthquake Spectral Acceleration (NEHRP, 1997)

Site Class	Mapped Maximum Considered Earthquake Spectral Response Acceleration at Short Periods				
	$S_s \leq 0.25$	$S_s = 0.50$	$S_s = 0.75$	$S_s = 1.00$	$S_s \geq 1.25$
A	0.8	0.8	0.8	0.8	0.8
B	1.0	1.0	1.0	1.0	1.0
C	1.2	1.2	1.1	1.0	1.0
D	1.6	1.4	1.2	1.1	1.0
E	2.5	1.7	1.2	0.9	<i>a</i>
F	<i>a</i>	<i>a</i>	<i>a</i>	<i>a</i>	<i>a</i>

NOTE: Use straight line interpolation for intermediate values of  $S_s$ .

\* Site-specific geotechnical investigation and dynamic site response analyses shall be performed.

Table 2.2 Values of  $F_v$  as a Function of Site Class and Mapped 1 Second Period Maximum Considered Earthquake Spectral Acceleration (NEHRP, 1997)

Site Class	Mapped Maximum Considered Earthquake Spectral Response Acceleration at 1 Second Periods				
	$S_1 \leq 0.1$	$S_1 = 0.2$	$S_1 = 0.3$	$S_1 = 0.4$	$S_1 \geq 0.5$
A	0.8	0.8	0.8	0.8	0.8
B	1.0	1.0	1.0	1.0	1.0
C	1.7	1.6	1.5	1.4	1.3
D	2.4	2.0	1.8	1.6	1.5
E	3.5	3.2	2.8	2.4	<i>a</i>
F	<i>a</i>	<i>a</i>	<i>a</i>	<i>a</i>	<i>a</i>

NOTE: Use straight line interpolation for intermediate values of  $S_1$ .

\* Site-specific geotechnical investigation and dynamic site response analyses shall be performed.

$$S_a = \frac{S_{D1}}{T} \quad (2.20)$$

The generated response spectrum based on the general procedure method specified above is presented in Figure 2.4.

## 2.5 Summary of Analytical Results

By determining the equation of sliding motion and solving it numerically, displacement and acceleration time histories for the sliding block are obtained. There are ninety different acceleration time history inputs, each scaled to have eight different values of HPGA, ranging from 0.3g~1.0g, with 0.1g increment.

Each of these eight horizontal time histories is combined with four different vertical acceleration inputs, which are scaled to 0, 1/4, 1/3, and 1/2 of the horizontal acceleration inputs, one at each time as the inputs for the analytical solutions. The ninety time histories are generated by SIMQKE as discussed in Section 2.4. Table 2.3 illustrates the time history inputs in a more systematic way.

Five different coefficients of dynamic friction, namely, 0.1, 0.2, 0.21, 0.3 and 0.4, are used to evaluate the frictional effect on the performance of the free-standing rigid block under seismic loading. The value of 0.21 is added to compare analytical and experimental results after it is determined experimentally, as described in Chapter 3. All of the time history combinations shown in Table 2.3 are repeated five times for the five different coefficients of dynamic friction.

### 2.5.1 Sliding Performance of Free-Standing Rigid Block

Only three parameters affect the pure sliding response of the free-standing rigid block once sliding has been initiated: the peak horizontal and vertical excitations, and the coefficient of dynamic friction. Figures 2.9~2.13 show relative displacement and absolute acceleration time histories from five typical time history inputs for the coefficient of dynamic friction equal to 0.21. The HPGA considered here is 0.7 g, with a vertical peak ground acceleration (VPGA) of 0.23g, which is 1/3 of the HPGA.

The block average relative peak displacements, which are obtained from the ninety peak displacements obtained from the ninety acceleration time history inputs for each of the combination of HPGA and VPGA for values of  $\mu_d$  equal to 0.1, 0.2, 0.3 and 0.4 are shown in Tables 2.4, 2.5, 2.6 and 2.7, respectively. In addition, the corresponding average absolute accelerations at which threshold displacements occur are also shown in these tables.

### 2.5.2 Analytical Fragility Curves

There are eight different relative displacement failure thresholds considered in the analysis. They are relative displacements of 0.1 inch, 0.2 inch, 0.5 inch, 0.75 inch, 1 inch, 2 inches, 2.5 inches and 3 inches. Consideration of the combination of the relative threshold displacement and the absolute acceleration at which threshold relative displacement occurs as the failure threshold for constructing the fragility curves for a specific coefficient of dynamic friction turns out to be unnecessary due to the analytical results obtained, which will be analyzed in Section 2.5.3.



Table 2.3 Number of Time History Inputs for Each Dynamic Friction Coefficient.

Number of runs for each combination of HPGA and VPGA for different dynamic friction coefficients.										
Proportional Constants for Vertical PGA	Horizontal PGA, g									
	0.3	0.4	0.5	0.6	0.7	0.8	0.9	1		
0	90	90	90	90	90	90	90	90	90	90
1/4	90	90	90	90	90	90	90	90	90	90
1/3	90	90	90	90	90	90	90	90	90	90
1/2	90	90	90	90	90	90	90	90	90	90
<b>TOTAL</b>	<b>360</b>	<b>360</b>	<b>360</b>	<b>360</b>	<b>360</b>	<b>360</b>	<b>360</b>	<b>360</b>	<b>360</b>	<b>360</b>

Table 2.4 Summary of Analytical Solution for  $\mu_d = 0.1$

**Average Peak Displacement, inch**

*Horizontal Peak Ground Acceleration, g*

<b>k</b>	<b>0.3</b>	<b>0.4</b>	<b>0.5</b>	<b>0.6</b>	<b>0.7</b>	<b>0.8</b>	<b>0.9</b>	<b>1</b>
<b>0</b>	0.871877	1.963674	3.316905	4.84207	6.445563	8.142414	9.858388	11.60008
<b>1/4</b>	0.921384	2.104202	3.569039	5.199697	6.942406	8.789935	10.58951	12.36227
<b>1/3</b>	0.962143	2.228275	3.766617	5.496397	7.344542	9.245172	11.12079	12.92271
<b>1/2</b>	1.101465	2.557681	4.359464	6.321035	8.379994	10.40032	12.41299	14.39003

**Average Acceleration at which Peak Displacement Occurs, g**

*Horizontal Peak Ground Acceleration, g*

<b>k</b>	<b>0.3</b>	<b>0.4</b>	<b>0.5</b>	<b>0.6</b>	<b>0.7</b>	<b>0.8</b>	<b>0.9</b>	<b>1</b>
<b>0</b>	0.100495	0.101066	0.102031	0.103067	0.104109	0.105126	0.106381	0.107264
<b>1/4</b>	0.100765	0.102114	0.103406	0.10445	0.106927	0.108995	0.109897	0.111781
<b>1/3</b>	0.100985	0.102439	0.104555	0.105821	0.108929	0.11122	0.112196	0.11464
<b>1/2</b>	0.101406	0.103789	0.106686	0.109926	0.11409	0.115631	0.117889	0.121681

Table 2.5 Summary of Analytical Solution for  $\mu_d = 0.2$

**Average Peak Displacement, inch**

*Horizontal Peak Ground Acceleration, g*

<b>k</b>	<b>0.3</b>	<b>0.4</b>	<b>0.5</b>	<b>0.6</b>	<b>0.7</b>	<b>0.8</b>	<b>0.9</b>	<b>1</b>
<b>0</b>	0.050998	0.320753	0.911822	1.74912	2.768411	3.94449	5.252241	6.632879
<b>1/4</b>	0.059841	0.385287	1.111411	2.206614	3.549732	5.142256	6.866747	8.726916
<b>1/3</b>	0.070863	0.440108	1.280512	2.538945	4.110351	5.944972	7.930333	10.05775
<b>1/2</b>	0.095742	0.586989	1.728973	3.43085	5.560253	8.052521	10.74478	13.52066

**Average Acceleration at which Peak Displacement Occurs, g**

*Horizontal Peak Ground Acceleration, g*

<b>k</b>	<b>0.3</b>	<b>0.4</b>	<b>0.5</b>	<b>0.6</b>	<b>0.7</b>	<b>0.8</b>	<b>0.9</b>	<b>1</b>
<b>0</b>	0.200027	0.200162	0.200425	0.20097	0.201442	0.202171	0.202678	0.203965
<b>1/4</b>	0.198913	0.199432	0.200514	0.203377	0.205114	0.20743	0.210553	0.212546
<b>1/3</b>	0.197997	0.199118	0.200961	0.204043	0.207114	0.208798	0.212754	0.215389
<b>1/2</b>	0.195402	0.199043	0.201428	0.204238	0.208484	0.213552	0.220483	0.224917

Table 2.6 Summary of Analytical Solution for  $\mu_d = 0.3$

**Average Peak Displacement, inch**

*Horizontal Peak Ground Acceleration, g*

<b>k</b>	<b>0.3</b>	<b>0.4</b>	<b>0.5</b>	<b>0.6</b>	<b>0.7</b>	<b>0.8</b>	<b>0.9</b>	<b>1</b>
<b>0</b>	0	0.032062	0.16661	0.484541	1.022189	1.736777	2.622881	3.610839
<b>1/4</b>	0.002776	0.048267	0.238398	0.710567	1.535561	2.702194	4.156455	5.796023
<b>1/3</b>	0.003739	0.0572	0.2947	0.875968	1.898381	3.350913	5.096362	7.153305
<b>1/2</b>	0.006102	0.085666	0.438896	1.288715	2.763771	4.852727	7.406389	10.32595

**Average Acceleration at which Peak Displacement Occurs, g**

*Horizontal Peak Ground Acceleration, g*

<b>k</b>	<b>0.3</b>	<b>0.4</b>	<b>0.5</b>	<b>0.6</b>	<b>0.7</b>	<b>0.8</b>	<b>0.9</b>	<b>1</b>
<b>0</b>	0.300000	0.300013	0.300097	0.300197	0.300461	0.300821	0.30136	0.301971
<b>1/4</b>	0.300016	0.299007	0.298809	0.299678	0.301386	0.303952	0.30624	0.309779
<b>1/3</b>	0.299980	0.294329	0.295592	0.299129	0.301413	0.303394	0.305485	0.312039
<b>1/2</b>	0.299978	0.292087	0.294498	0.299552	0.298781	0.301419	0.308011	0.314566

Table 2.7 Summary of Analytical Solution for  $\mu_d = 0.4$

**Average Peak Displacement, inch**

*Horizontal Peak Ground Acceleration, g*

<b>k</b>	<b>0.3</b>	<b>0.4</b>	<b>0.5</b>	<b>0.6</b>	<b>0.7</b>	<b>0.8</b>	<b>0.9</b>	<b>1</b>
<b>0</b>	0	0	0.027903	0.106349	0.294062	0.656252	1.177117	1.827146
<b>1/4</b>	0	0.006243	0.048001	0.192107	0.535539	1.179736	2.147652	3.48398
<b>1/3</b>	0	0.007759	0.062028	0.24896	0.695578	1.535042	2.761142	4.461842
<b>1/2</b>	0	0.014172	0.096248	0.39307	1.092654	2.33019	4.173504	6.637165

**Average Acceleration at which Peak Displacement Occurs, g**

*Horizontal Peak Ground Acceleration, g*

<b>k</b>	<b>0.3</b>	<b>0.4</b>	<b>0.5</b>	<b>0.6</b>	<b>0.7</b>	<b>0.8</b>	<b>0.9</b>	<b>1</b>
<b>0</b>	0.300000	0.400000	0.400013	0.400051	0.400132	0.400224	0.400508	0.400772
<b>1/4</b>	0.300000	0.396667	0.396252	0.397343	0.396613	0.399183	0.401645	0.40217
<b>1/3</b>	0.300000	0.396688	0.396227	0.39852	0.394437	0.398538	0.402789	0.402723
<b>1/2</b>	0.300000	0.395433	0.395374	0.392508	0.39626	0.396192	0.399953	0.400695

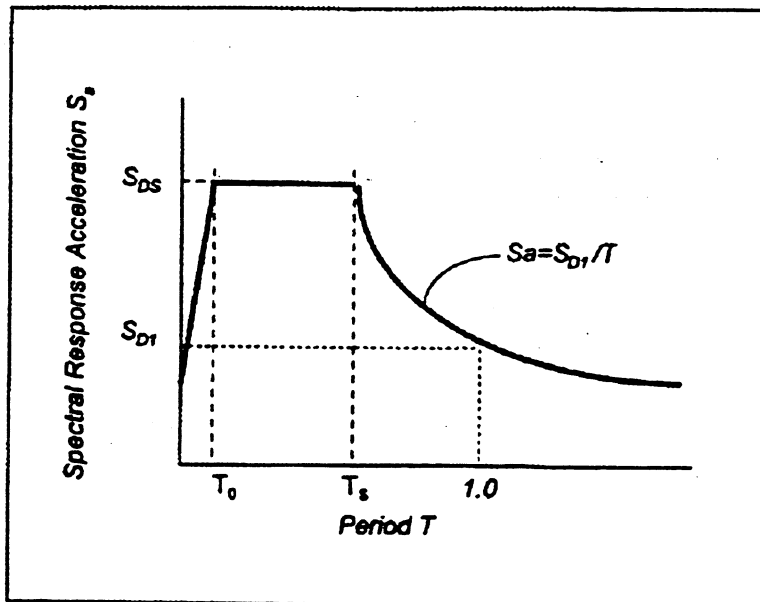


Figure 2.3 General Procedure Response Spectrum (NEHRP, 1997)

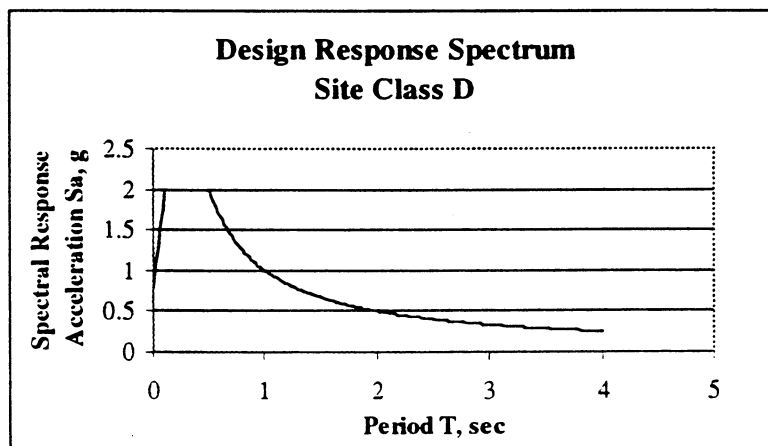


Figure 2.4 Generated Response Spectrum

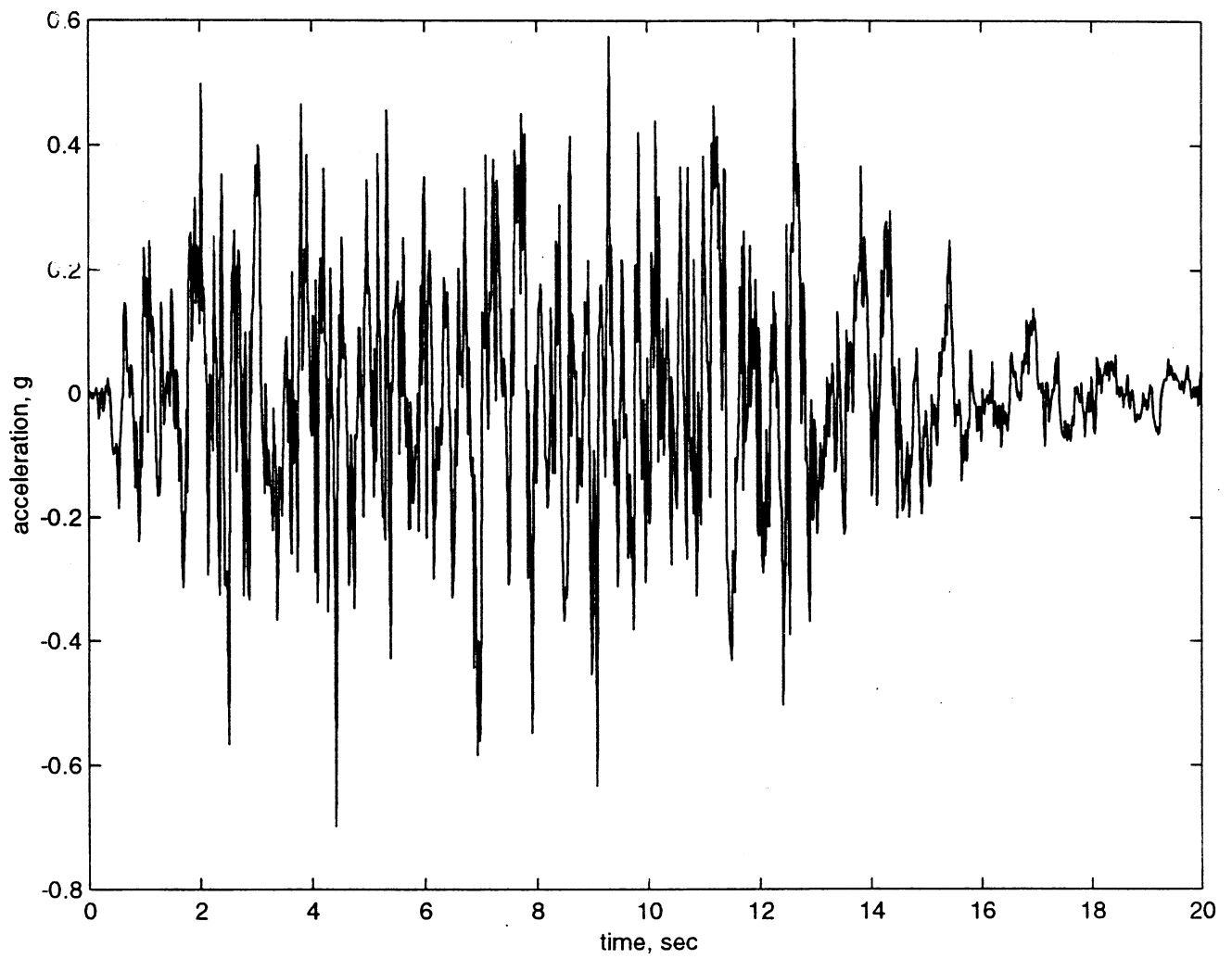


Figure 2.5 Generated Time History Input I : HPGA = 0.7g

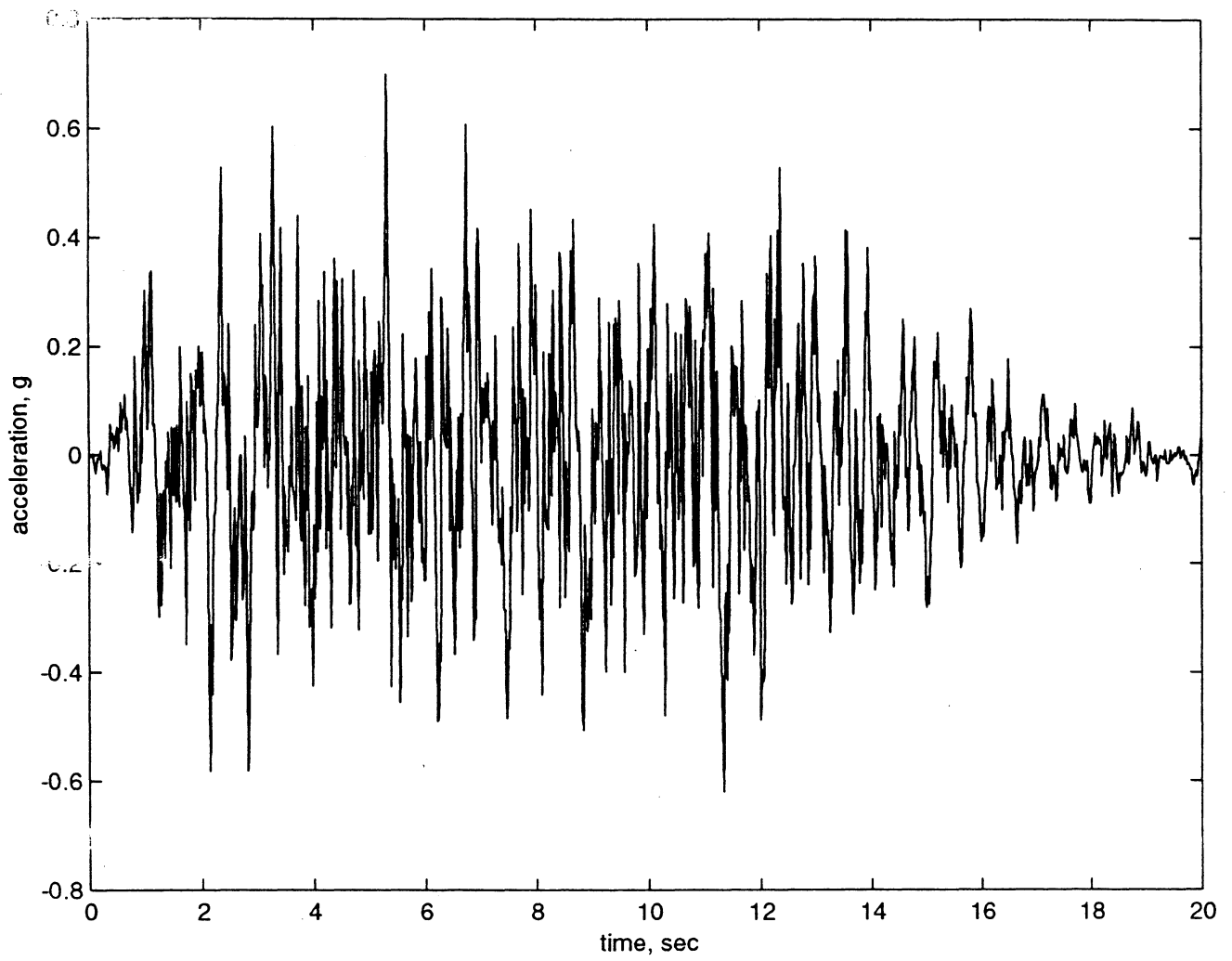


Figure 2.6 Generated Time History Input II : HPGA = 0.7g

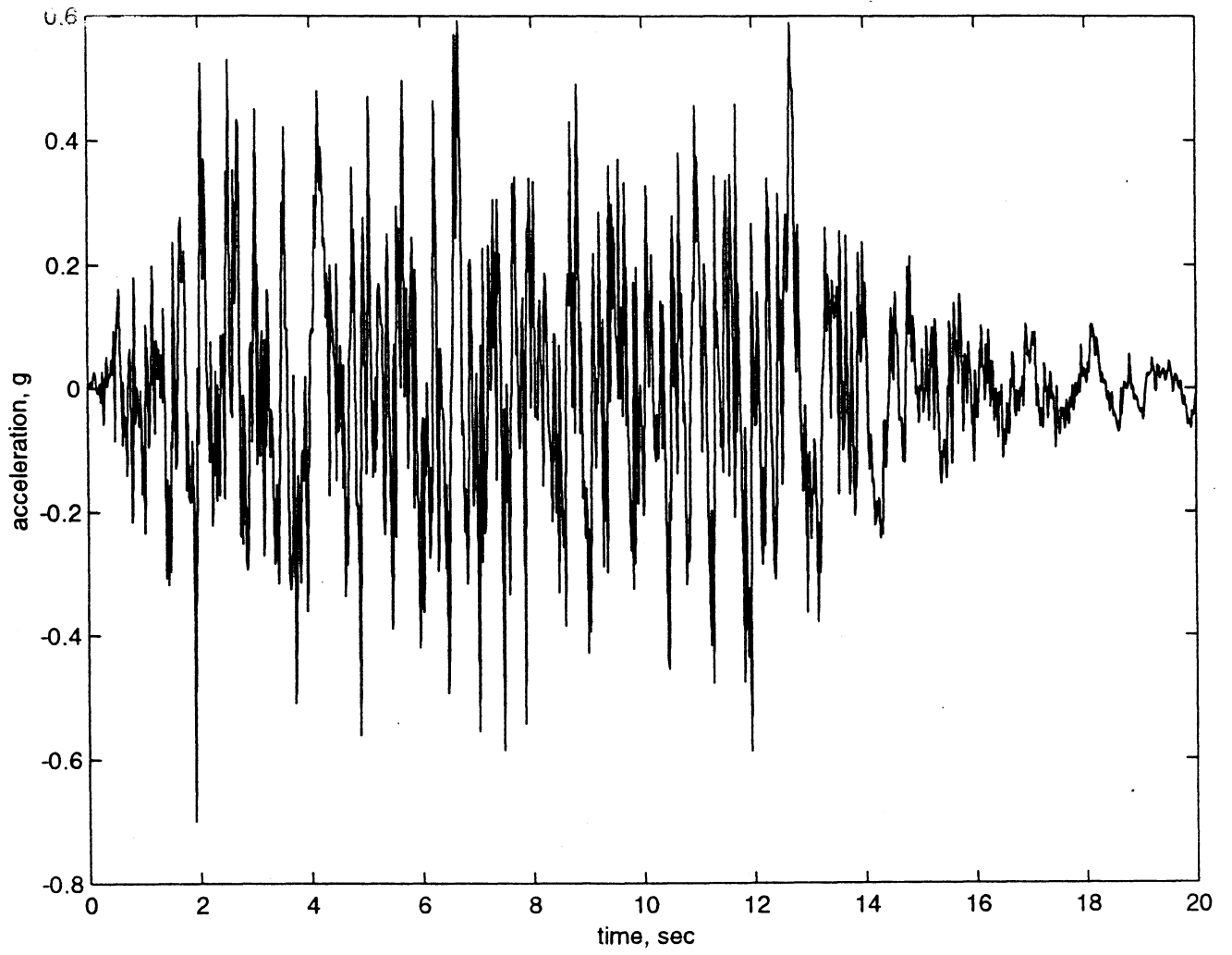


Figure 2.7 Generated Time History Input III : HPGA = 0.7g

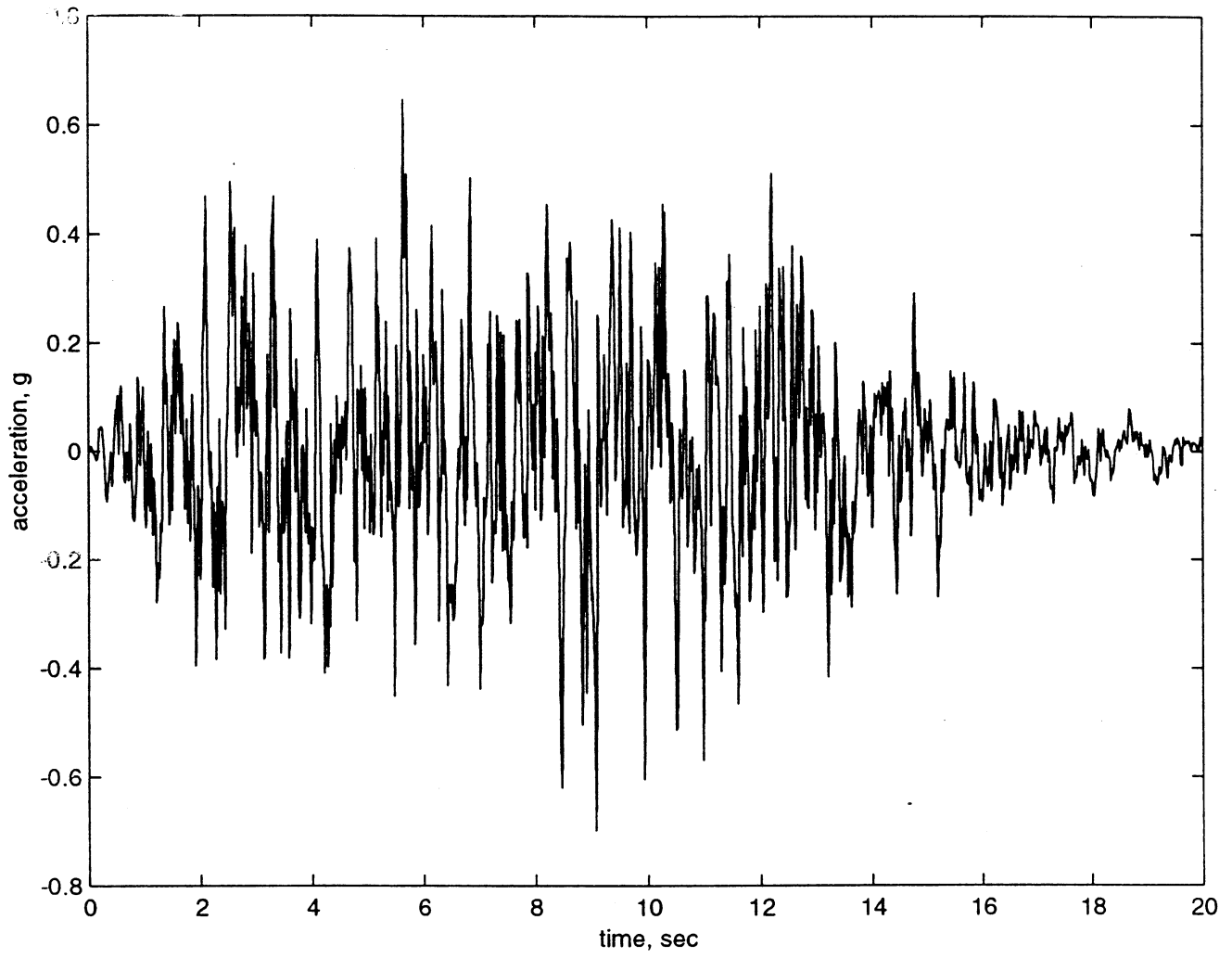


Figure 2.8 Generated Time History Input IV : HPGA = 0.7g



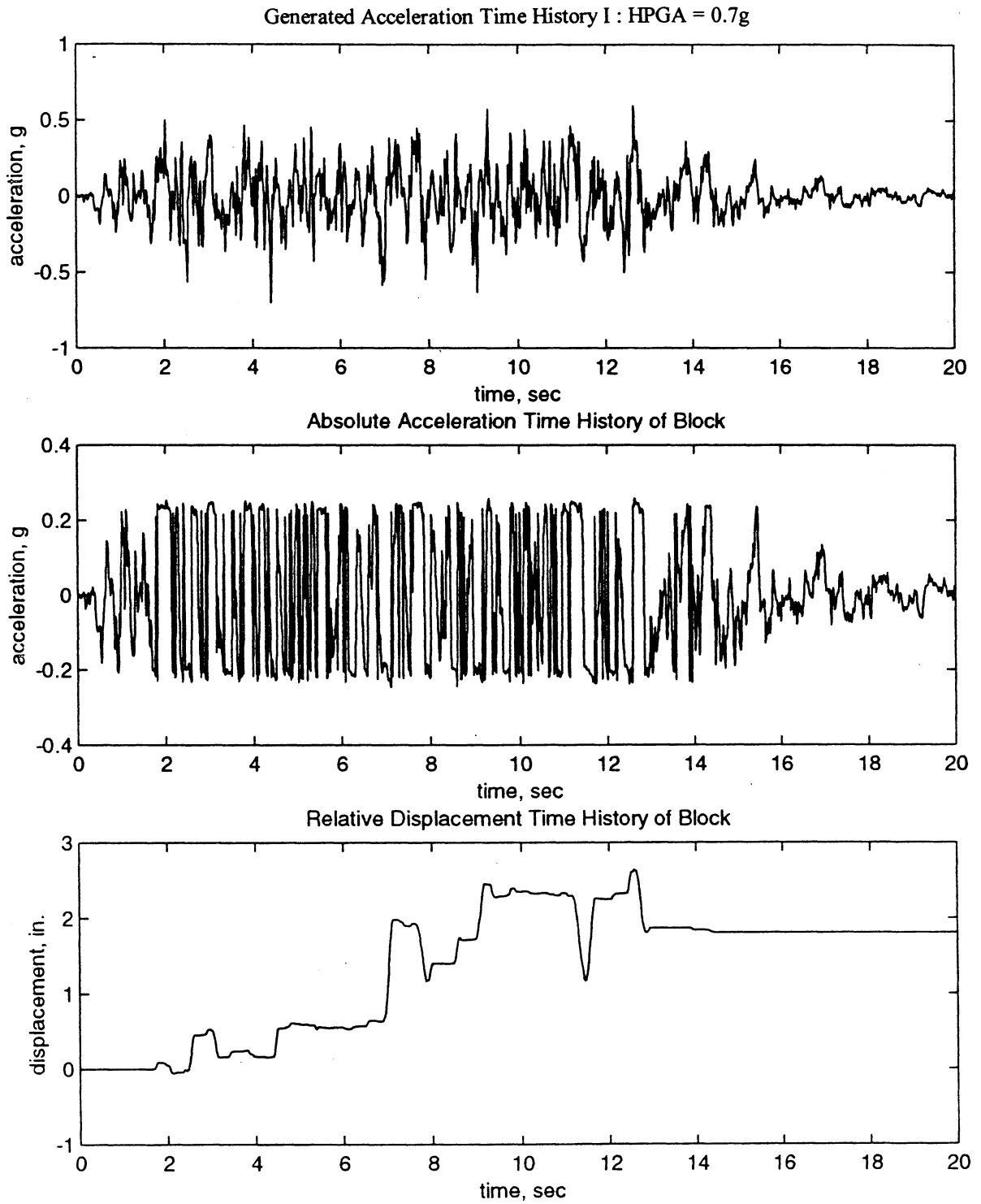


Figure 2.9 Analytical Solution I

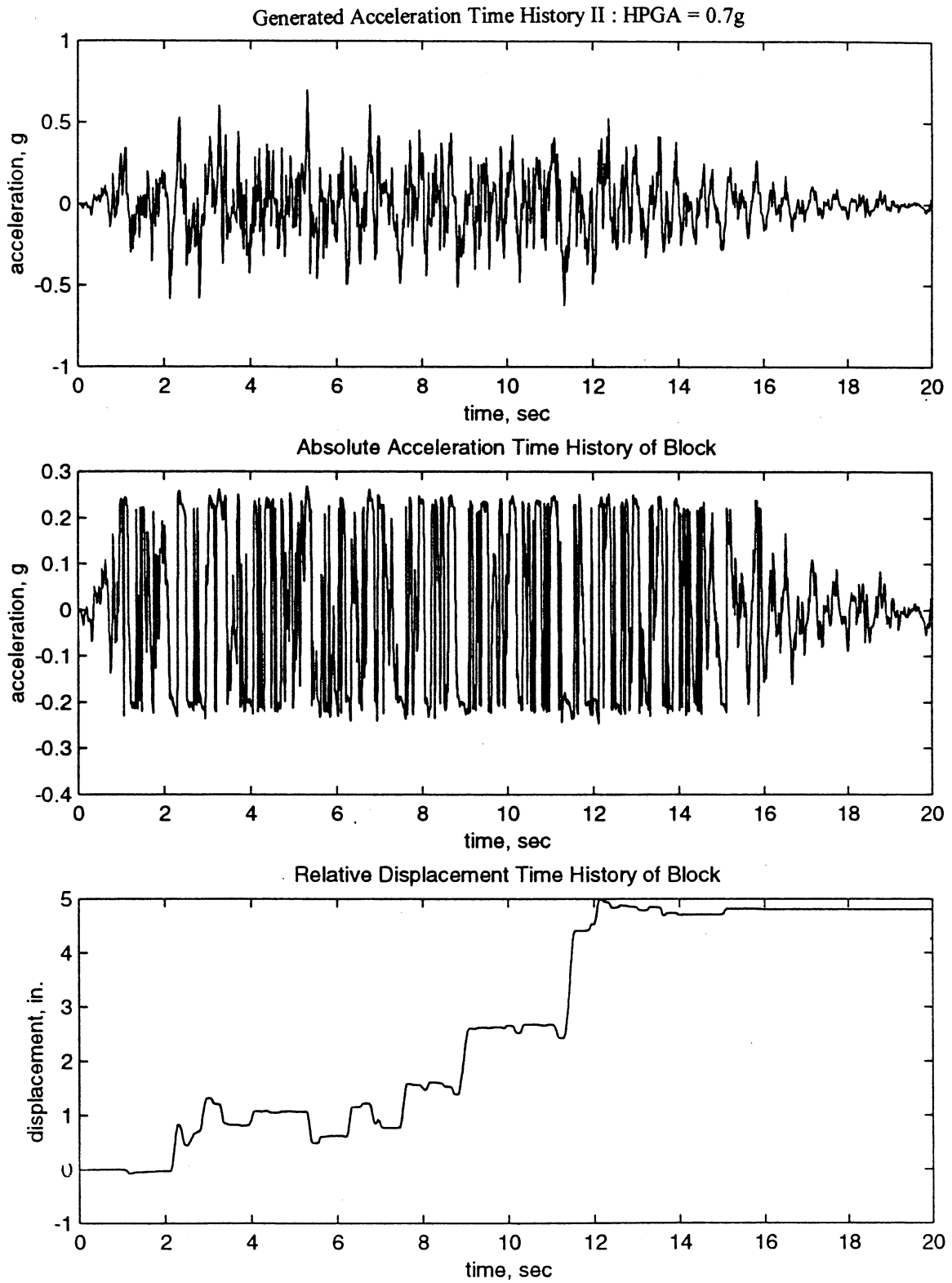


Figure 2.10 Analytical Solution II

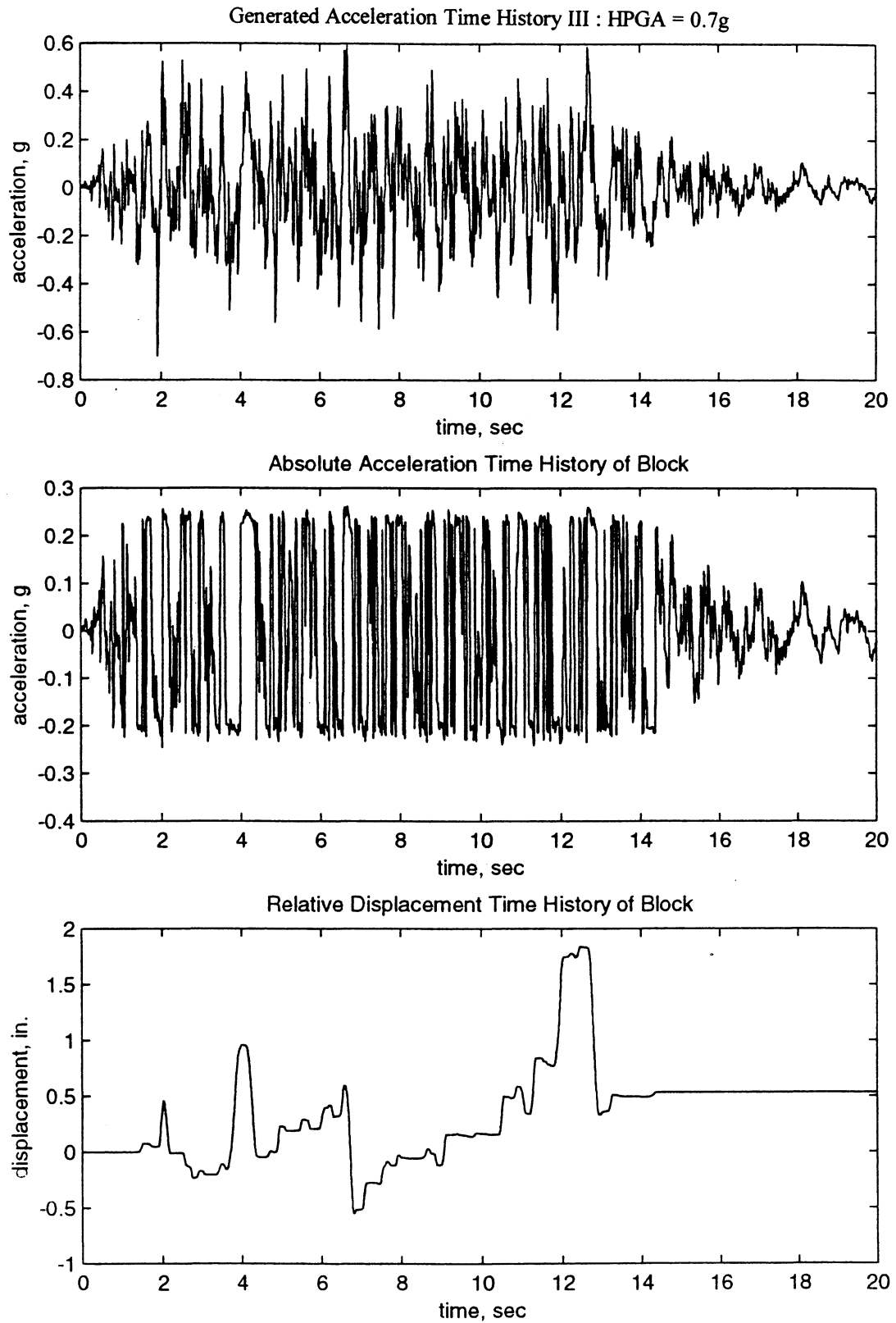


Figure 2.11 Analytical Solution III

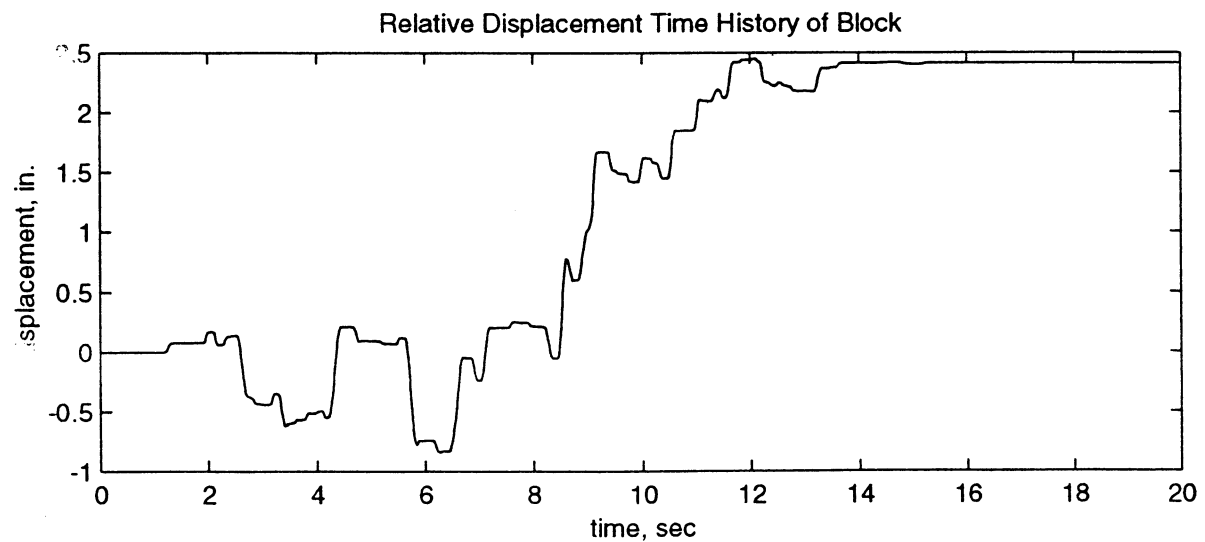
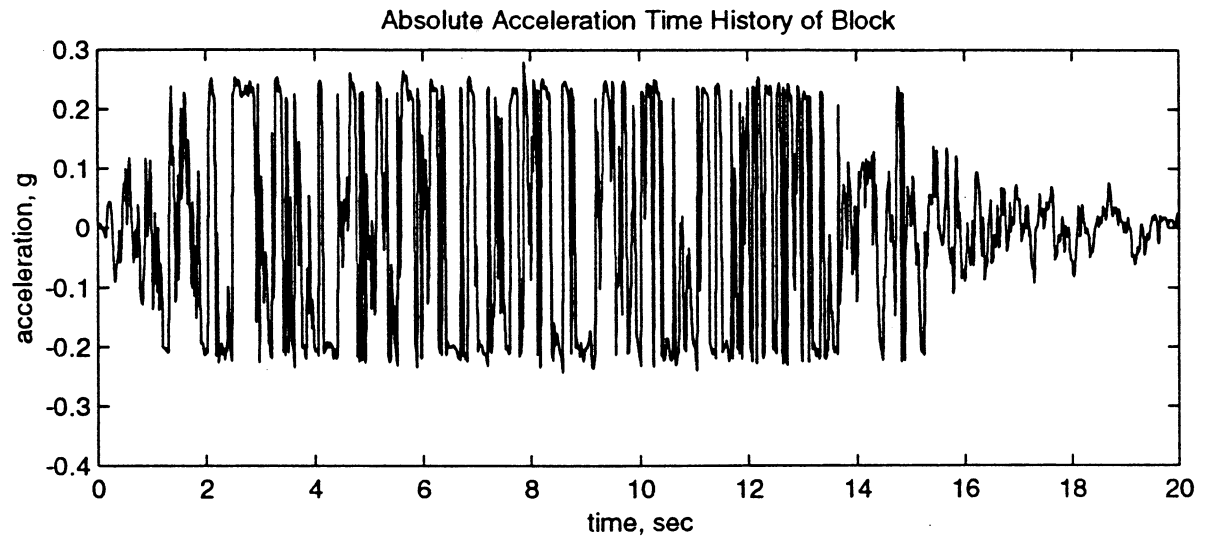
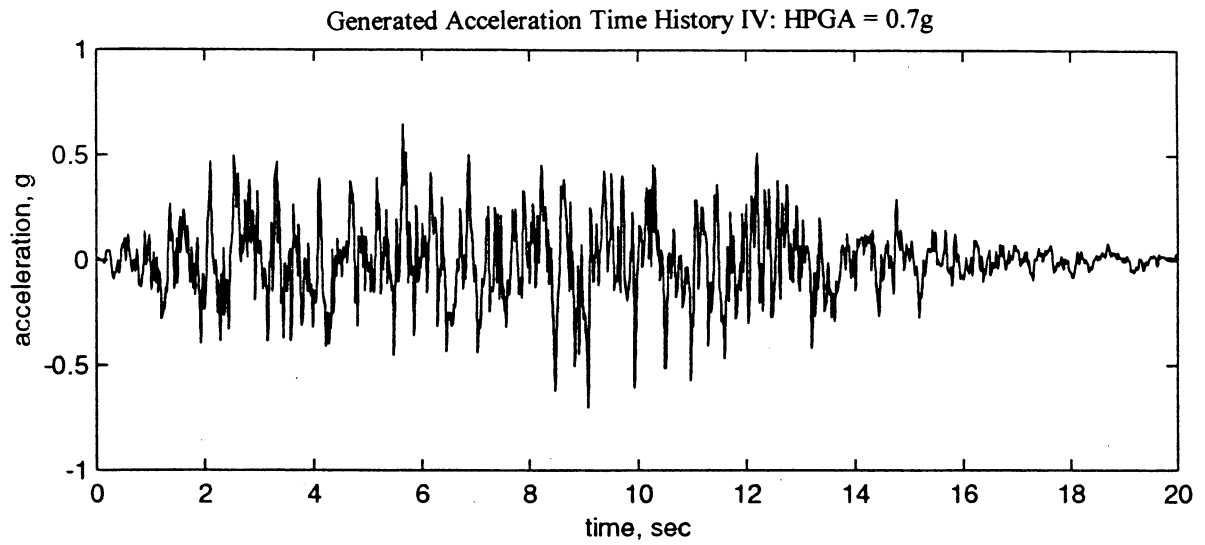


Figure 2.12 Analytical Solution IV

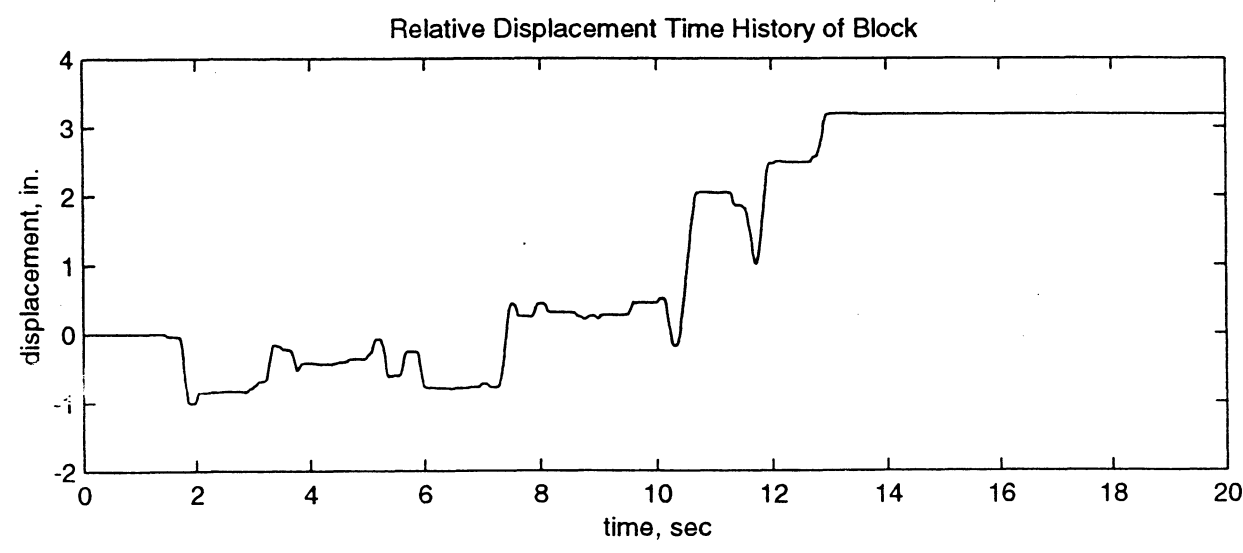
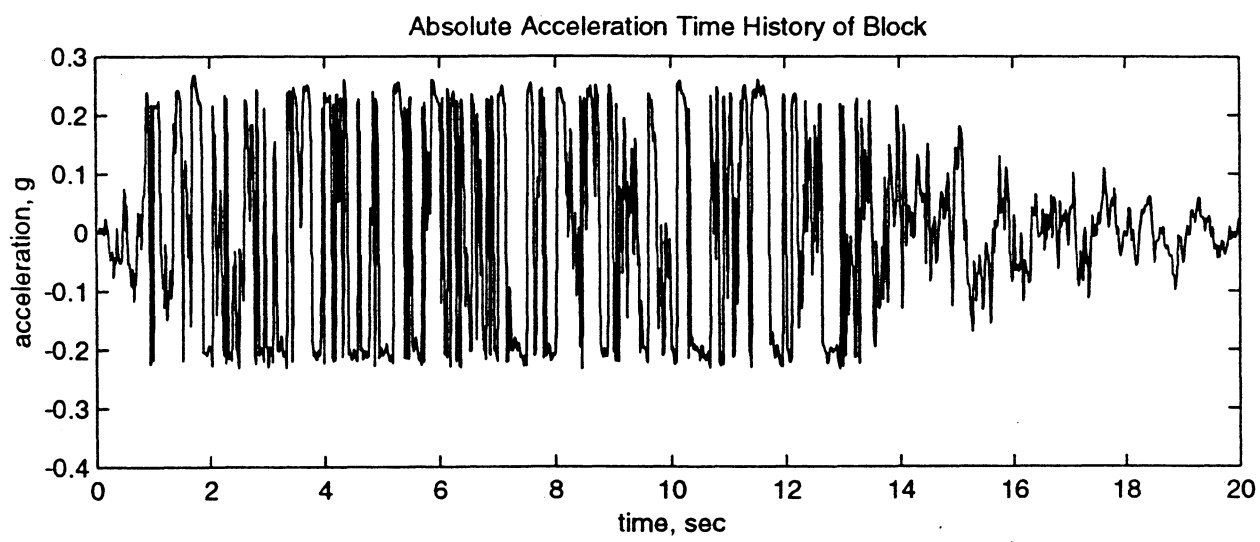
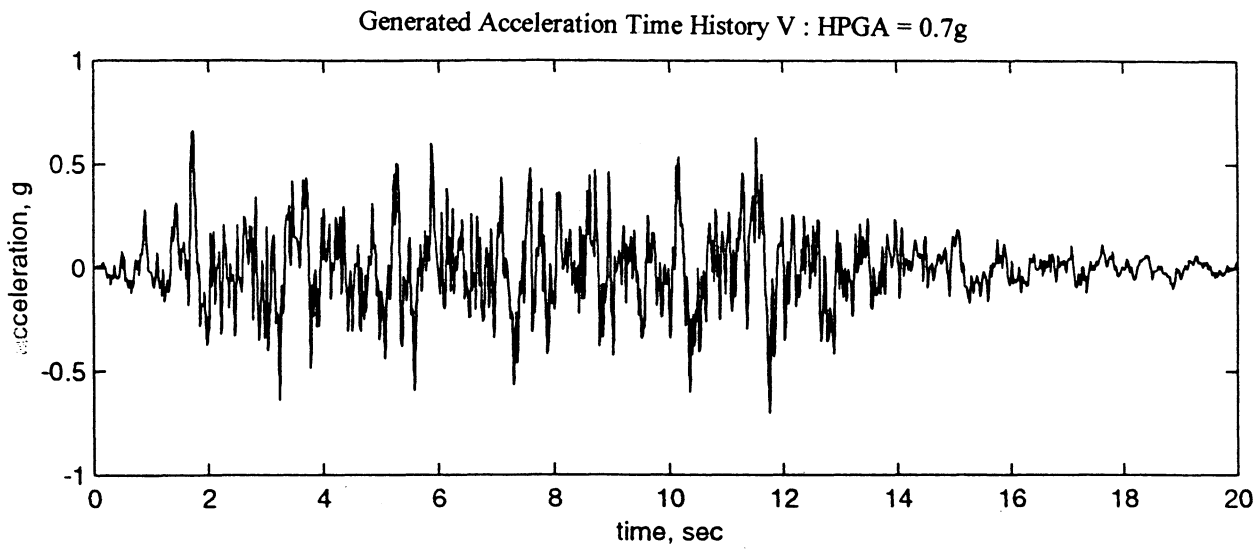


Figure 2.13 Analytical Solution V

The fragility curves for failure thresholds of 1 inch and 2 inches, for the four different coefficients of dynamic friction, (0.1,0.2,0.3,0.4) are shown in Figures 2.15~2.22. A comprehensive presentation of the probabilities of failure for all of the failure thresholds considered are shown in Tables 2.8~2.11.

### 2.5.3 Discussion of Results

There are three sensitive parameters that determine the sliding performance of a free-standing block-type equipment during an earthquake. They are the peak horizontal acceleration, peak vertical acceleration and coefficient of dynamic friction. As can be seen in Tables 2.4~2.7, every combination of HPGA and VPGA inputs has an almost same effect on the absolute acceleration for a given coefficient of dynamic friction. Thus, it is unnecessary to construct fragility curves for the failure threshold of the combination of relative displacement and the absolute acceleration at which threshold displacement occurs for a specific dynamic friction coefficient, as the fragility will always be either one or zero. On the other hand, as expected, the peak displacement increases as the vertical and horizontal peak accelerations increase.

As can be seen from the results, as  $k=0$ , the absolute peak accelerations for each peak ground acceleration are almost exactly the same and they are almost perfectly matched with the coefficient of dynamic friction. As for other  $k$  values, the absolute acceleration increases as the  $k\ddot{x}_g$  value increases, generally, but not significantly.

Although the magnitudes of HPGA and VPGA have no significant impact on the absolute acceleration at which threshold displacement occurs, but the coefficient of dynamic friction has. As the coefficient of dynamic friction increases, the peak displacement decreases, while the absolute acceleration increases, as shown in Figure 2.14.

As for the fragility curves, as the coefficient of dynamic friction increases, the probability of failure for a free-standing block-type equipment decreases under a specific threshold. As the vertical acceleration increases, under a specific horizontal acceleration, the free-standing block is more prone to failure.

Table 2.8 Analytical Probabilities of Failure for  $\mu_d = 0.1$

**k = 0**

**Maximum Sliding Distance, in.**

HPGA	0.1	0.2	0.5	0.75	1	2	2.5	3
0.3	1	1	0.833333	0.588889	0.277778	0.022222	0	0
0.4	1	1	1	0.988889	0.933333	0.455556	0.177778	0.088889
0.5	1	1	1	1	1	0.888889	0.677778	0.5
0.6	1	1	1	1	1	0.988889	0.966667	0.855556
0.7	1	1	1	1	1	1	1	0.988889
0.8	1	1	1	1	1	1	1	1
0.9	1	1	1	1	1	1	1	1
1	1	1	1	1	1	1	1	1

**k = 1/4**

**Maximum Sliding Distance, in.**

HPGA	0.1	0.2	0.5	0.75	1	2	2.5	3
0.3	1	1	0.866667	0.522222	0.322222	0.011111	0.011111	0
0.4	1	1	1	1	0.922222	0.455556	0.3	0.177778
0.5	1	1	1	1	1	0.9	0.722222	0.566667
0.6	1	1	1	1	1	1	0.977778	0.922222
0.7	1	1	1	1	1	1	1	1
0.8	1	1	1	1	1	1	1	1
0.9	1	1	1	1	1	1	1	1
1	1	1	1	1	1	1	1	1

**k = 1/3**

**Maximum Sliding Distance, in.**

HPGA	0.1	0.2	0.5	0.75	1	2	2.5	3
0.3	1	1	0.877778	0.533333	0.411111	0.022222	0.011111	0
0.4	1	1	1	1	0.966667	0.488889	0.333333	0.222222
0.5	1	1	1	1	1	0.911111	0.777778	0.6
0.6	1	1	1	1	1	1	0.966667	0.933333
0.7	1	1	1	1	1	1	1	1
0.8	1	1	1	1	1	1	1	1
0.9	1	1	1	1	1	1	1	1
1	1	1	1	1	1	1	1	1

**k = 1/2**

**Maximum Sliding Distance, in.**

HPGA	0.1	0.2	0.5	0.75	1	2	2.5	3
0.3	1	1	0.877778	0.666667	0.488889	0.066667	0.011111	0
0.4	1	1	1	0.977778	0.977778	0.611111	0.477778	0.322222
0.5	1	1	1	1	1	0.944444	0.877778	0.766667
0.6	1	1	1	1	1	1	0.977778	0.911111
0.7	1	1	1	1	1	1	0.988889	0.988889
0.8	1	1	1	1	1	1	1	1
0.9	1	1	1	1	1	1	1	1
1	1	1	1	1	1	1	1	1

Table 2.9 Analytical Probabilities of Failure for  $\mu_d = 0.2$

**k = 0**

**Maximum Sliding Distance, in.**

HPGA	0.1	0.2	0.5	0.75	1	2	2.5	3
0.3	0.1	0	0	0	0	0	0	0
0.4	0.944444	0.744444	0.144444	0	0	0	0	0
0.5	1	1	0.8	0.622222	0.322222	0.033333	0	0
0.6	1	1	1	0.944444	0.833333	0.3	0.122222	0.077778
0.7	1	1	1	1	0.977778	0.711111	0.488889	0.355556
0.8	1	1	1	1	1	0.944444	0.822222	0.655556
0.9	1	1	1	1	1	0.988889	0.955556	0.9
1	1	1	1	1	1	1	0.988889	0.988889

**k = 1/4**

**Maximum Sliding Distance, in.**

HPGA	0.1	0.2	0.5	0.75	1	2	2.5	3
0.3	0.144444	0.022222	0	0	0	0	0	0
0.4	0.988889	0.822222	0.211111	0.077778	0.011111	0	0	0
0.5	1	1	0.9	0.677778	0.488889	0.1	0.011111	0.011111
0.6	1	1	1	0.966667	0.9	0.5	0.366667	0.222222
0.7	1	1	1	1	0.977778	0.833333	0.622222	0.533333
0.8	1	1	1	1	1	0.977778	0.933333	0.822222
0.9	1	1	1	1	1	1	1	0.966667
1	1	1	1	1	1	1	1	1

**k = 1/3**

**Maximum Sliding Distance, in.**

HPGA	0.1	0.2	0.5	0.75	1	2	2.5	3
0.3	0.188889	0.033333	0	0	0	0	0	0
0.4	0.988889	0.8	0.355556	0.122222	0.044444	0	0	0
0.5	1	1	0.9	0.733333	0.6	0.144444	0.077778	0.011111
0.6	1	1	1	0.977778	0.877778	0.611111	0.466667	0.311111
0.7	1	1	1	1	1	0.866667	0.811111	0.7
0.8	1	1	1	1	1	0.955556	0.911111	0.888889
0.9	1	1	1	1	1	1	0.977778	0.944444
1	1	1	1	1	1	1	1	1

**k = 1/2**

**Maximum Sliding Distance, in.**

HPGA	0.1	0.2	0.5	0.75	1	2	2.5	3
0.3	0.377778	0.1	0	0	0	0	0	0
0.4	0.988889	0.955556	0.544444	0.266667	0.122222	0	0	0
0.5	1	1	0.977778	0.933333	0.777778	0.333333	0.155556	0.1
0.6	1	1	1	1	0.977778	0.8	0.7	0.588889
0.7	1	1	1	1	1	0.966667	0.955556	0.855556
0.8	1	1	1	1	1	1	0.977778	0.966667
0.9	1	1	1	1	1	1	1	1
1	1	1	1	1	1	1	1	1



Table 2.10 Analytical Probabilities of Failure for  $\mu_d = 0.3$

**k = 0**

Maximum Sliding Distance, in.

HPGA	0.1	0.2	0.5	0.75	1	2	2.5	3
0.3	0	0	0	0	0	0	0	0
0.4	0.011111	0	0	0	0	0	0	0
0.5	0.777778	0.3	0	0	0	0	0	0
0.6	1	0.888889	0.377778	0.144444	0.055556	0	0	0
0.7	1	1	0.888889	0.688889	0.444444	0.044444	0	0
0.8	1	1	0.966667	0.933333	0.833333	0.255556	0.144444	0.077778
0.9	1	1	1	1	0.977778	0.666667	0.466667	0.288889
1	1	1	1	1	1	0.866667	0.755556	0.6

**k = 1/4**

Maximum Sliding Distance, in.

HPGA	0.1	0.2	0.5	0.75	1	2	2.5	3
0.3	0	0	0	0	0	0	0	0
0.4	0.1	0.011111	0	0	0	0	0	0
0.5	0.822222	0.5	0.077778	0.011111	0	0	0	0
0.6	1	0.933333	0.588889	0.388889	0.222222	0	0	0
0.7	1	1	0.944444	0.844444	0.688889	0.255556	0.133333	0.088889
0.8	1	1	1	0.977778	0.911111	0.644444	0.511111	0.377778
0.9	1	1	1	1	0.988889	0.855556	0.8	0.688889
1	1	1	1	1	1	0.966667	0.877778	0.866667

**k = 1/3**

Maximum Sliding Distance, in.

HPGA	0.1	0.2	0.5	0.75	1	2	2.5	3
0.3	0	0	0	0	0	0	0	0
0.4	0.133333	0.011111	0	0	0	0	0	0
0.5	0.9	0.633333	0.133333	0.033333	0	0	0	0
0.6	1	0.988889	0.777778	0.522222	0.333333	0.022222	0	0
0.7	1	1	0.988889	0.933333	0.844444	0.411111	0.222222	0.133333
0.8	1	1	1	0.988889	0.977778	0.788889	0.7	0.533333
0.9	1	1	1	1	1	0.966667	0.877778	0.788889
1	1	1	1	1	1	0.988889	0.966667	0.966667

**k = 1/2**

Maximum Sliding Distance, in.

HPGA	0.1	0.2	0.5	0.75	1	2	2.5	3
0.3	0	0	0	0	0	0	0	0
0.4	0.322222	0.055556	0	0	0	0	0	0
0.5	0.988889	0.888889	0.311111	0.1	0.033333	0	0	0
0.6	1	1	0.988889	0.855556	0.655556	0.122222	0.022222	0
0.7	1	1	1	1	0.988889	0.733333	0.566667	0.4
0.8	1	1	1	1	1	0.988889	0.955556	0.877778
0.9	1	1	1	1	1	0.988889	0.988889	0.988889
1	1	1	1	1	1	1	1	1

Table 2.11 Analytical Probabilities of Failure for  $\mu_d = 0.4$

**k = 0**

**Maximum Sliding Distance, in.**

HPGA	0.1	0.2	0.5	0.75	1	2	2.5	3
0.3	0	0	0	0	0	0	0	0
0.4	0	0	0	0	0	0	0	0
0.5	0.011111	0	0	0	0	0	0	0
0.6	0.422222	0.088889	0	0	0	0	0	0
0.7	0.933333	0.666667	0.122222	0	0	0	0	0
0.8	1	0.944444	0.666667	0.333333	0.155556	0	0	0
0.9	1	1	0.922222	0.744444	0.555556	0.1	0.022222	0
1	1	1	1	0.966667	0.822222	0.333333	0.166667	0.122222

**k = 1/4**

**Maximum Sliding Distance, in.**

HPGA	0.1	0.2	0.5	0.75	1	2	2.5	3
0.3	0	0	0	0	0	0	0	0
0.4	0	0	0	0	0	0	0	0
0.5	0.066667	0.011111	0	0	0	0	0	0
0.6	0.711111	0.377778	0.033333	0	0	0	0	0
0.7	0.966667	0.9	0.444444	0.188889	0.1	0	0	0
0.8	1	0.988889	0.888889	0.688889	0.566667	0.122222	0.044444	0
0.9	1	1	0.977778	0.933333	0.911111	0.488889	0.322222	0.188889
1	1	1	1	0.988889	0.988889	0.811111	0.7	0.577778

**k = 1/3**

**Maximum Sliding Distance, in.**

HPGA	0.1	0.2	0.5	0.75	1	2	2.5	3
0.3	0	0	0	0	0	0	0	0
0.4	0	0	0	0	0	0	0	0
0.5	0.188889	0.011111	0	0	0	0	0	0
0.6	0.855556	0.511111	0.1	0.011111	0	0	0	0
0.7	1	0.966667	0.655556	0.4	0.177778	0	0	0
0.8	1	1	0.988889	0.9	0.755556	0.211111	0.111111	0.044444
0.9	1	1	1	0.988889	0.966667	0.733333	0.533333	0.366667
1	1	1	1	1	1	0.944444	0.9	0.788889

**k = 1/2**

**Maximum Sliding Distance, in.**

HPGA	0.1	0.2	0.5	0.75	1	2	2.5	3
0.3	0	0	0	0	0	0	0	0
0.4	0	0	0	0	0	0	0	0
0.5	0.355556	0.077778	0	0	0	0	0	0
0.6	0.988889	0.788889	0.255556	0.088889	0.011111	0	0	0
0.7	1	1	0.955556	0.733333	0.522222	0.055556	0	0
0.8	1	1	1	1	0.988889	0.588889	0.344444	0.2
0.9	1	1	1	1	1	0.988889	0.922222	0.8
1	1	1	1	1	1	1	1	0.988889

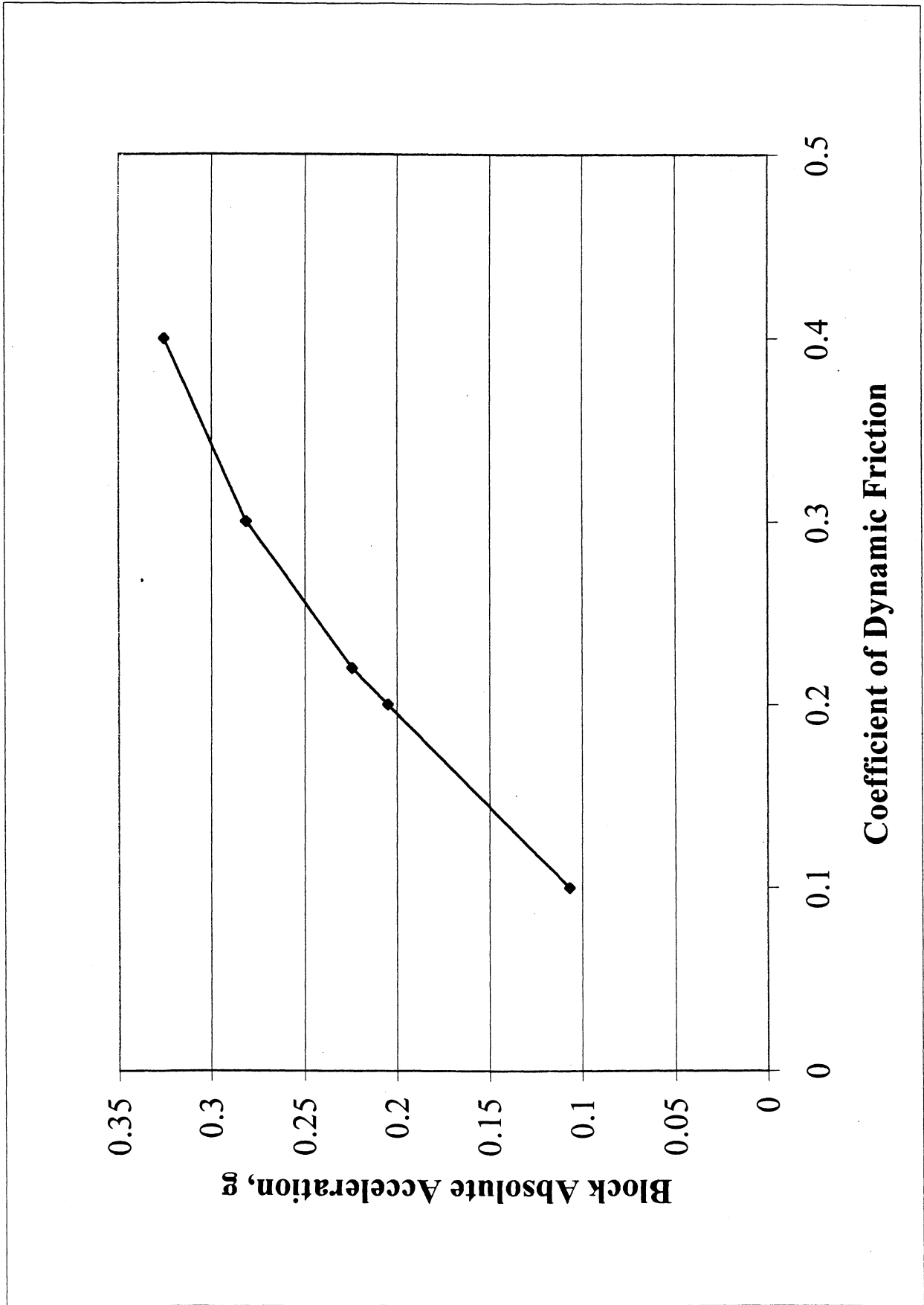


Figure 2.14 Effect of Dynamic Friction Coefficient on the Acceleration-at-which-Threshold-Displacement-Occur

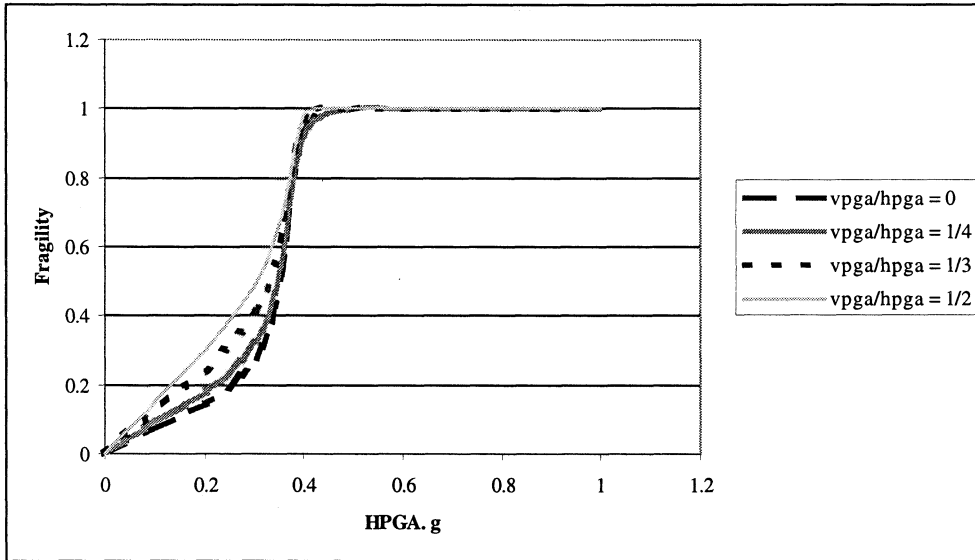


Figure 2.15 Fragility Curves for  $\mu_d = 0.1$ ; Failure Threshold = 1 inch

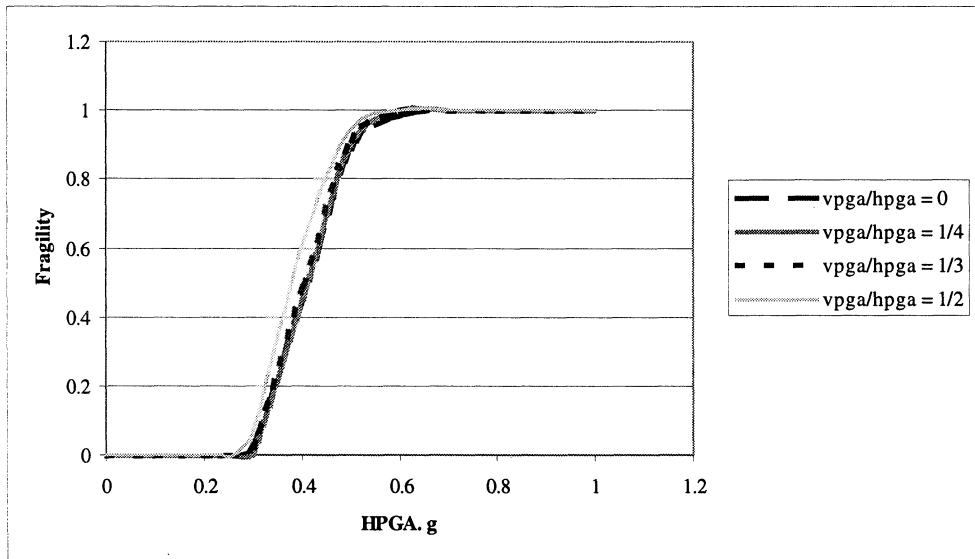


Figure 2.16 Fragility Curves for  $\mu_d = 0.1$ ; Failure Threshold = 2 inches

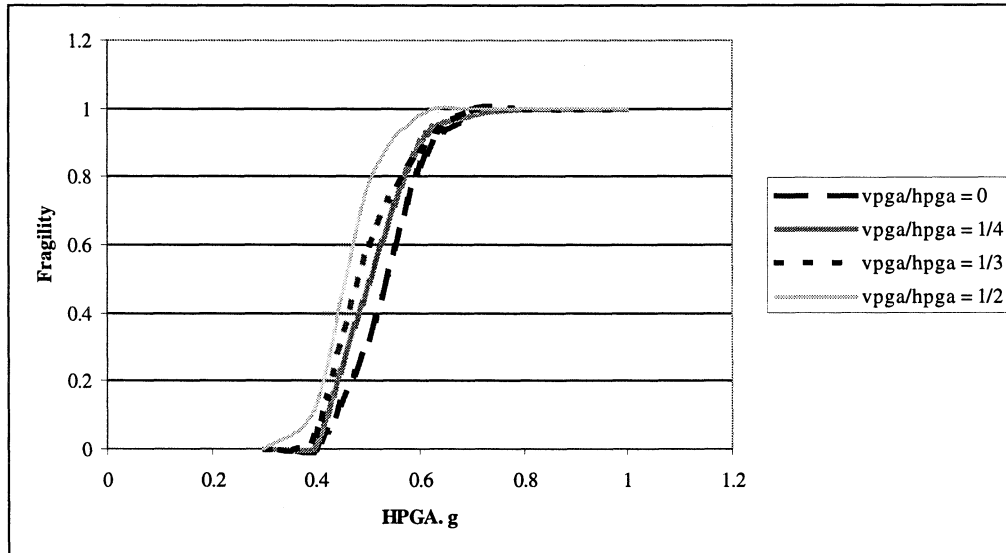


Figure 2.17 Fragility Curves for  $\mu_d = 0.2$  ; Failure Threshold = 1 inch

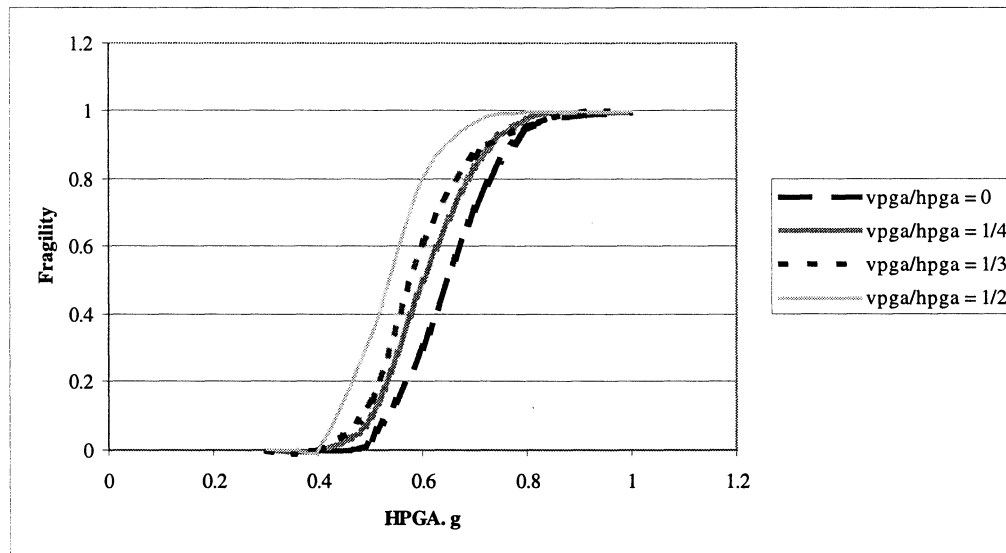


Figure 2.18 Fragility Curves for  $\mu_d = 0.2$  ; Failure Threshold = 2 inches

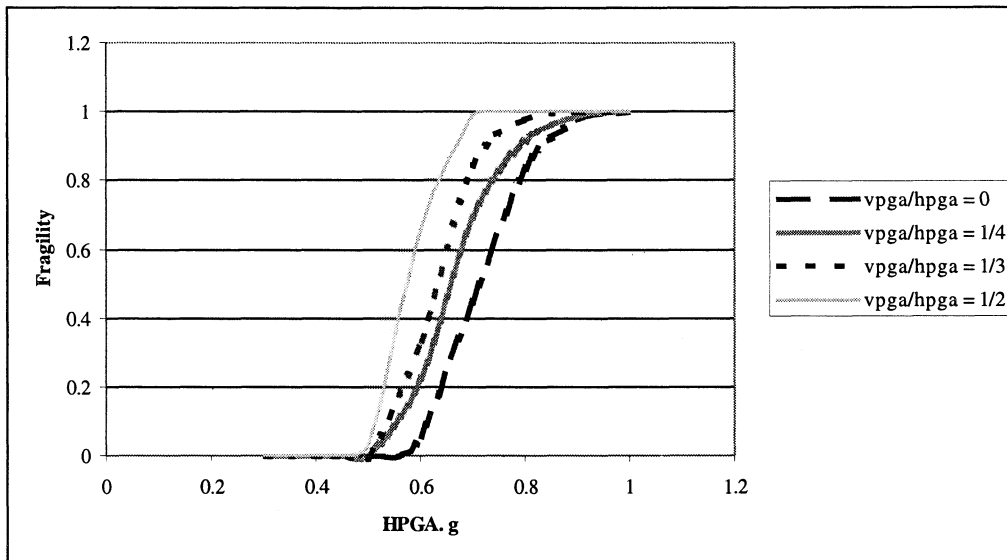


Figure 2.19 Fragility Curves for  $\mu_d = 0.3$ ; Failure Threshold = 1 inch

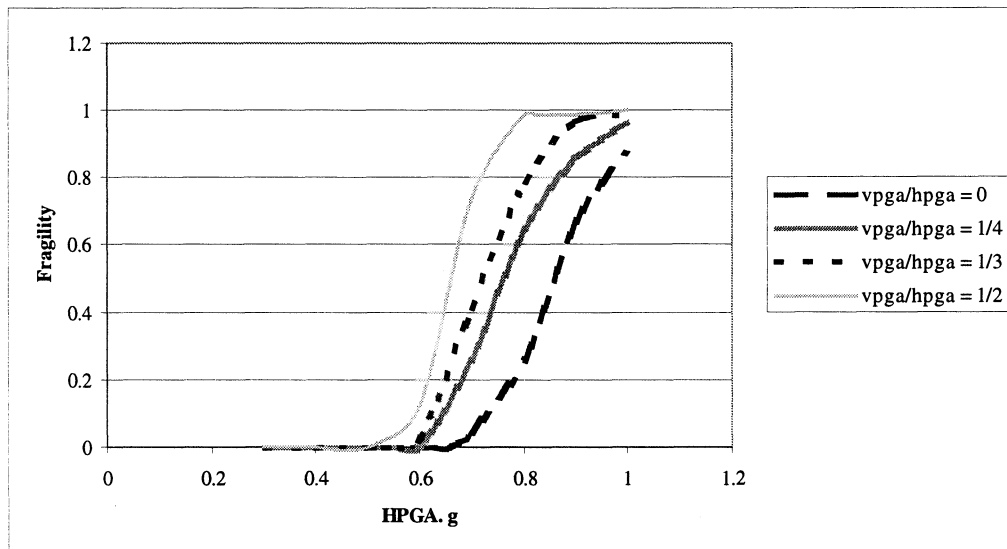


Figure 2.20 Fragility Curves for  $\mu_d = 0.3$ ; Failure Threshold = 2 inches

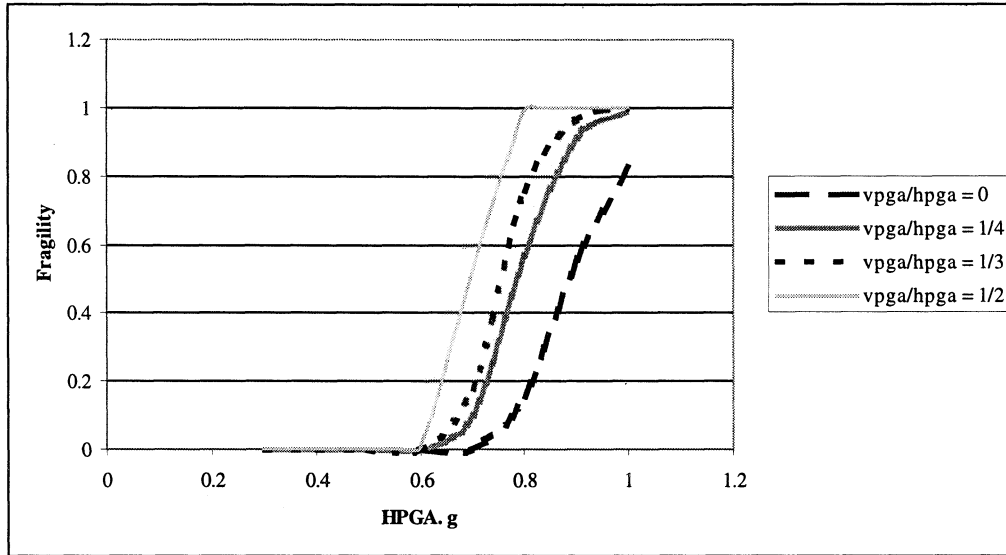


Figure 2.21 Fragility Curves for  $\mu_d = 0.4$  ; Failure Threshold = 1 inch

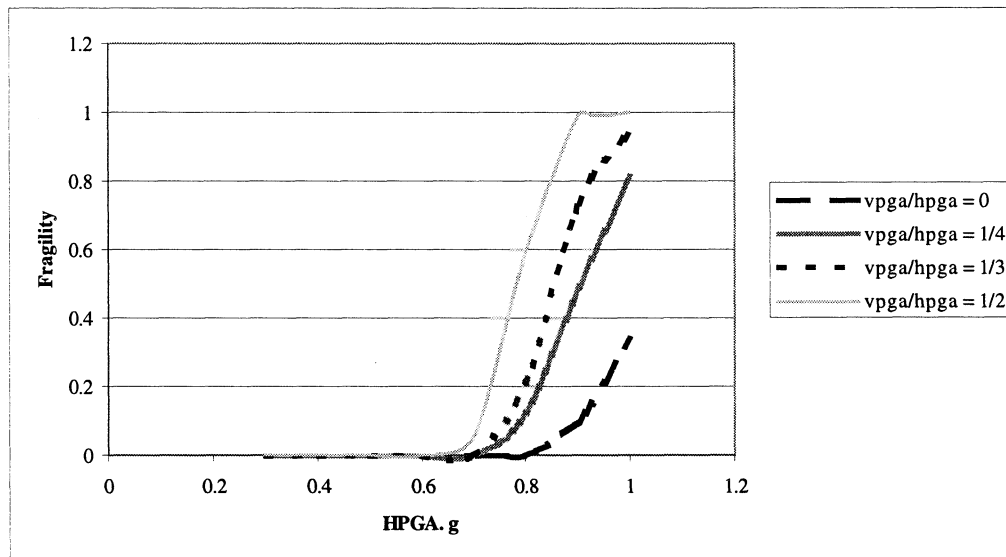


Figure 2.22 Fragility Curves for  $\mu_d = 0.4$  ; Failure Threshold = 2 inches

## **SECTION 3**

### **EXPERIMENTS FOR SLIDING PROBLEM**

The basic objective of the experiments described in this chapter was to investigate the sliding response of a free-standing rigid block under seismic loading in order to verify the validity of the analytical solution described in Section 2. The sliding motion of a rigid block against the surface of a raised floor was tested on a shaking table using five randomly chosen earthquake time histories. In addition, two different friction tests were conducted to determine the static coefficient of friction of the two sliding surfaces for a quantitative comparison of the experimental and analytical results. This comparison will later be described in the end of this section.

#### **3.1 Test Set-Up**

The experiments were set-up on a shaking table, which provides the earthquake motion. The free standing rigid block was tested on a 1.83 m x 1.83 m ( 6 ft x 6 ft ) raised floor surface that was fixed on top of a concrete slab attached to the shaking table, shown in Figure 3.1. Five randomly chosen earthquake time histories were used as the earthquake inputs, with a scale of 0.3g~0.7g of peak ground acceleration (PGA) in the horizontal direction and four proportional scales of the horizontal acceleration, ranging between 0~1, in the vertical direction. Displacement and acceleration measurements were of interest in these experiments.

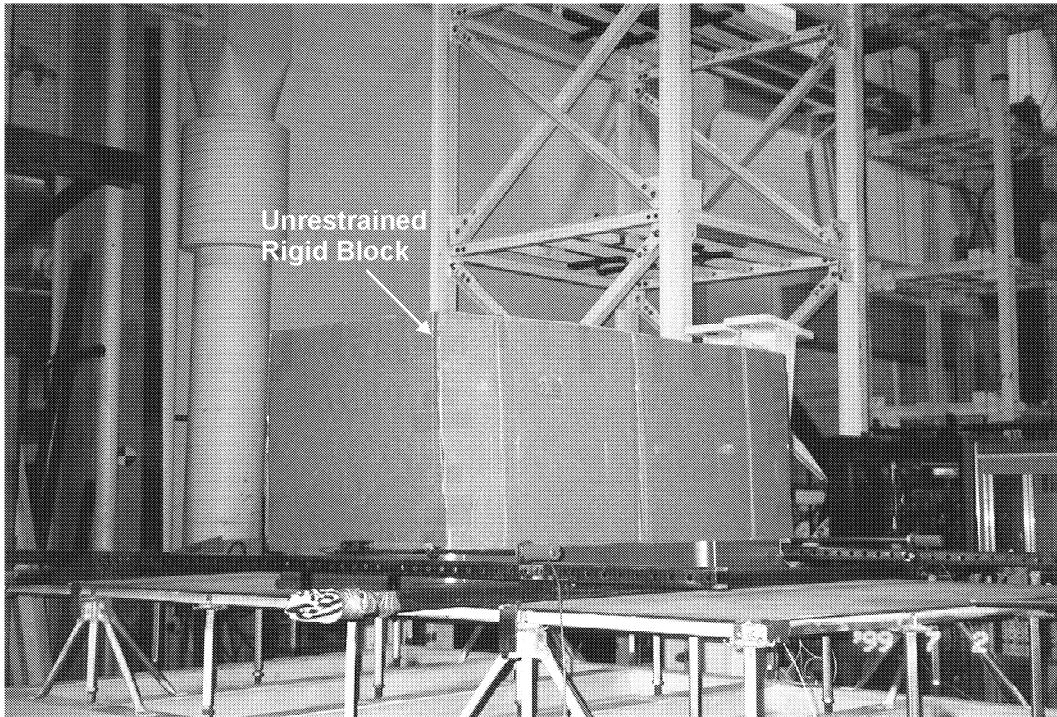
##### **3.1.1 The Shaking Table**

The shaking table has a dimension of 3.66 m x 3.66 m (12 ft x 12 ft) with a capacity of 50 mtons (110 kips). It has a total of five degrees of freedom (DOF) with three programmable DOFs (horizontal, vertical, and roll) and the other two DOFs corrected for cross coupling only. The system has two horizontal actuators with a capacity of 32 mtons (70 kips), which can provide a maximum horizontal acceleration of 0.625 g with maximum payload. Four vertical actuators with a total capacity of 100 mtons (220 kips) can accelerate the system to 1.05 g at maximum payload. With lighter payloads, the system can produce larger accelerations (up to 4.0g horizontally and 8.0g vertically). A schematic sketch of the system is shown in Figure 3.2 (Kosar et al., 1993).

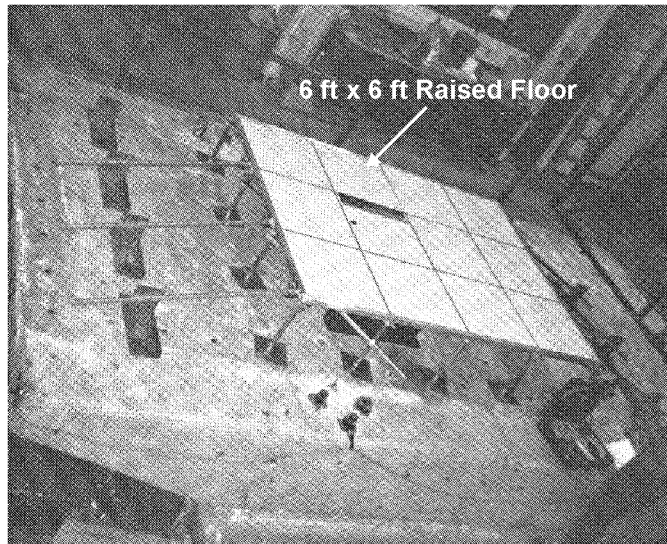
##### **3.1.2 The Sliding Surfaces**

The two sliding surfaces used in the experiments were a raised floor surface, shown in Figure 3.1(b), and the surface of a free-standing rigid block. Two steel bars were placed closely to the sides of the rigid block to prevent any rotation to occur while the block was sliding. In addition, two more steel bars were placed perpendicular to the sliding direction of the rigid block to prevent the block from falling off the edge of the raised floor when the relative displacement was too large. The descriptions above are clearly shown in Figure 3.3.





(a)



(b)

Figure 3.1 Shaking Table and Experimental Set-up

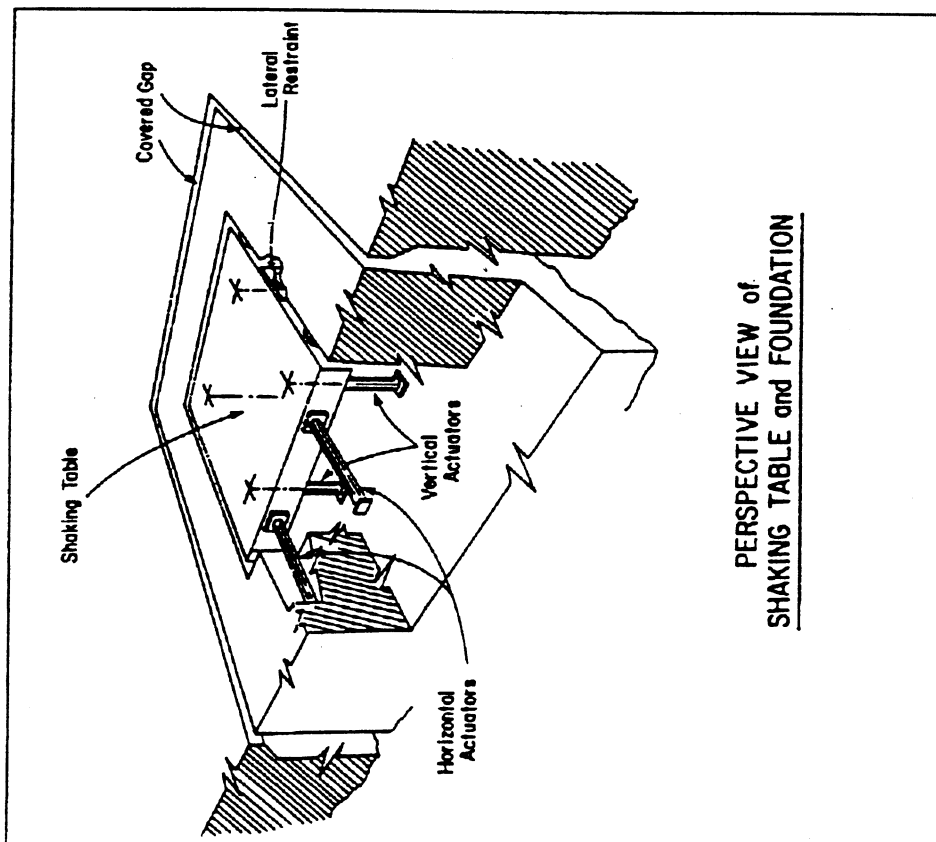
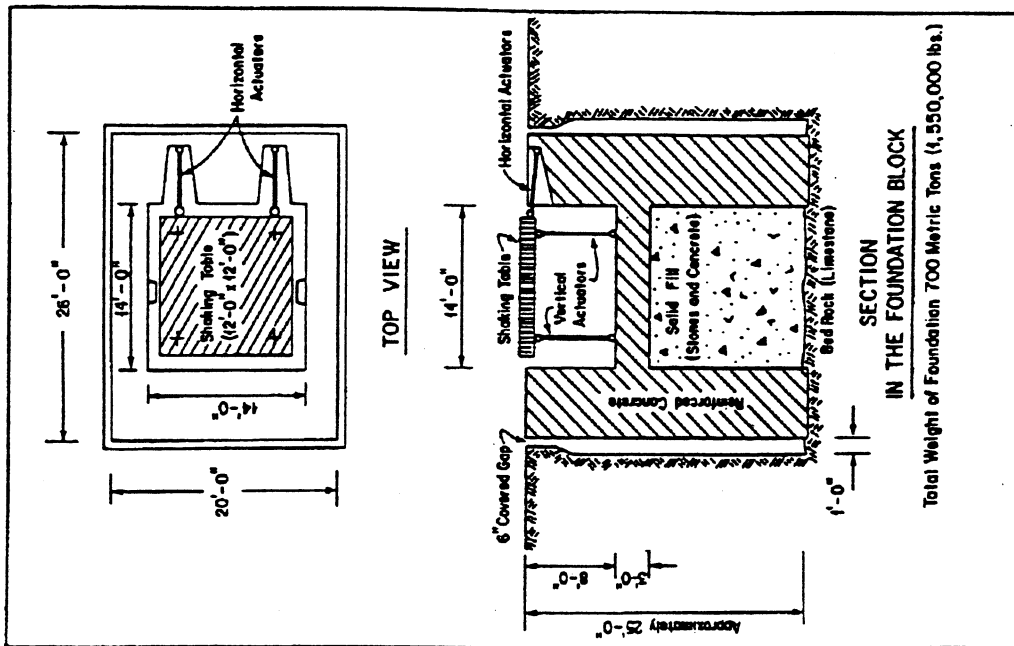
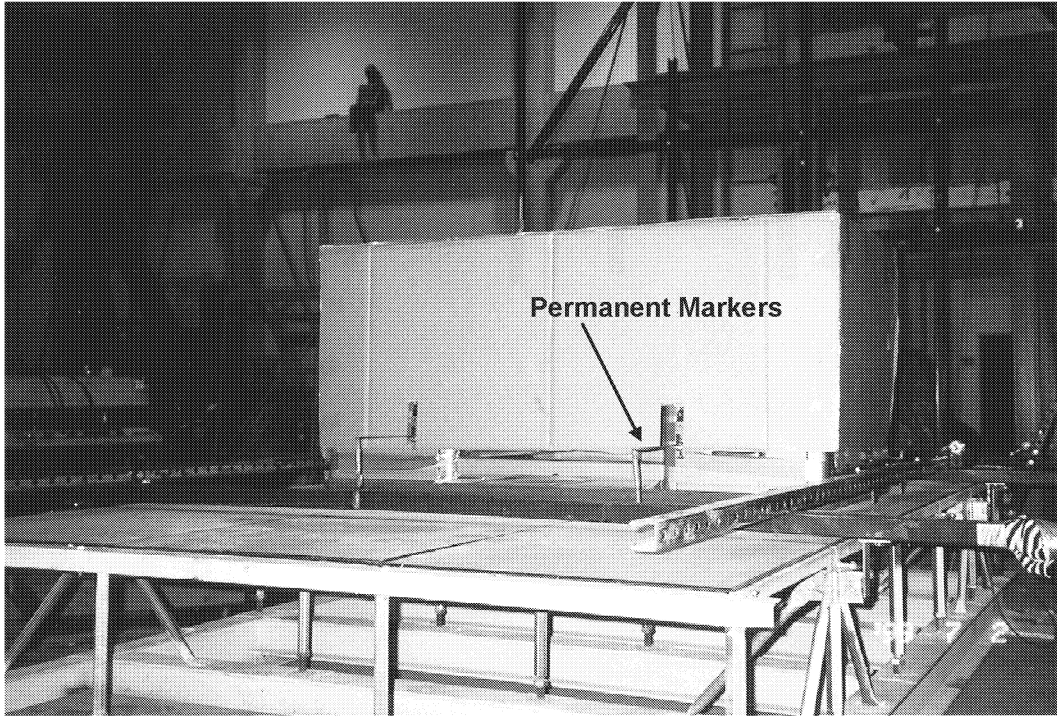
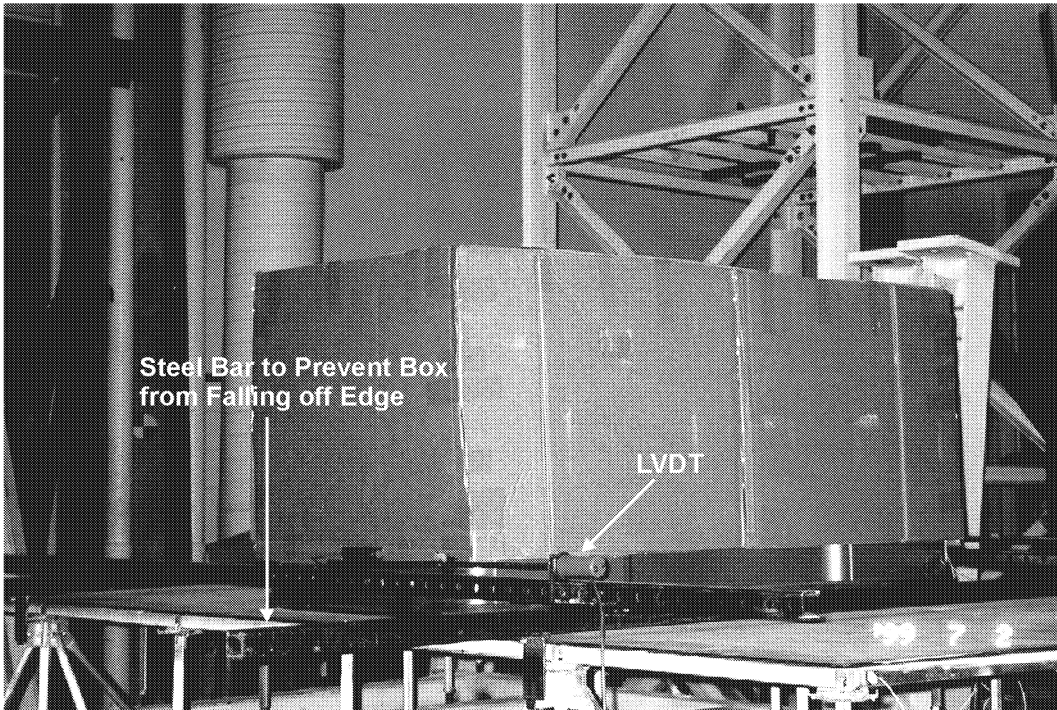


Figure 3.2 Schematic Sketch of Shaking Table System (Kosar, et al., 1993)



(a)



(b)

Figure 3.3 Steel Bars to Constrain Sliding Performance

### 3.1.3 Instrumentation

Horizontal and vertical acceleration measurements using accelerometers were made at several locations on the shaking table, the raised floor, and the free standing rigid block. The placements and designations for the accelerometers attached to the block are shown in Figure 3.4. For all measurements, the sampling rate was set at 100 samples/second.

The horizontal displacements of the block were measured by Temposonic displacement transducers ( LVDT ) as well as two permanent markers attached to the left and right side on the surface facing the sliding direction. The locations of the Temposonic transducers attached to the sliding block are shown in Figure 3.5. Figure 3.6 shows the locations of the permanent markers.

### 3.1.4 Acceleration Time History Inputs

Five acceleration time histories representing some typical past earthquakes were randomly chosen as excitation inputs in these experiments. The particular earthquake inputs selected were El Centro, Taft, Pacoima, Kobe, and Northridge earthquake records. They are shown in Figure 3.7~3.11.

Horizontal and vertical accelerations were considered in these experiments. There were five HPGAs being considered in the experiments. They are, namely, 0.3g, 0.4g, 0.5g, 0.6g, and 0.7g. Due to displacement limitations of the shaking table, the HPGA being tested can only be increased up to a maximum acceleration of 0.7g. As for the VPGA, four different scale factors were used to represent them in terms of HPGA. They were 0,  $\frac{1}{4}$ ,  $\frac{1}{3}$ ,  $\frac{1}{2}$ . For each HPGA, these four different VPGA values were applied, individually, with the horizontal acceleration. Three repeated tests, from the same earthquake input, were conducted for most of the combinations of horizontal and vertical accelerations. Some combinations were only tested for two runs due to the constraints experienced during the experiments. Table 3.1, presented in Section 3.3, shows all the combinations of horizontal and vertical accelerations and the number of tests conducted for each combination.

Table 3.1 Number of Runs for Each Combination of HPGA and VPGA in Experiment

Proportional Constants for Vertical PGA	Horizontal PGA, g				
	0.3	0.4	0.5	0.6	0.7
0	10	10	13	13	11
$\frac{1}{4}$	10	10	13	13	11
$\frac{1}{3}$	10	10	13	13	11
$\frac{1}{2}$	10	10	13	13	11
<b>TOTAL</b>	<b>40</b>	<b>40</b>	<b>52</b>	<b>52</b>	<b>44</b>

\* there are five different time history inputs used in each combination of horizontal and vertical PGA.

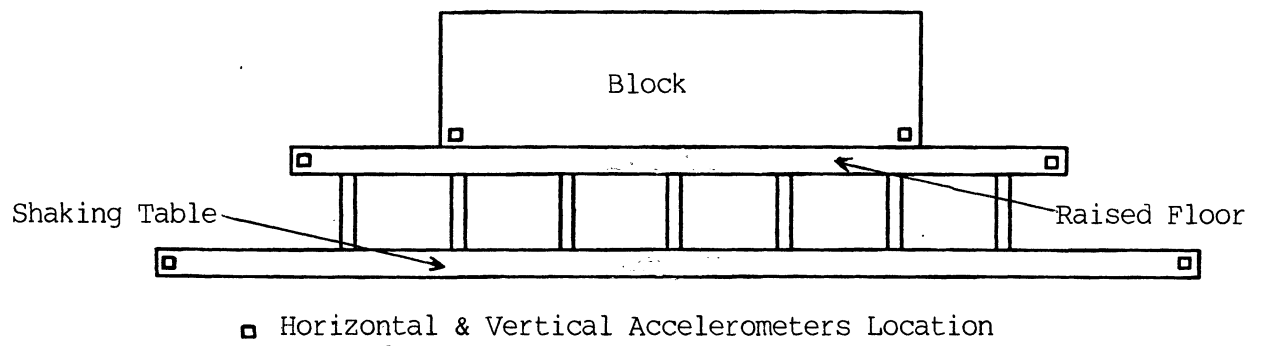


Figure 3.4(a) Locations of Horizontal and Vertical Accelerometers



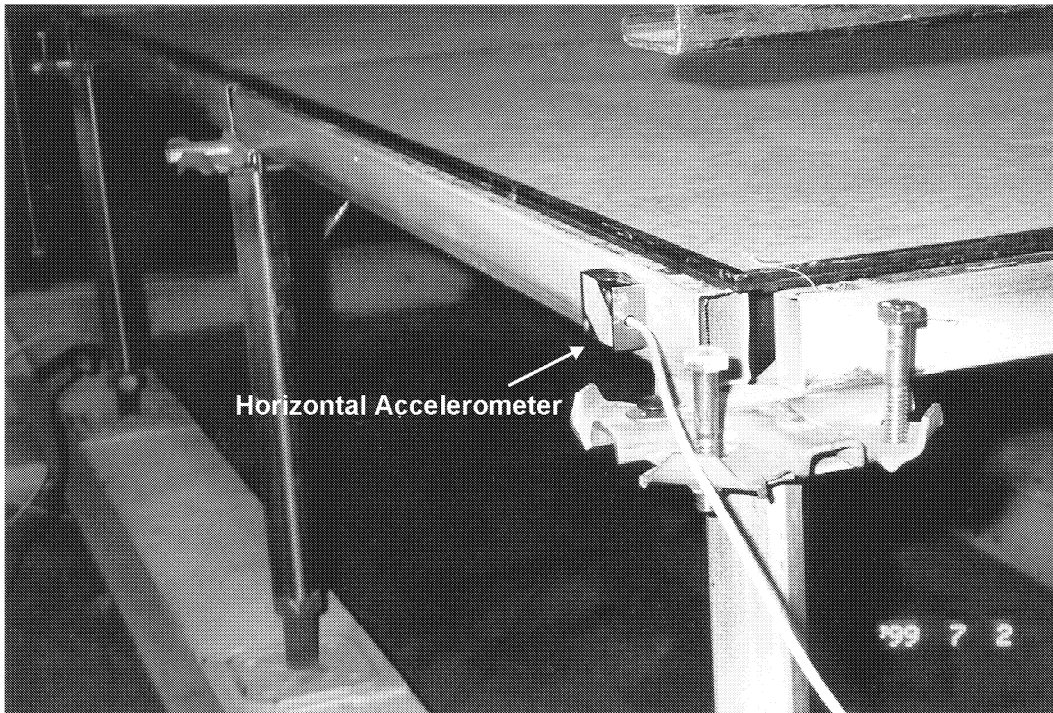


Figure 3.4(b) Location of Horizontal Accelerometer

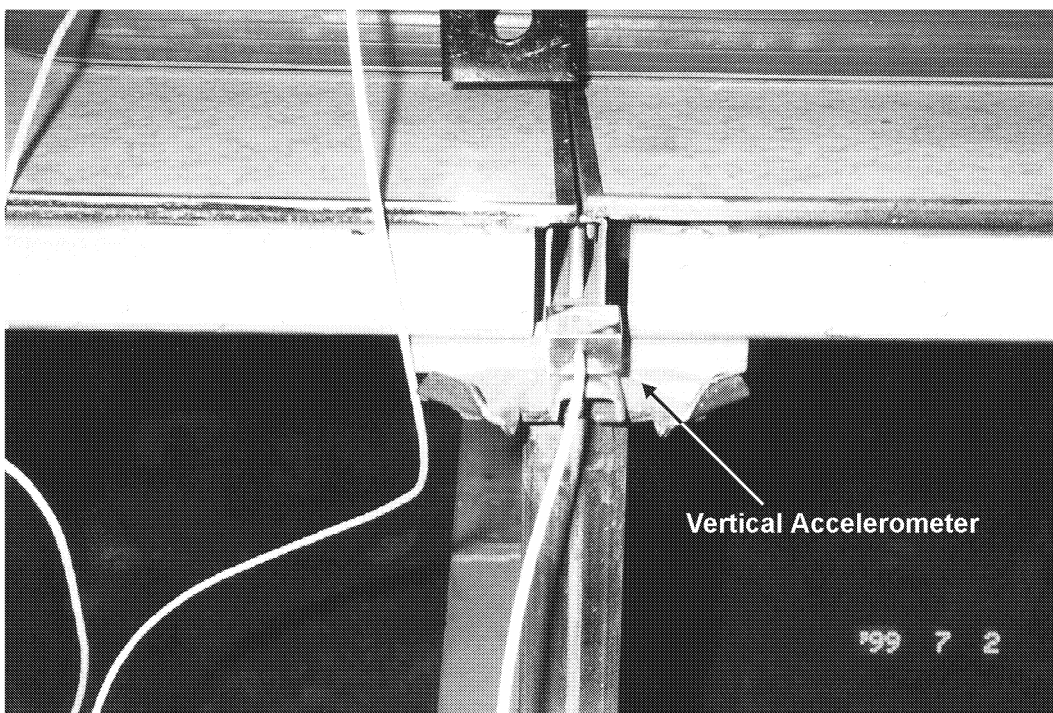


Figure 3.4(c) Location of Vertical Accelerometer

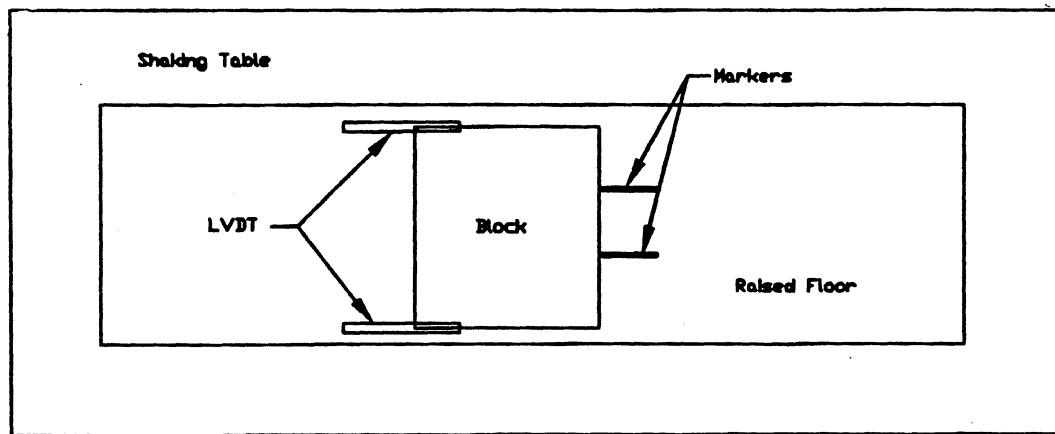


Figure 3.5(a) Locations of Horizontal LVDT and Markers

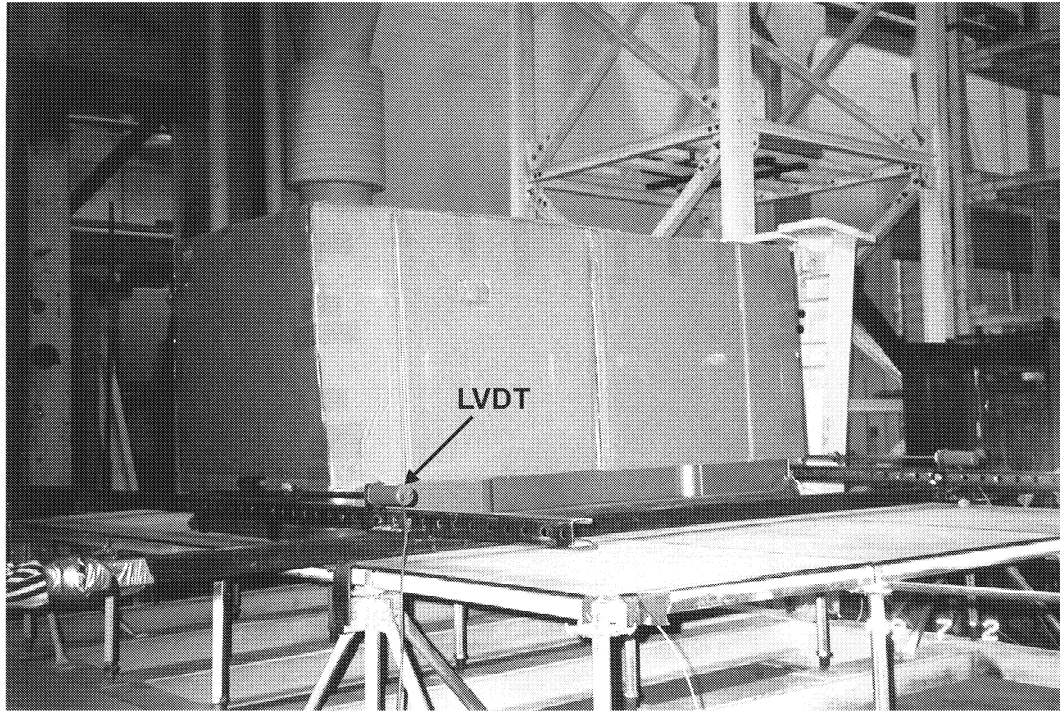


Figure 3.5(b) Front View of Rigid Block with LVDT attached

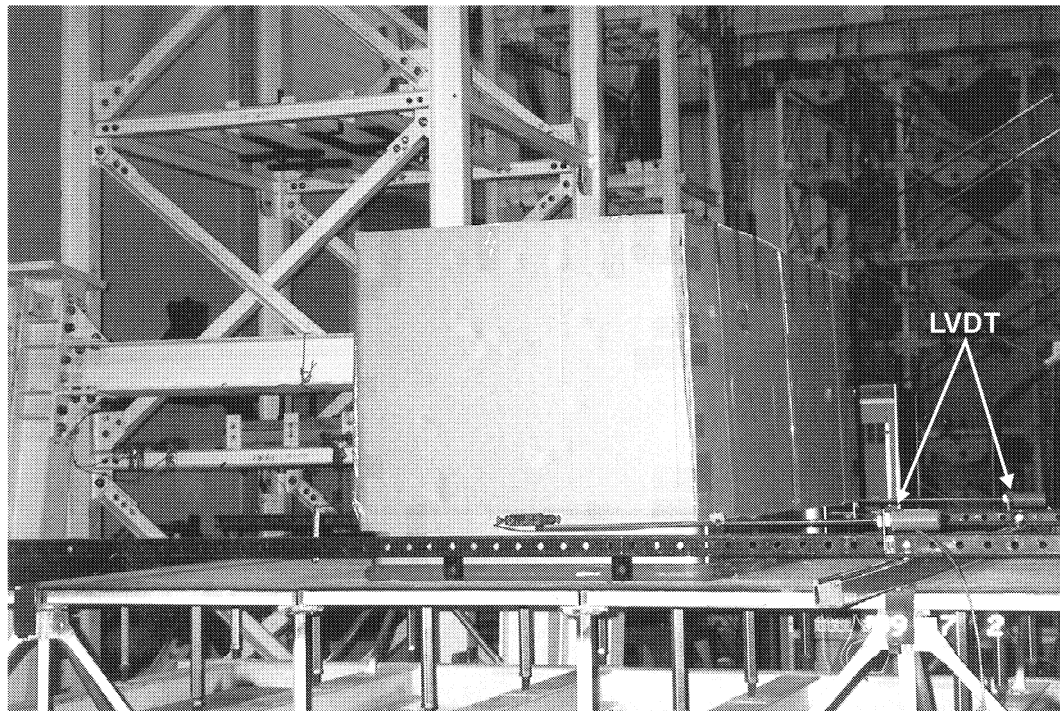


Figure 3.5(c) Side View of Rigid Block with LVDT attached



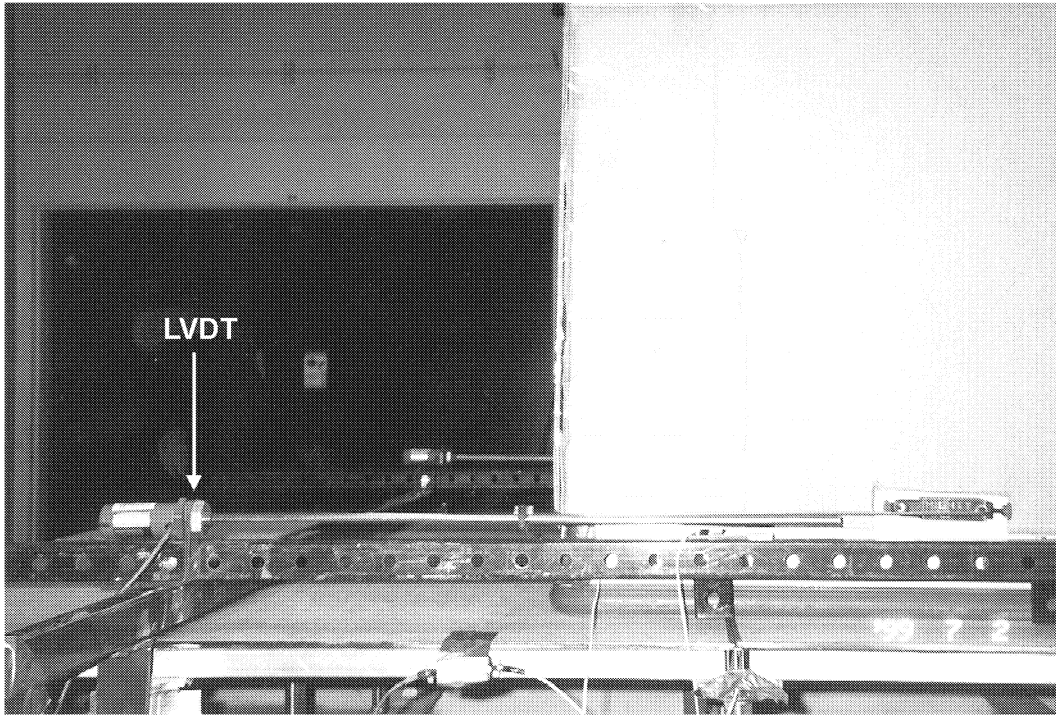


Figure 3.5(d) Side View of LVDT

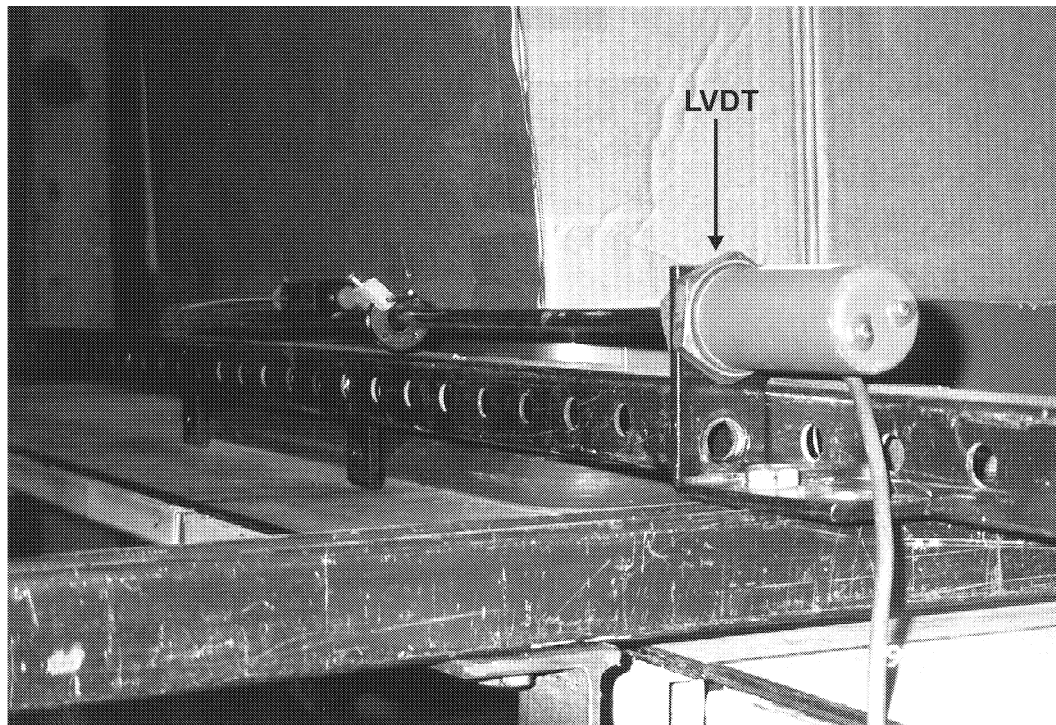
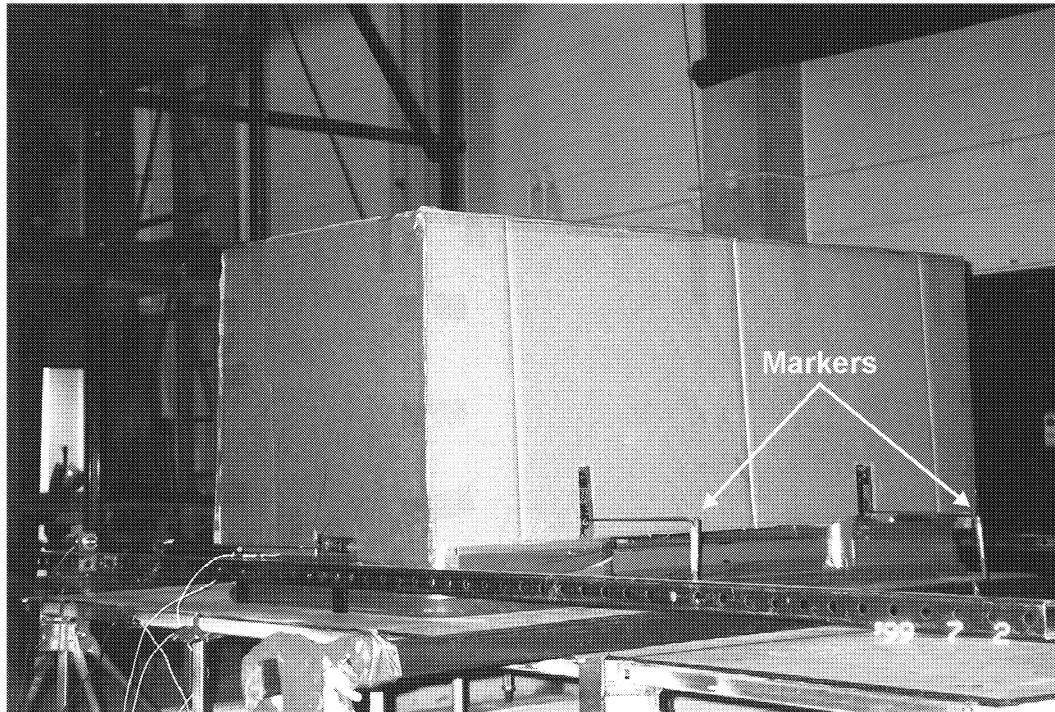
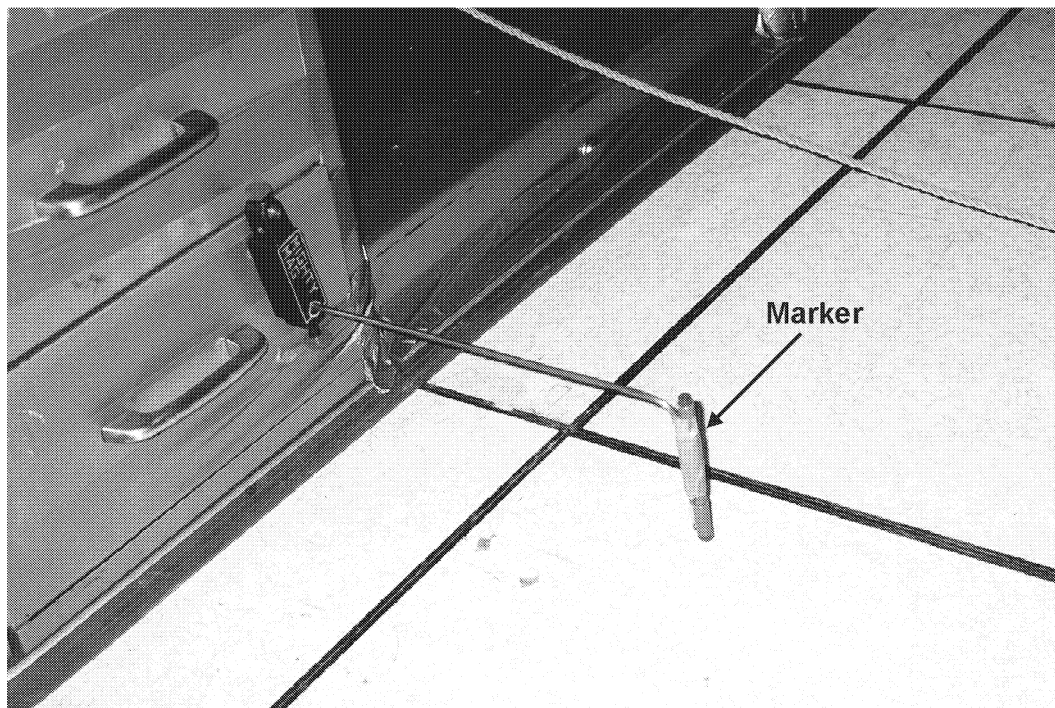


Figure 3.5(e) Front View of LVDT



(a)



(b)

Figure 3.6 Locations of Permanent Markers

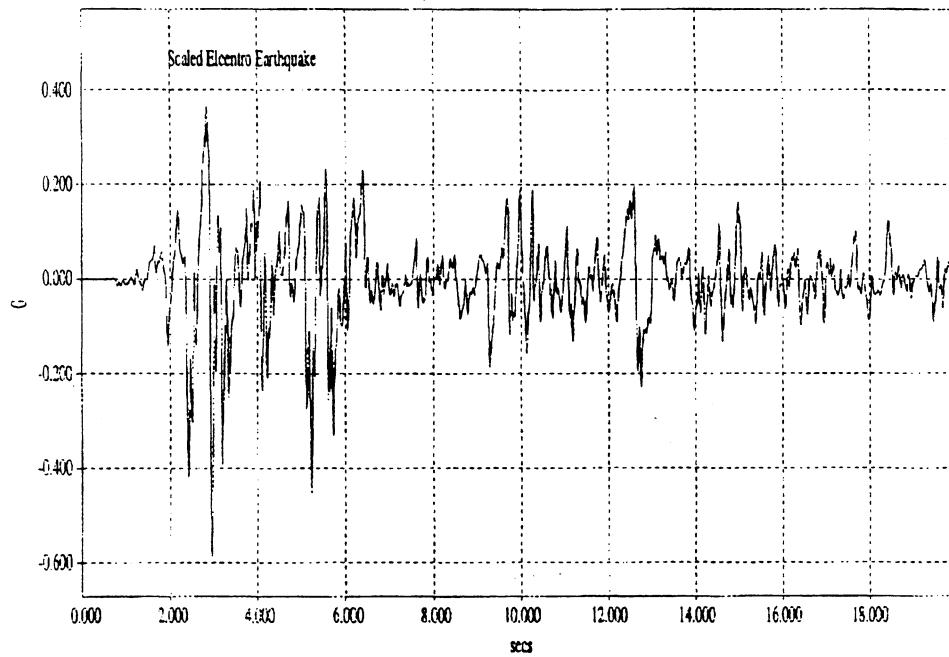


Figure 3.7 Scaled El Centro Earthquake Time History

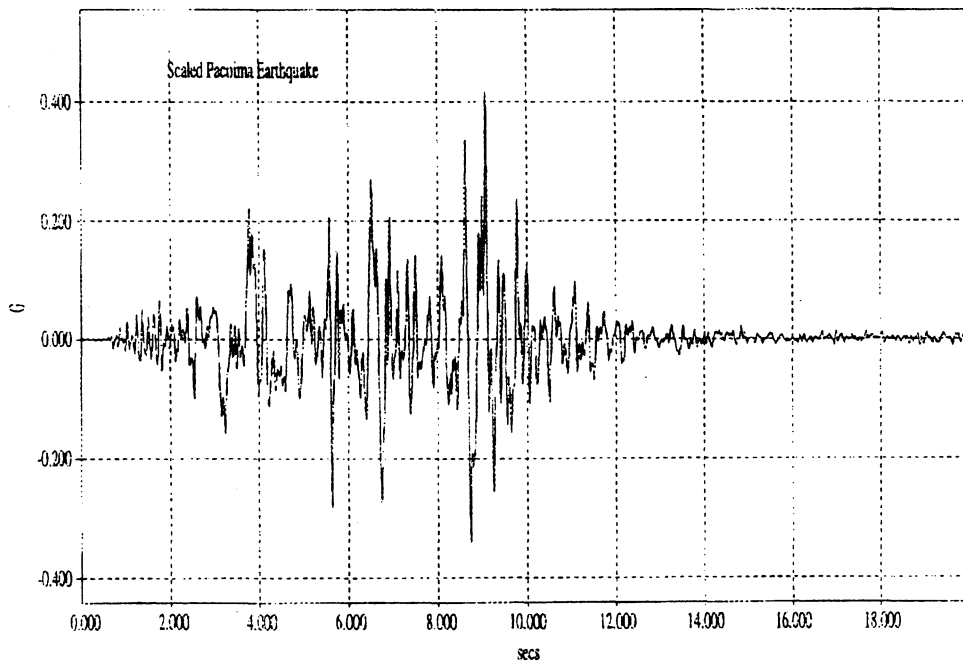


Figure 3.8 Scaled Pacoima Earthquake Time History

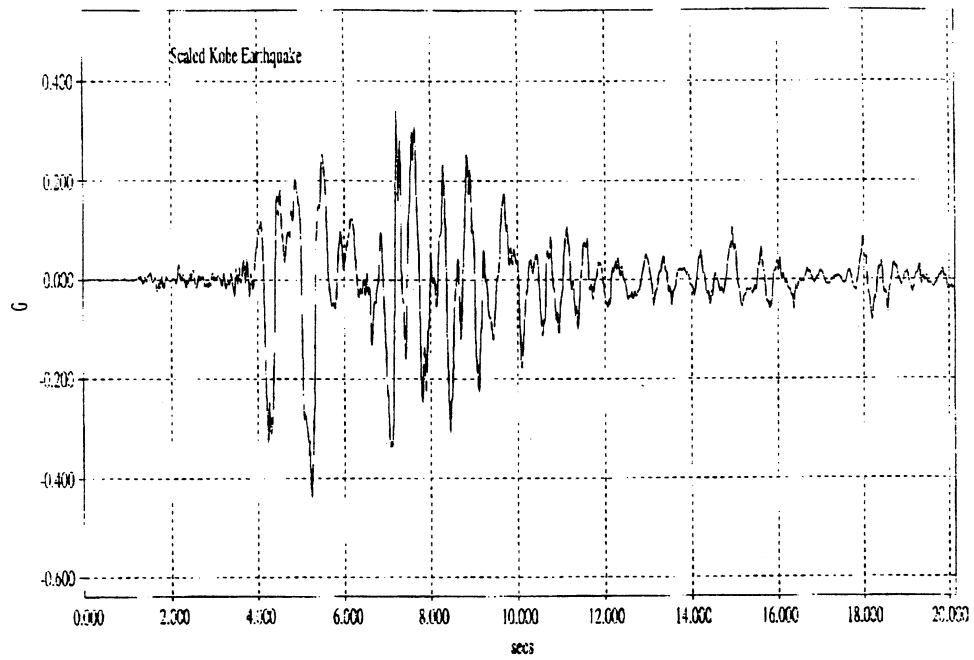


Figure 3.9 Scaled Kobe Earthquake Time History

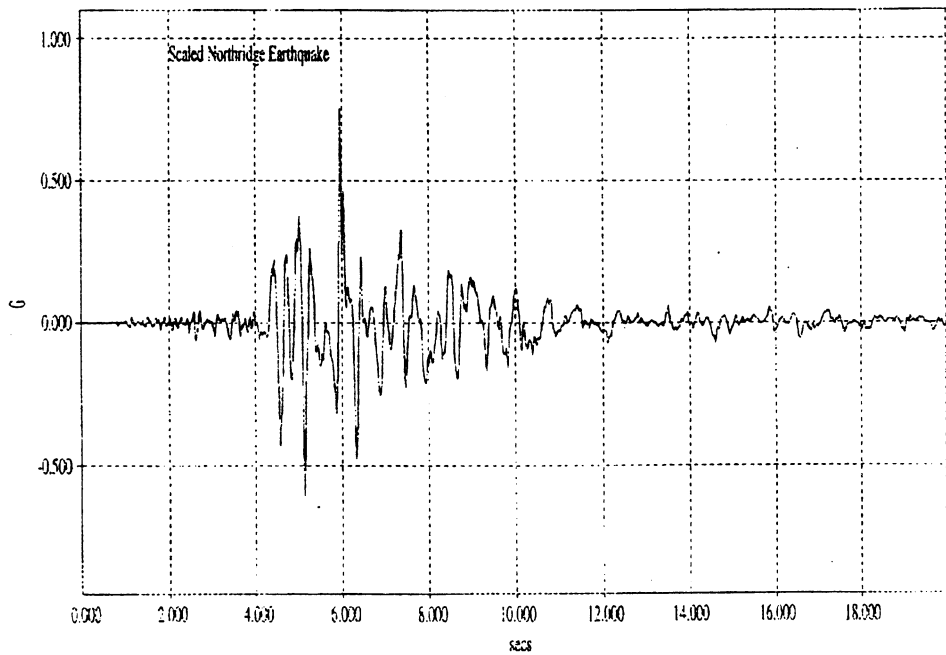


Figure 3.10 Scaled Northridge Earthquake Time History

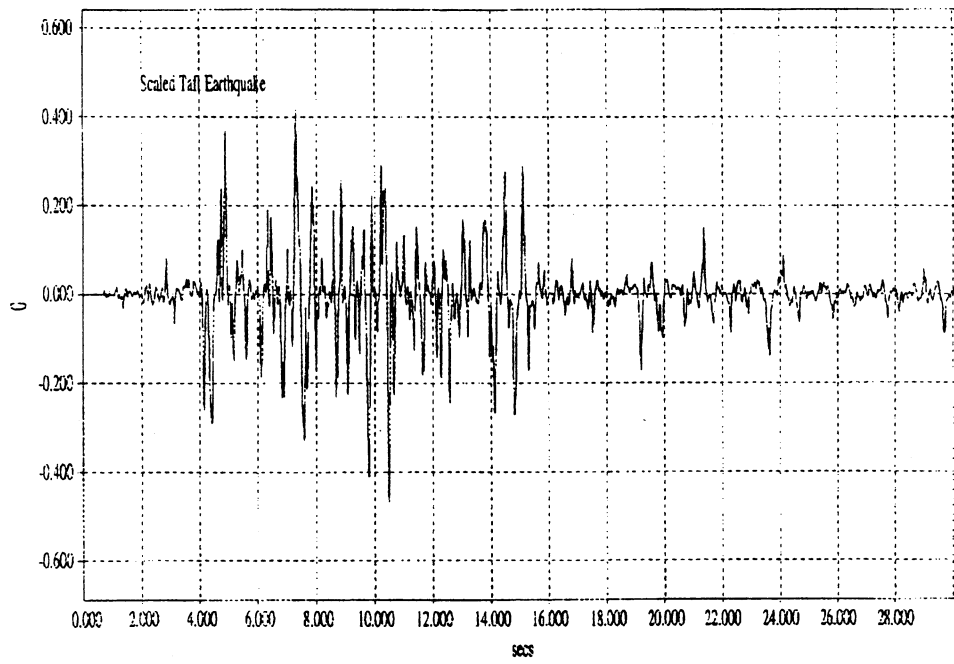


Figure 3.11 Scaled Taft Earthquake Time History

## 3.2 Determination of Coefficient of Static Friction

Determination of the static coefficient of friction for the two sliding surfaces is a very important part of this experiment in the sense that, with the static coefficient of friction determined, comparison between the experimental and analytical results become possible and this leads to the evaluation of accuracy of the analytical solution. There were two tests conducted for the determination of static coefficient of friction : the pulling test and the tilting test as described below.

### 3.2.1 The Pulling Test

The schematic representation of the test setup is shown in Figure 3.12. The determination of the static coefficient of friction is based on the following equation which described the relationship between the static frictional force,  $F_s$ , and the normal force,  $N$  :

$$F_s = \mu_s N \quad (3.1)$$

where  $\mu_s$  is the coefficient of static friction.

In this test, a rope was tied to the sliding block, which was pulled during the test. A load cell was used to measure the force applied in pulling the sliding block,  $F_s$ . The block was pulled until it started to slide. The weight of the sliding block,  $N$ , was then measured. A total of five tests were repeated to obtain an accurate static coefficient of friction, which in this case is 0.143.

### 3.2.2 The Tilting Test

A schematic representation of the test setup in the tilting test is shown in Figure 3.13. Equation (3.2) shown below was used to determine the static coefficient of friction, which is a simpler experiment than the pulling test.

$$\mu_s = \tan \theta \quad (3.2)$$

where  $\theta$  is the angle between the tilted surface and the original surface.

In this case, the whole equipment setup, the sliding block and the raised floor surface, was tilted slowly at one side by a crane, as shown in Figure 3.14, until the block started to slide. The angle at which the rigid block started to slide was measured using an angle measuring instrument shown in Figure 3.15. Two repeated tests were done. A result of 0.455 for the static coefficient of friction was obtained.

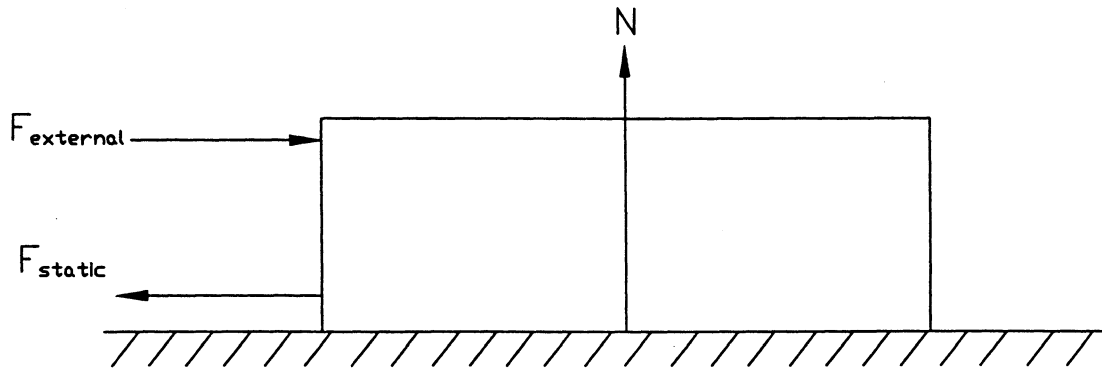


Figure 3.12 The Pulling Test Assembly

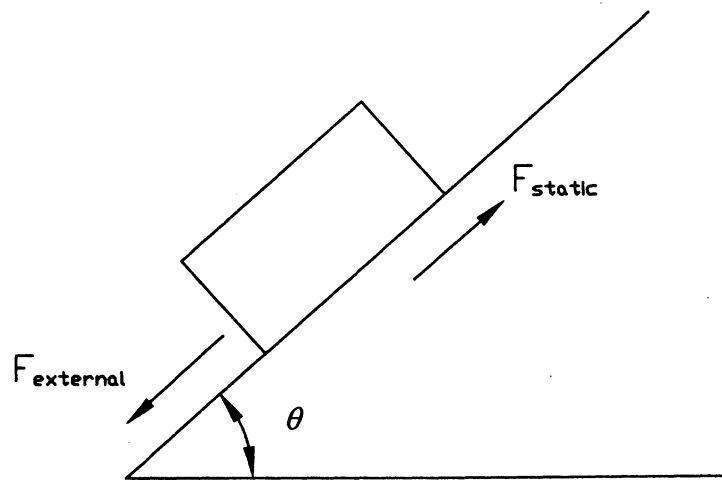


Figure 3.13 The Tilting Test Assembly

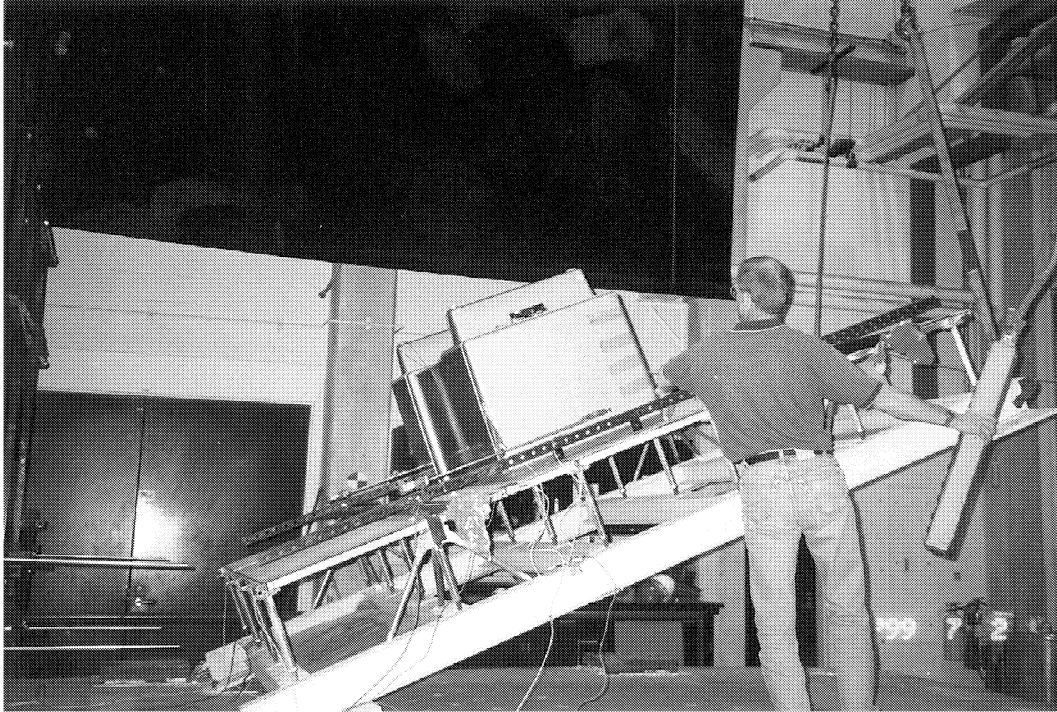


Figure 3.14 The Tilting Test Procedure





(a)



(b)

Figure 3.15 Instrument for Angle Measurement

### 3.2.3 Average Static Coefficient of Friction

Due to the fact that the results obtained for the static coefficient of friction in the two tests described above were significantly different, averaging the results obtained from both tests was necessary. The averaged value of the coefficient of static friction was taken as 0.3.

### 3.3 Summary of Experimental Results

There were five different sets of acceleration time history inputs used in the experiments. They are the acceleration time history records from El Centro, Kobe, Pacoima, Northridge and Taft earthquakes.

Horizontal and vertical excitations were considered in the experiments, as considered in the analytical calculations. In every of the five excitation inputs mentioned above, five different horizontal intensities, which represented by the peak PGA ranging from 0.3g to 0.7g, were tested. As for the vertical acceleration inputs, they were scaled from the horizontal acceleration inputs. There were four different scale factors used in the vertical accelerations : 0, 1/4, 1/3 and 1/2. Table 3.1 illustrates these combinations clearly. For each of the combinations of the HPGA and VPGA in each set of the time history inputs (i.e. El Centro Earthquake, Kobe Earthquake,...etc), two or three repeated test were done for the sake of accuracy of the results.

#### 3.3.1 Sliding Performance of Free-Standing Rigid Block

Once sliding is initiated, there are three parameters which affect the sliding response of the free-standing rigid block. They are the peak horizontal and vertical excitations, and the dynamic coefficient of friction. These three parameters were investigated in the experiments.

Figures 3.16~3.20 show relative displacement and absolute acceleration time histories from the five time history earthquake inputs mentioned before. The HPGA considered here is 0.7 g, with a VPGA of 0.23g, which is 1/3 of the horizontal PGA.

The block average relative peak displacements for each of the combinations of HPGA and VPGA are shown in Table 3.2, together with the corresponding average absolute accelerations at which threshold displacements occur. In addition, based on an approximate correlation between static and dynamic friction coefficients found in TABLE C1. (Dimarogonas, 1996) in Appendix C, an assumed coefficient of dynamic friction of 0.21 which was estimated from the determined coefficient of static friction between the tested sliding surfaces was used as a parameter in the analytical solution procedure for comparison. A summary of these results is presented in Table 3.3.

#### 3.3.2 Experimental Failure Curves

There were eight different failure thresholds considered in the experimental analysis, as in the analytical solutions. They are relative displacements of 0.1 inch, 0.2 inch, 0.5 inch, 0.75 inch, 1 inch, 2 inches, 2.5 inches and 3 inches. The fragility curves for failure threshold of 1 inch and 2

Table 3.2 Summary of Experimental Results

**Average Peak Displacement, inch**

*Horizontal Peak Ground Acceleration, g*

k	0.3	0.4	0.5	0.6	0.7
0	0.1473	0.43132	0.763692	1.813846	3.029818
1/4	0.1326	0.4463	0.821385	2.064538	3.192909
1/3	0.1309	0.4042	0.876	2.317769	3.215273
1/2	0.1292	0.418	0.882462	2.287846	3.843091

**Average Acceleration at which Peak Displacement Occurs, g**

*Horizontal Peak Ground Acceleration, g*

k	0.3	0.4	0.5	0.6	0.7
0	0.2187	0.2052	0.231538	0.256923	0.196909
1/4	0.1929	0.2462	0.237154	0.241692	0.21
1/3	0.2346	0.2423	0.214692	0.231	0.246636
1/2	0.2191	0.2601	0.186846	0.255846	0.163091

Table 3.3 Summary of Analytical Solution for  $\mu_d = 0.21$

**Average Peak Displacement, inch**

*Horizontal Peak Ground Acceleration, g*

k	0.3	0.4	0.5	0.6	0.7	0.8	0.9	1
0	0.027586	0.208377	0.665909	1.385792	2.317321	3.39103	4.598406	5.894688
1/4	0.034412	0.2584	0.835573	1.805412	3.065873	4.564104	6.245473	8.093002
1/3	0.038549	0.296323	0.979537	2.11098	3.573012	5.342662	7.355268	9.50258
1/2	0.053762	0.4073	1.350192	2.929514	4.9672	7.415218	10.16441	13.09147

**Average Acceleration at which Peak Displacement Occurs, g**

*Horizontal Peak Ground Acceleration, g*

k	0.3	0.4	0.5	0.6	0.7	0.8	0.9	1
0	0.220012	0.220102	0.220313	0.220662	0.221277	0.221902	0.222909	0.222913
1/4	0.219328	0.219373	0.220117	0.222542	0.224652	0.227457	0.229738	0.232046
1/3	0.216208	0.218529	0.220116	0.223239	0.225861	0.228754	0.232716	0.237841
1/2	0.215276	0.218409	0.220737	0.22343	0.225846	0.233291	0.237565	0.244355

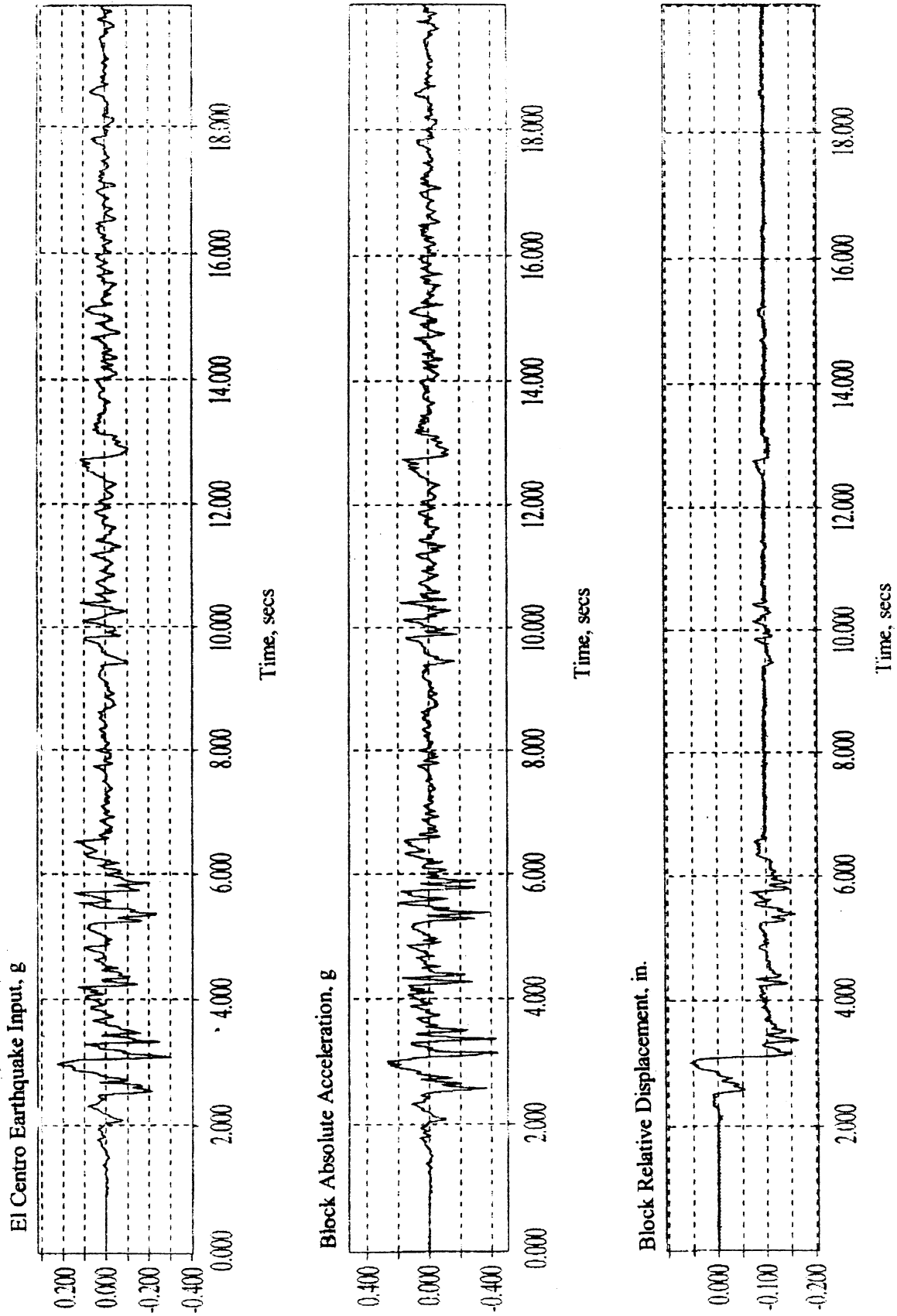


Figure 3.16 Typical Experimental Result from El Centro Earthquake Input

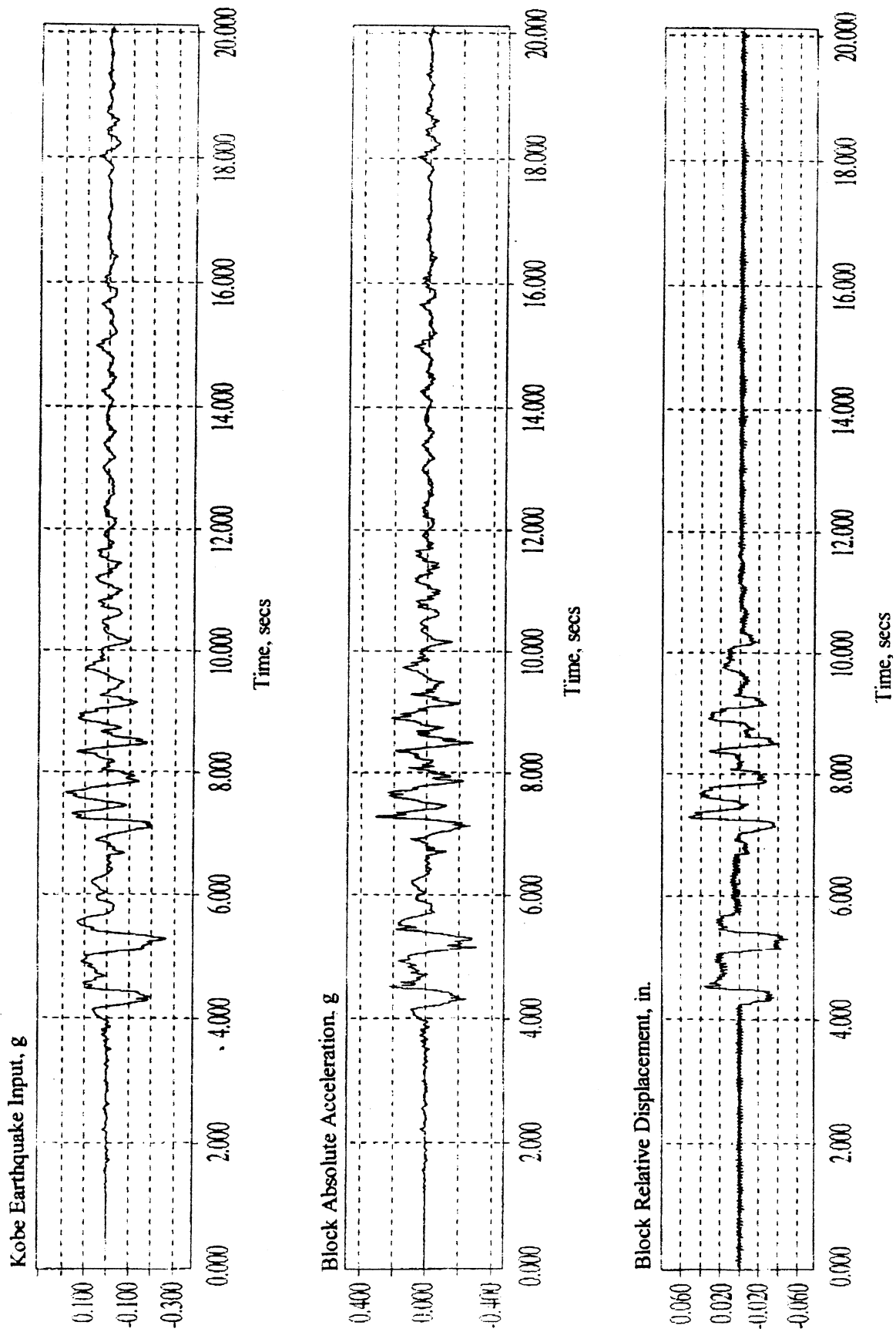


Figure 3.17 Typical Experimental Result from Kobe Earthquake Input

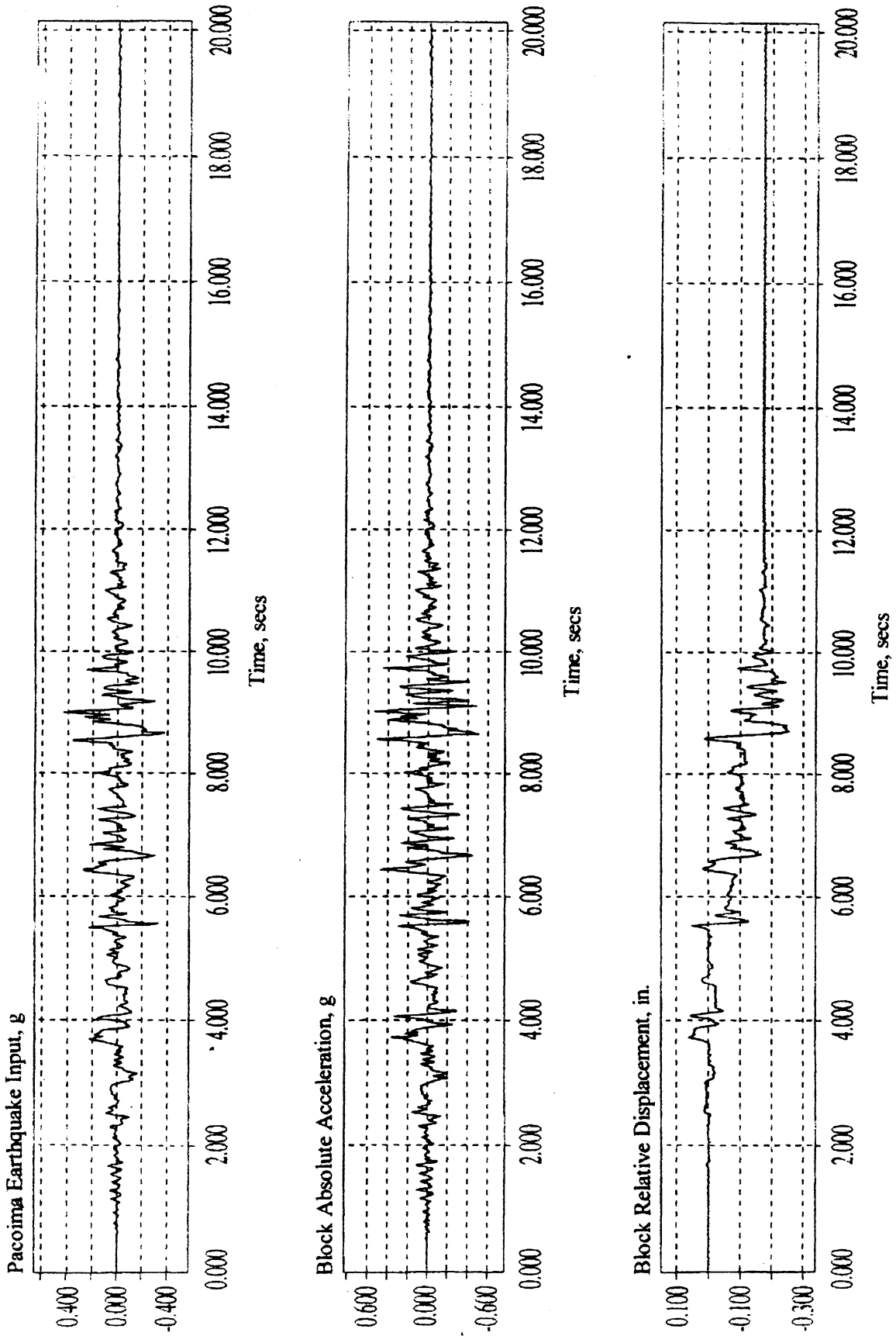


Figure 3.18 Typical Experimental Result from Pacoima Earthquake Input

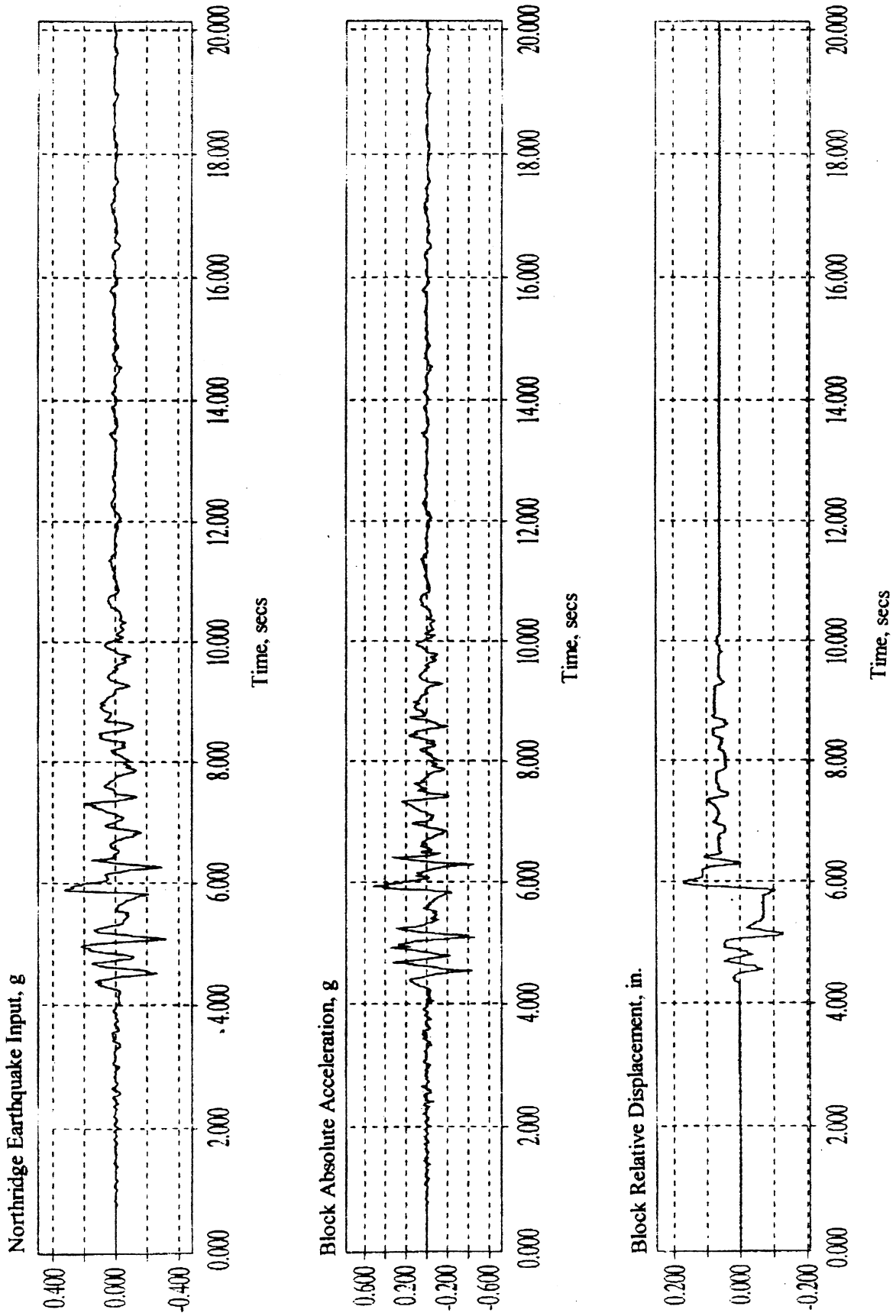


Figure 3.19 Typical Experimental Result from Northridge Earthquake Input

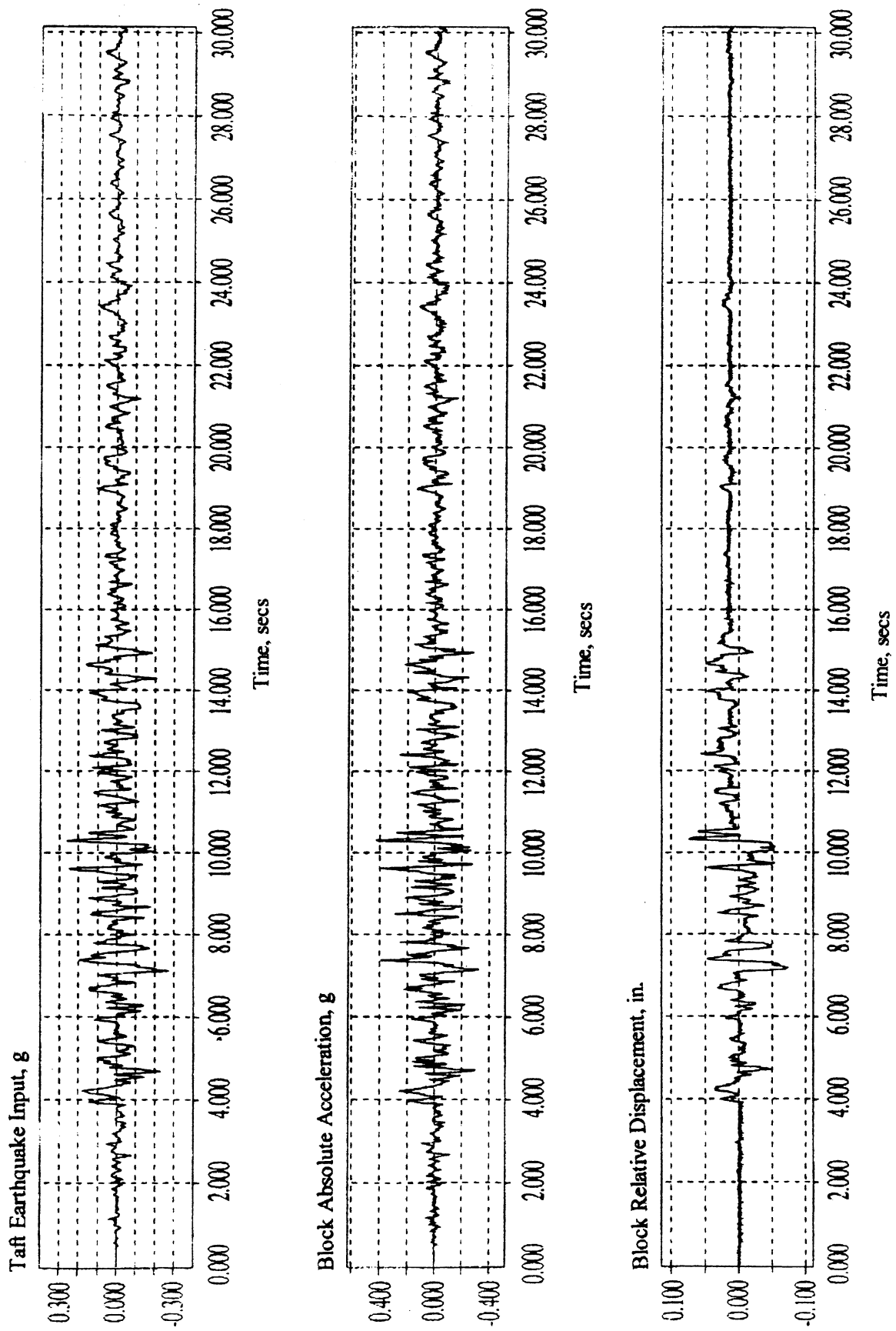


Figure 3.20 Typical Experimental Result from Taft Earthquake Input



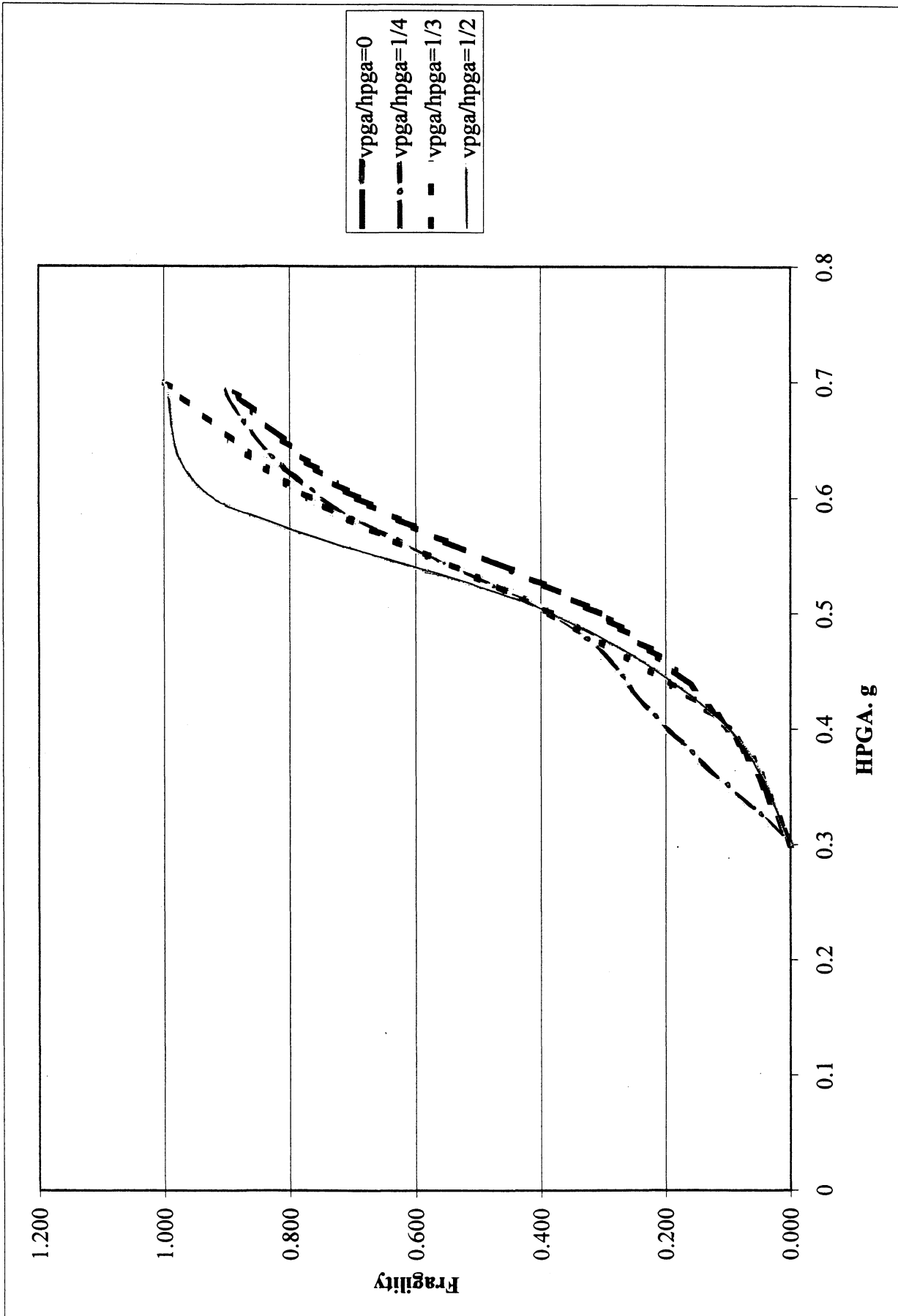


Figure 3.21 Experimental Fragility Curves for Failure Threshold = 1 inch

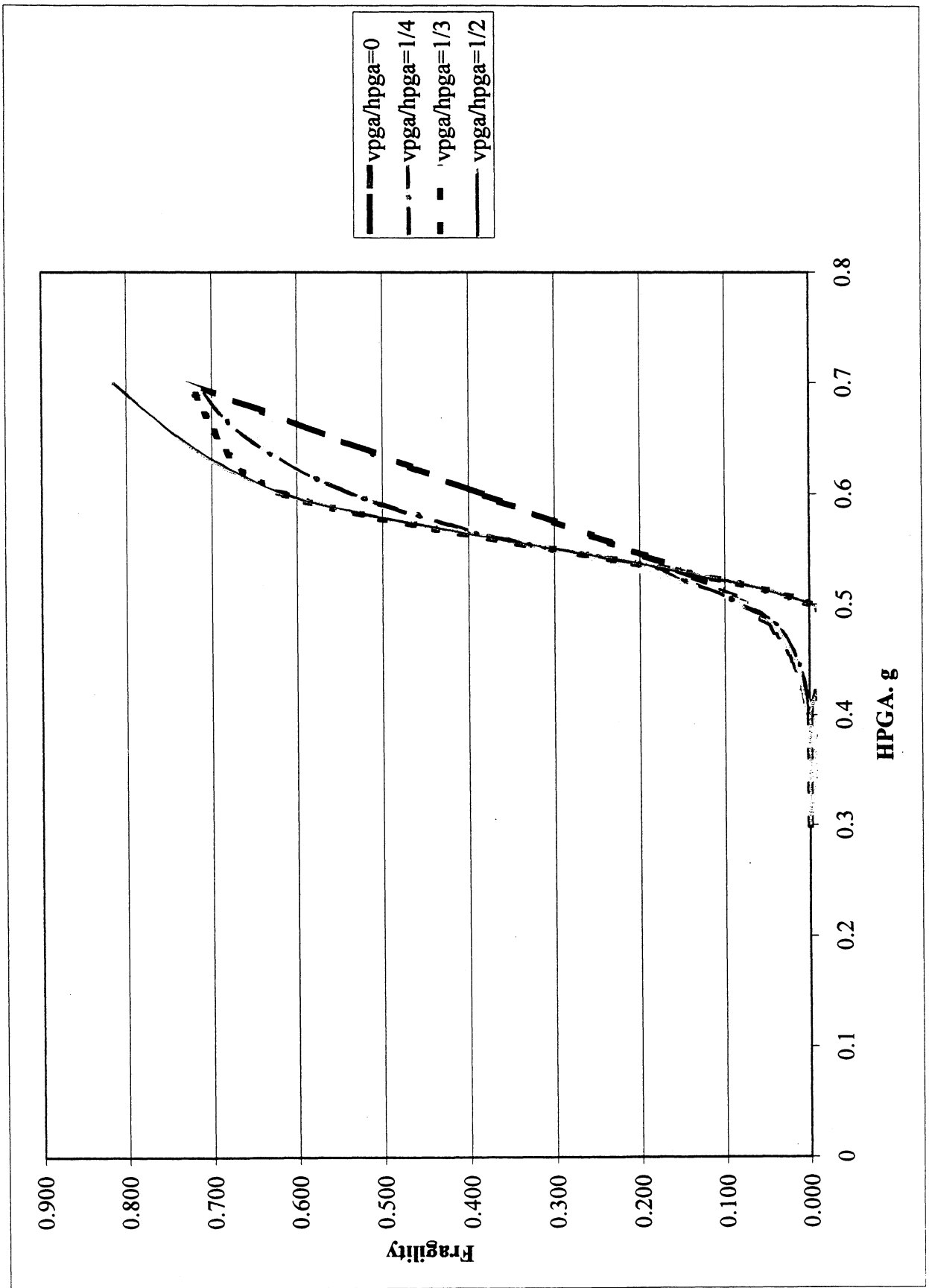


Figure 3.22 Experimental Fragility Curves for Failure Threshold = 2 inches

inches are shown in Figure 3.21 and 3.22, respectively. A comprehensive presentation of the probabilities of failure for all of the failure thresholds considered is given in Table 3.4.

### **3.3.3 Discussion of Results**

The results obtained from the experiments are somewhat similar to the results obtained analytically. Most of the threshold displacements increase as magnitudes of the horizontal and vertical excitation inputs increase. Moreover, the insensitivity of the absolute acceleration at which threshold displacement occurs to the change of horizontal and vertical input excitations once again revealed in the experimental results, as in the analytical solutions. However, some experimental results show that, for a specific HPGA and coefficient of dynamic friction, the peak displacements do not always increase as the VPGA increases, as in the analytical results.

The experimental coefficient of dynamic friction was obtained through multiplying a scale factor to the coefficient of static friction obtained experimentally due to the fact that the coefficient of dynamic friction was difficult to determine by experimental means. Comparison of the analytical and experimental results is illustrated in more detail in the next section.

## **3.4 Comparison of Analytical and Experimental Results**

Based on the displacement failure thresholds, it can be seen from the analytical and experimental results that, as the coefficient of dynamic friction increases, the free-standing rigid block will have less vulnerability in resisting earthquake excitation. In other words, it will perform better in resisting earthquake load with a larger coefficient of dynamic friction of the contact surfaces. However, as the HPGA and VPGA of an excitation increase, the rigid block will have a larger probability of failure for a given sliding failure mode.

On the other hand, it was found that the fragility curves are not necessary to be constructed based on the threshold displacement together with the absolute accelerations at which threshold displacements occur for a specific dynamic friction coefficient. This is due to the fact that from a summary of those average absolute acceleration results for each of the cases considered in Section 2, it could be seen that no matter how the HPGA or VPGA changes, the average absolute accelerations for each case remain almost unchanged. The experimental results produce a somewhat similar pattern in this case.

As for a comparison of the analytical and experimental results, Figures 3.23 and 3.24 show the results for the displacement thresholds of 1 inch and 2 inches, respectively, obtained analytically and experimentally for a coefficient of dynamic friction of 0.3. As can be noticed in these figures, there is quite a difference between the analytical and experimental solutions. This difference can be explained by the use of the experimentally obtained static friction coefficient, 0.3, as the dynamic friction coefficient in obtaining analytical results.

The coefficient of friction determined in the experiments is for the static case. This value was used in the analytical solution procedure despite the fact that the dynamic friction coefficient, which is supposed to be smaller than 0.3, should be used in the analytical solution procedure.

Therefore, we can see from Figures 3.23 and 3.24 that the analytical failure curves are lower than those experimental solutions. This 'lower position' suggests that the probabilities of failure, determined analytically, are supposed to be higher than what are shown in Figures 3.23 and 3.24 if a proper coefficient of dynamic friction is used.

The proper coefficient of dynamic friction, which should be input into the analytical solution procedure, is supposed to be smaller than the determined static coefficient of friction of 0.3. Due to the fact that there is no suitable experimental procedure that we could perform to determine the dynamic coefficient of friction, a coefficient of 0.7 of the static coefficient of friction, which is 0.21, is taken to be the dynamic coefficient of friction. This value was selected based on Table C1 (Dimarogonas, 1996) for similar sliding surfaces. These analytical solutions obtained based on the scaled coefficient of dynamic friction of 0.21 agree well enough with the experimental results as shown in Figures 3.25 and 3.26 for the displacement failure thresholds of 1 inch and 2 inches.

Table 3.4 Experimental Probabilities of Failure

$v_{pga}/h_{pga} = 0$

Threshold Sliding Distance, in

PGA	0.1	0.2	0.5	0.75	1	2	2.5	3
0.300	0.700	0.400	0.000	0.000	0.000	0.000	0.000	0.000
0.400	0.800	0.700	0.400	0.200	0.100	0.000	0.000	0.000
0.500	1.000	0.846	0.538	0.385	0.308	0.077	0.000	0.000
0.600	1.000	1.000	0.846	0.692	0.692	0.385	0.308	0.154
0.700	1.000	1.000	1.000	0.909	0.909	0.727	0.455	0.364

$v_{pga}/h_{pga} = 1/4$

Threshold Sliding Distance, in

PGA	0.100	0.200	0.500	0.750	1.000	2.000	2.500	3.000
0.300	0.500	0.200	0.000	0.000	0.000	0.000	0.000	0.000
0.400	0.700	0.700	0.200	0.200	0.200	0.000	0.000	0.000
0.500	1.000	0.923	0.538	0.385	0.385	0.077	0.000	0.000
0.600	1.000	1.000	0.923	0.769	0.769	0.538	0.385	0.231
0.700	1.000	1.000	1.000	1.000	0.909	0.727	0.545	0.545

$v_{pga}/h_{pga} = 1/3$

Threshold Sliding Distance, in

PGA	0.100	0.200	0.500	0.750	1.000	2.000	2.500	3.000
0.300	0.500	0.200	0.000	0.000	0.000	0.000	0.000	0.000
0.400	0.700	0.700	0.200	0.200	0.100	0.000	0.000	0.000
0.500	1.000	1.000	0.538	0.462	0.385	0.000	0.000	0.000
0.600	1.000	1.000	0.923	0.923	0.769	0.615	0.538	0.308
0.700	1.000	1.000	1.000	1.000	1.000	0.727	0.545	0.545

$v_{pga}/h_{pga} = 1/2$

Threshold Sliding Distance, in

PGA	0.100	0.200	0.500	0.750	1.000	2.000	2.500	3.000
0.300	0.500	0.200	0.000	0.000	0.000	0.000	0.000	0.000
0.400	0.800	0.700	0.300	0.200	0.100	0.000	0.000	0.000
0.500	1.000	1.000	0.615	0.538	0.385	0.000	0.000	0.000
0.600	1.000	1.000	1.000	0.923	0.923	0.615	0.538	0.231
0.700	1.000	1.000	1.000	1.000	1.000	0.818	0.545	0.545

Table 3.5 Analytical Probabilities of Failure for  $\mu_d = 0.21$

$vp_{ga}/hp_{ga} = 0$

PGA	0.1 in	0.2 in	0.5 in	0.75 in	1 in	2 in	2.5 in	3 in
0.3	0.011111	0	0	0	0	0	0	0
0.4	0.855556	0.411111	0	0	0	0	0	0
0.5	1	0.977778	0.644444	0.322222	0.166667	0	0	0
0.6	1	1	0.955556	0.844444	0.7	0.133333	0.066667	0.033333
0.7	1	1	1	1	0.977778	0.566667	0.344444	0.2
0.8	1	1	1	1	1	0.855556	0.688889	0.555556
0.9	1	1	1	1	1	0.988889	0.911111	0.822222
1	1	1	1	1	1	1	0.988889	0.944444

$vp_{ga}/hp_{ga} = 1/4$

PGA	0.1 in	0.2 in	0.5 in	0.75 in	1 in	2 in	2.5 in	3 in
0.3	0.044444	0	0	0	0	0	0	0
0.4	0.877778	0.522222	0.1	0.011111	0	0	0	0
0.5	1	1	0.711111	0.477778	0.311111	0.011111	0	0
0.6	1	1	1	0.9	0.788889	0.366667	0.211111	0.133333
0.7	1	1	1	1	0.955556	0.733333	0.533333	0.455556
0.8	1	1	1	1	1	0.911111	0.844444	0.733333
0.9	1	1	1	1	1	0.977778	0.966667	0.888889
1	1	1	1	1	1	1	1	0.988889

$vp_{ga}/hp_{ga} = 1/3$

PGA	0.1 in	0.2 in	0.5 in	0.75 in	1 in	2 in	2.5 in	3 in
0.3	0.077778	0	0	0	0	0	0	0
0.4	0.9	0.588889	0.155556	0.033333	0	0	0	0
0.5	1	1	0.788889	0.611111	0.433333	0.044444	0.011111	0
0.6	1	1	0.988889	0.933333	0.844444	0.488889	0.322222	0.188889
0.7	1	1	1	1	0.988889	0.811111	0.722222	0.555556
0.8	1	1	1	1	1	0.922222	0.877778	0.855556
0.9	1	1	1	1	1	0.977778	0.944444	0.911111
1	1	1	1	1	1	1	1	0.966667

$vp_{ga}/hp_{ga} = 1/2$

PGA	0.1 in	0.2 in	0.5 in	0.75 in	1 in	2 in	2.5 in	3 in
0.3	0.111111	0.011111	0	0	0	0	0	0
0.4	0.977778	0.855556	0.255556	0.088889	0.011111	0	0	0
0.5	1	1	0.944444	0.855556	0.666667	0.144444	0.055556	0.011111
0.6	1	1	1	0.988889	0.966667	0.744444	0.622222	0.433333
0.7	1	1	1	1	1	0.966667	0.922222	0.811111
0.8	1	1	1	1	1	0.988889	0.977778	0.966667
0.9	1	1	1	1	1	1	1	0.977778
1	1	1	1	1	1	1	1	1

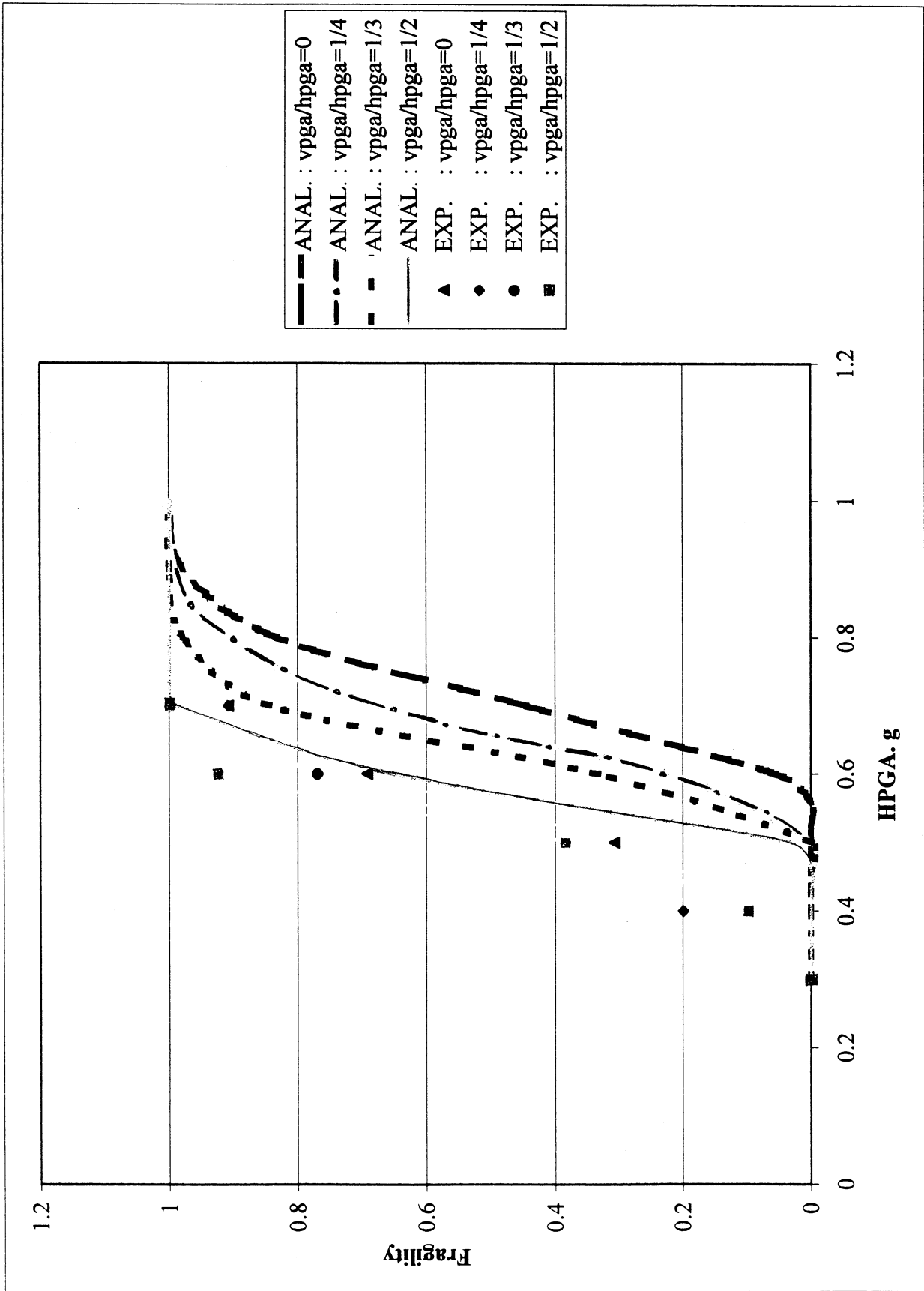


Figure 3.23 Comparison of Experimental and Analytical Fragility Curves with  $\mu_d = 0.3$ , Failure Threshold = 1 inch

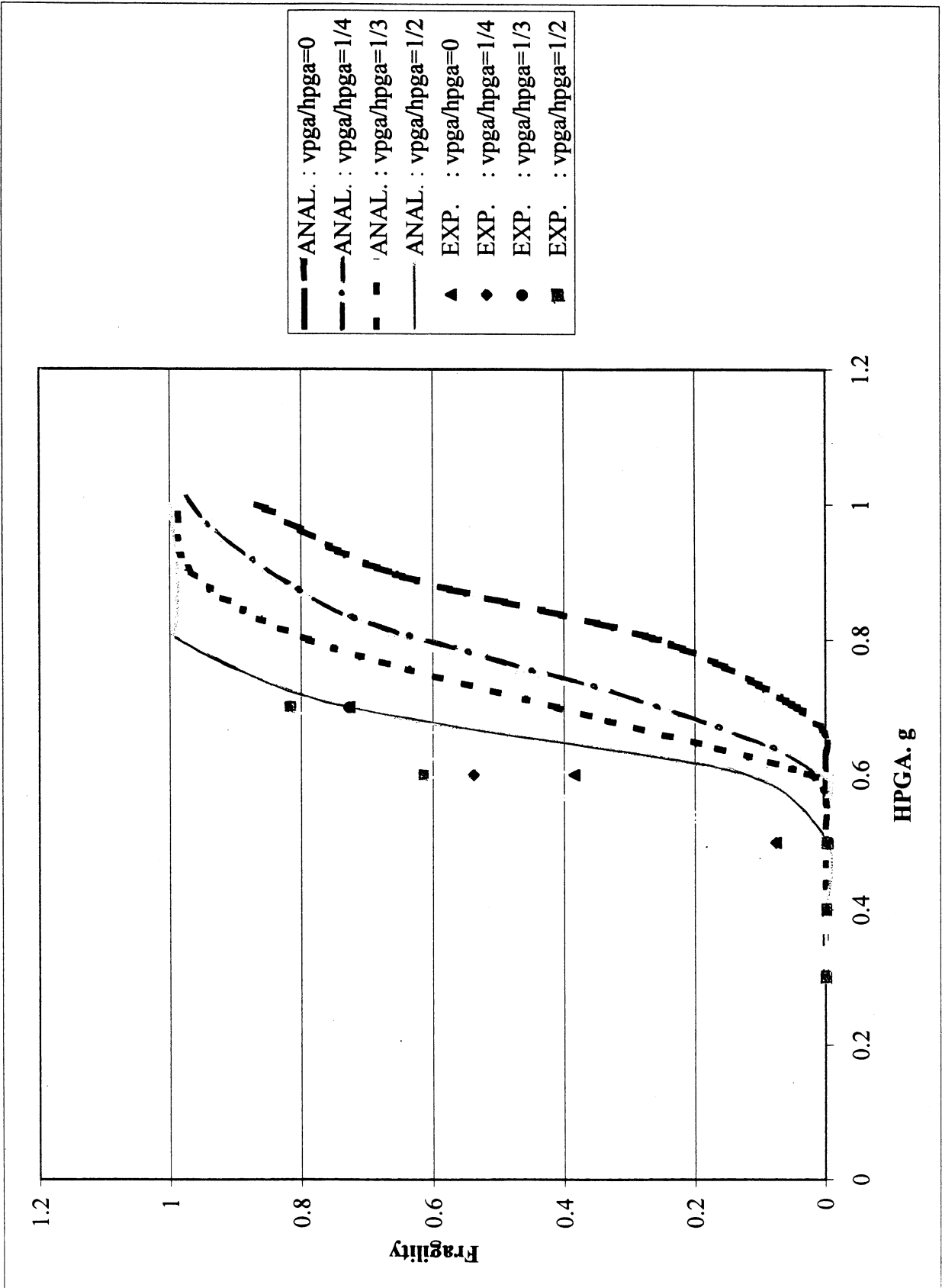


Figure 3.24 Comparison of Experimental and Analytical Fragility Curves with  $\mu_d = 0.3$ , Failure Threshold = 2 inches



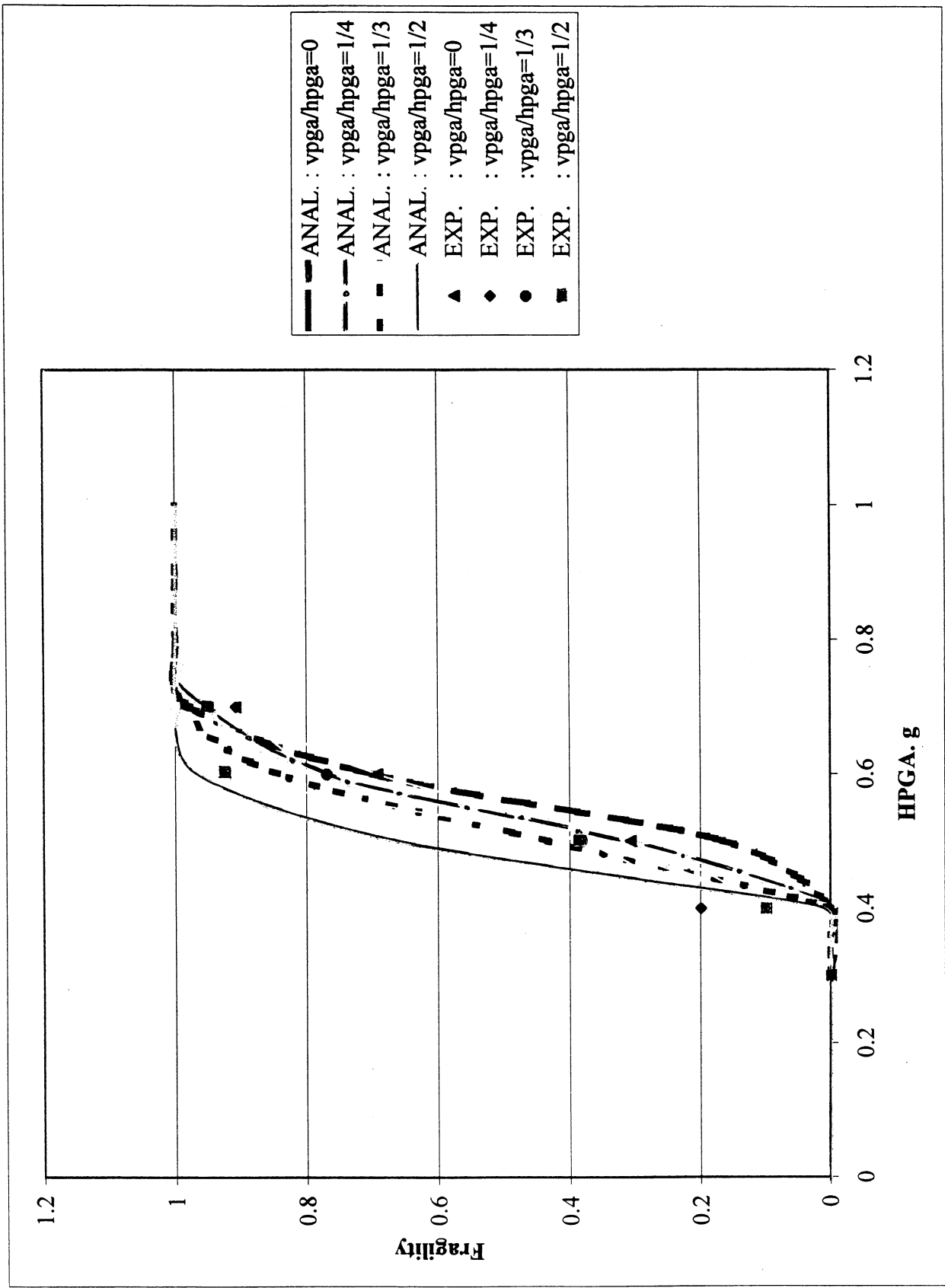


Figure 3.25 Comparison of Experimental and Analytical Fragility Curves with  $\mu_d = 0.21$ , Failure Threshold = 1 inch

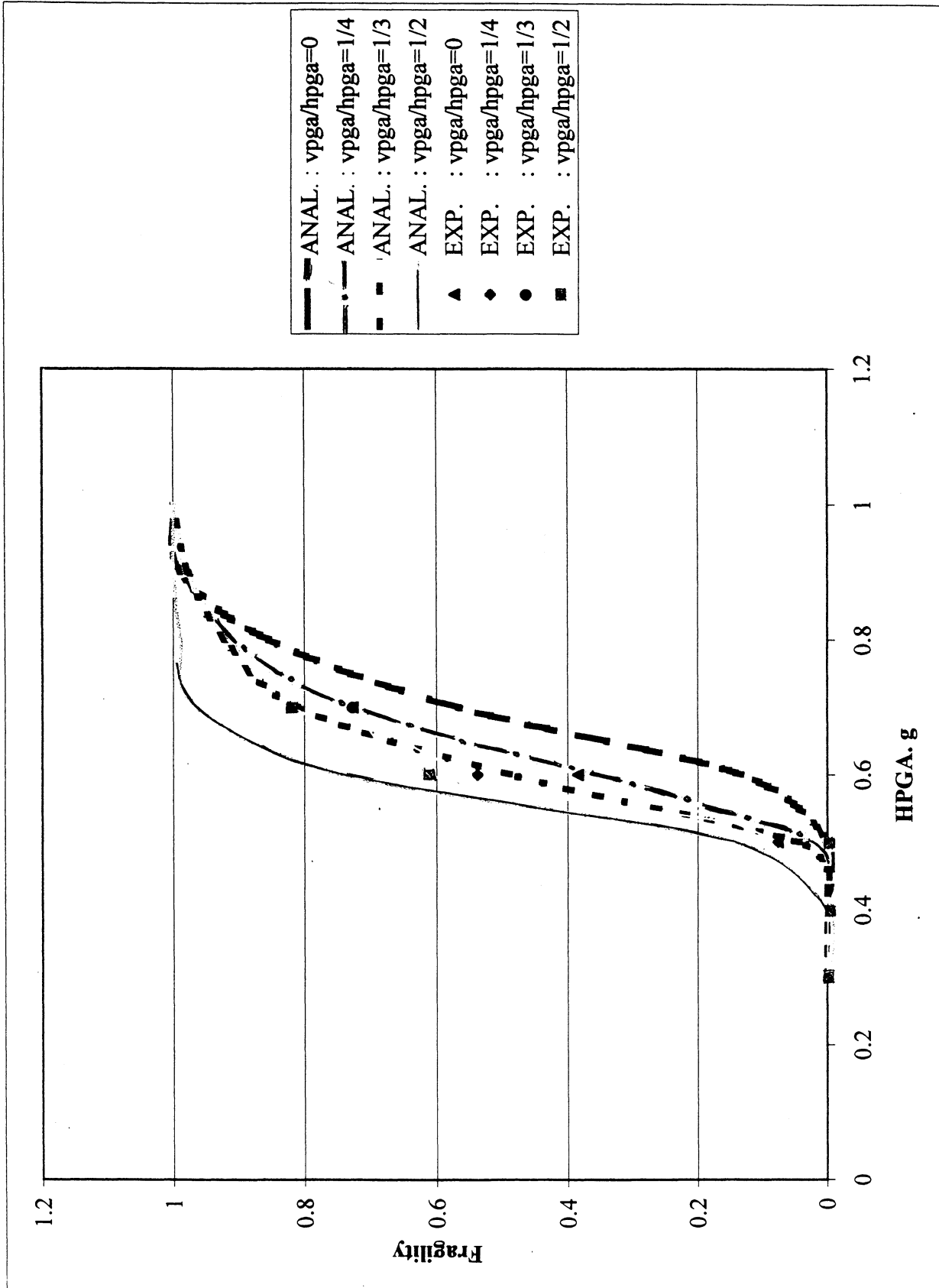


Figure 3.26 Comparison of Experimental and Analytical Fragility Curves with  $\mu_d = 0.21$ , Failure Threshold = 2 inches

## **SECTION 4 CONCLUSION**

### **4.1 Conclusion**

A free-standing rigid block resting on a rigid supporting base subjected to horizontal and vertical base excitations is an excellent model of an unrestrained block-type equipment under seismic excitations. There are, basically, four types of response of this rigid block that can be initiated under base excitations, depending on the excitation level, the aspect ratio ( $b/h$ ), and the static friction coefficient. They are the at-rest state, sliding motion, rocking motion, and jumping motion. A graphical representation of sliding and rocking motion types can be used to determine the motion of the free-standing rigid block once the peak value of the base excitation level is known. This representation is developed by assigning static friction coefficient as the abscissa and aspect ratio as the ordinate.

A combined analytical and experimental approach has been implemented to assess the fragility of free-standing rigid block under pure sliding motion. The equation of sliding motion has been derived in term of horizontal force balance. SIMQKE was used to generate base excitations, for the analytical solution procedure, based on the response spectrum specified by NEHRP. On the other hand, the base excitations used in the experiments were from past earthquake data. A comparison of the analytical and experimental results was made possible by multiplying a scale factor into the experimentally determined static friction coefficient, in order to match the dynamic friction coefficient used in the analytical solution procedure.

Three sensitive parameters have been studied in this research. They are the coefficient of dynamic friction, the HPGA and the VPGA. From the results obtained, both analytical and experimental, relative displacement increases as the HPGA and VPGA increases and decreases as the coefficient of friction increases, as expected. On the other hand, the absolute acceleration at which threshold acceleration occurs is insensitive to changes as the HPGA and VPGA change while the coefficient of dynamic friction remains unchanged. However, it increases as the coefficient of dynamic friction increases, and in fact, it has an almost perfectly correlation with the dynamic friction coefficient.

### **4.2 Recommendations for Future Research**

Theoretical assumptions were made in this research in order to simplify the problem and obtain analytical solutions. In regards to this, investigation and modifications of the theoretical model should further be implemented to verify its validity and to improve upon performance predictions. This section addresses some specific issues for future improvements on this analytical model and accuracy of results.

#### **4.2.1 Sliding-Rocking Motion Type and Jumping Motion Type**

It was assumed in this research that the restraining moment is large enough to prevent rocking motion of a sliding block and no jumping will occur during sliding. However, in realistic situations, these assumptions may not always be true. Rocking motion may also occur if the restoring moment is not large enough and jumping will happen if VPGA is too large. Thus, these

motion types may also need to be incorporated into this study. In this case, the equation of sliding motion may break down and new equations of motion need to be derived, which may be much more complicated than the equation of sliding motion.

#### **4.2.2 Deviation from Horizontal Supporting Base**

The surface of supporting base was assumed to be horizontal in this research. This assumption may not be valid in realistic situations, and thus introducing the sliding angle parameter in the equation of motion is necessary to better predict the sliding performance of unrestrained block-type equipment.

#### **4.2.3 Experimental Estimation of Dynamic Friction Coefficient**

Determination of the actual dynamic friction coefficient experimentally is an important subject in validating the accuracy of the analytical model in this research. Due to this importance, further effort should be concentrated on the method for this determination.

## SECTION 5 REFERENCES

1. Blau, P. J., (1996), *Friction Science and Technology*, Marcel Dekker, Inc., New York, NY. 43-163.
2. Chopra, A. K., (1995), *Dynamics of Structures*, Prentice-Hall, Inc., Upper Saddle River, NJ.
3. Dimarogonas, A., (1996), *Vibration for Engineers- 2<sup>nd</sup> Edition*, Prentice-Hall, Inc., Upper Saddle River, NJ.
4. Earthquake Engineering Research Institute (EERI), (1984), *Nonstructural Issues of Seismic Design and Construction*, EERI, Oakland, CA.
5. Federal Emergency Management Agency (FEMA), (1997), *NEHRP Recommended Provisions for Seismic Regulations for New Buildings and Other Structures*, Building Seismic Safety Council, Washington, D.C. 33-41.
6. Gates, W.E. and Scawthorn, C., (1982), "Mitigation of Earthquake Effects on Data Processing Equipment," Presented at the Session on Performance of Electrical Power and Communications Systems During Earthquakes, ASCE National Spring Convention, Las Vegas, NV.
7. Ishiyama, Y., (1981), "Motions of Rigid Bodies and Criteria for Overturning by Earthquake Excitations," *Earthquake Engineering and Structural Dynamics*, Vol. 10, 635-650.
8. Kosar, K., Soong, T. T., Shen, K. L., HoLung, J.A., Lin, Y. K., (1993), *Seismic Testing of Installation Methods for Computers and Data Processing Equipment*, Report NCEER-93-00007, National Center for Earthquake Engineering Research, Buffalo, NY.
9. Lagorio, H. J., (1990), *Earthquakes*, John Wiley & Sons, Inc., New York, NY.
10. Perry, C.L., Fierro, E.A., Freeman, S.A., (1994), *Reducing the Risks of Nonstructural Earthquake Damage – A Practical Guide, 3<sup>rd</sup> Edition (FEMA 74)*, Wiss, Janney, Elstner Associates, Inc. 1-20.
11. Sakamoto, I., (1978), *Seismic Performance of Nonstructural and Secondary Structural Elements*, Report No. UCB/EERC-78/10, Earthquake Engineering Research Center, U.C. Berkeley, Berkeley, CA.
12. Shultz, P., Jones, N. P., (1994), "Experimental Determination of Slide-Rock Behavior of Rigid Blocks Subjected to Base Motion," *Proceedings of Fifth U.S. National Conference on Earthquake Engineering*, Vol. II, Chicago, IL.
13. Vanmarcke, E. H., Cornell, C. A., Gasparini, D. A., Hou, S. N., (1976), "SIMQKE: A Program for Artificial Motion Generation – User's Manual and Documentation," Department of Civil Engineering, M.I.T., Cambridge, MA

14. Zhu, Z. Y., Soong, T. T., (1998), "Toppling Fragility of Unrestrained Equipment," Earthquake Spectra, Vol. 14, No.4, 695-711.

## APPENDIX A DISCRETE SYSTEM ANALYSIS FOR SLIDING PROBLEM

```

/* slide-stick program for a block on ground attached with tendons */ /*
Written by Rahul Rana, Modified by Woon Hui Chong */

#include<stdio.h>
#include<math.h>

main(){

FILE *f1;
FILE *f2;
FILE *f10;
/*FILE *f5;*/
/*FILE *f3;
FILE *f4;
FILE *f5;
FILE *f6;
FILE *f7;
FILE *f8;
FILE *f9;*/

int i,j,k,N,NUM,n,l,parts;
int counter,stick,sgn,index,loop;

float quake[1024];
float s1,sd1,s2,sd2,sdd2,z2,zd2,zdd2,xg1,xg2,P1,Q2,Teq,ratio;
float
a,b,c,d,e,blah,tau,one,two,peak_displ,peak_vel,peak_acc,peak_displ_acc;
float minvel,DT,dt,mu,W,Wd,xi,T,D,theta,M;

char c1[]={'s','i','m','l','0','h','.', 'h','s','t','\0'};
char infile[20], outfile[20];
printf("enter the inputfile name:\n");
scanf("%s",infile);
printf("enter the outputfile name:\n");
scanf("%s",outfile);

f10=fopen(outfile,"w+");
f2=fopen(infile,"r");

for(loop=10;loop<100;loop++)

{

c1[3]=(loop/10)+48;
c1[4]=loop%10+48;

if ((f1=fopen(c1,"r"))==NULL) {
printf("sorry, cannot open file %s\n",c1);
}

/*f3=fopen("summary29","w");

f4=fopen("p_disp29","w");*/
/*f5=fopen("p_acc29","w");*/
/*f6=fopen("p_vel29","w");

f7=fopen("disp29_h","w");
f8=fopen("acc29_h","w");
f9=fopen("vel29_h","w");
*/
fscanf(f2,"%f %f %f %d",&minvel,&DT,&dt, &NUM);
/* minvel: If velocity falls below minvel, block is considered stuck. */
/* DT: The excitation data interval */
/* dt: Interval of integration */
/* NUM: total number of points to read from file 'excitation' */

```

```

n=ceil(DT/dt);
/* Input data file should have DT and dt such that DT/dt is an integer. 'ceil'
   is used here since DT/dt will be float which otherwise can't be assigned
   to int variable n */

N=(NUM-1)*n+1;

fscanf(f2, "%f %f %f %f %d", &mu, &W, &one, &two, &parts);

/* mu: coeff of friction */
/* W: natural frequency */
/* xi: damping ratio */

fscanf(f2, "%f %f %f %f %f", &T, &D, &a, &M, &ratio);
theta=a*M_PI/180.0;

/* T: Pretension in cable */
/* D: depth */
/* a: angle in degrees, theta: angle in radians.*/
/* M: Block mass */
/* Vertical ground acc = horizontal ground acc (file 'excitation') * ratio */

Teq=2*T*sin(theta);

for (i=0;i<NUM;i++){
    fscanf(f1, "%f %f", &a, &b);
    quake[i]=b*0.3;
}

for (l=0;l<=parts;l++) { /* looping over damping ratio */
peak_displ=peak_acc=peak_vel=0.0;

xi=one+(two-one)*l/parts;

Wd=W*sqrt(1-xi*xi);

blah=xi*W*dt;

stick=1; s1=sd1=xg1=0.0; index=0;

if ((parts==1) && (l==0)) {
/* save time-history if no damping ratio looping is done */

/*fprintf(f7, "%5.2f %10.5f\n", 0.0, 0.0);
fprintf(f8, "%5.2f %10.5f\n", 0.0, 0.0);
fprintf(f9, "%5.2f %10.5f\n", 0.0, 0.0);
*/
}

counter=0; /* counter for when to store results. the big for loop follows*/
for (k=0;k<N;k++){

/* now xg2 by interpolation of quake[] vector */

xg2=9.81*(quake[index]+(quake[index+1]-quake[index])*counter/n);

if (stick == 1) { /* block is sticking */
d=mu*(9.81+(Teq/M)+(xg1*ratio)); e=fabs(W*W*s1+xg1);

/* vertical acceleration = xg1*ratio. Teq is equivalent pretension in cable. */

if (d < e) {
stick=0; sgn=((xg1 > 0)? -1:+1);
}
else {

```



```

        s2=s1; sd2=0.0; sdd2=0.0;
    }
} /* if stick == 1 */

if (stick == 0) { /* block is sliding */
    P1=-(xg1+mu*(9.81+Teq/M+xg1*ratio)*sgn);
    Q2=-(xg2-xg1)-mu*sgn*(xg2-xg1)*ratio;
    c=pow(M_E,-blah);

    z2=c*(-((1-2*xi*xi)/(W*W*Wd*dt))*sin(Wd*dt)+((2*xi)/(W*W*W*dt))*cos(Wd*dt))*Q2 + c*((1/Wd)
    s2 = z2 + (1/(W*W))*(P1+(1-(2*xi)/(W*dt))*Q2);

    zd2 = -xi*W*z2 + Wd*c*(-((1-2*xi*xi)/(W*W*Wd*dt))*cos(Wd*dt)-((2*xi)/(W*W*W*dt))*sin(Wd*dt);
    sd2 = zd2 + Q2/(W*W*dt);

    zdd2 = -2*xi*W*zd2 - W*W*z2;

    sdd2 = zdd2;
    if (fabs(sd2)<minvel) stick=1; /* if vel < minvel, block sticks */
}

counter++;
if (counter == n) {
    index++;

    if ((parts==1) && (l==0))
{ /* save time-history if no damping ratio looping is done */

    tau=DT*index;
    /* fprintf(f7, "%5.2f %10.5f\n", tau,s2);
    fprintf(f8, "%5.2f %10.5f\n", tau,(sdd2+xg2)/9.81);
    fprintf(f9, "%5.2f %10.5f\n", tau,sd2);
    */
}
    if (counter==n) counter=0;

a=peak_displ;b=peak_vel;c=peak_acc;
d=sdd2+xg2;
if (fabs(s2) > fabs(a)) { peak_displ=fabs(s2); peak_displ_acc=fabs(d);}
if (fabs(sd2) > fabs(b)) peak_vel=fabs(sd2);

if (fabs(d) > fabs(c)) peak_acc=fabs(d);

    xg1=xg2; s1=s2; sd1=sd2; sgn=((sd2 > 0)? 1:-1);

} /* The big for loop */

fprintf(f10,"%10.5f %14.7f %14.7f\n",xi,peak_displ,peak_displ_acc);
/*fprintf(f4,"%10.5f %14.7f\n",xi,peak_displ);*/
/*fprintf(f5,"%10.5f %14.7f\n",xi,peak_acc/9.81);*/
/*fprintf(f6,"%10.5f %14.7f\n",xi,peak_vel);
*/

}/* looping over damping ratio */

fclose(f1);

}
fclose(f2);
/*fclose(f3);
fclose(f4);
fclose(f5);
fclose(f6);
fclose(f7);

```

```
fclose(f8);  
fclose(f9);*/  
fclose(f10);  
  
}
```

## APPENDIX B SIMQKE PROGRAM

```

PROGRAM SIMQK                                SIMQ  1
C                                             SIMQ  2
C   - SIMULATION OF EARTHQUAKE GROUND MOTIONS - SIMQ  3
C                                             SIMQ  4
C   DEVELOPED BY - E. H. VANMARCKE, C. A. CORNELL, SIMQ  5
C               D. A. GASPARINI AND S. N. HOU    SIMQ  6
C               DEPARTMENT OF CIVIL ENGINEERING SIMQ  7
C               MASSACHUSETTS INSTITUTE OF TECHNOLOGY SIMQ  8
C               CAMBRIDGE, MASSACHUSETTS 02139   SIMQ  9
C                                             SIMQ 10
C   PROGRAM DATE - AUGUST 1969, REVISED SEPTEMBER 1976 SIMQ 11
C                                             SIMQ 12
C   NOTES - THIS SOURCE DECK HAS BEEN MODIFIED FOR A CDC6400 SIMQ 13
C           - DUMMY SUBROUTINE PLOT CALLS (SC4020) HAVE BEEN INSERTED SIMQ 14
C                                             SIMQ 15
C           installiert auf VAX-11/780, H.G.Hartmann, 1-Jun-1988 SIMQ 16
C           - Bestimmung der Zufallszahl ver{ndert
C           - umgestellt von Inch auf Meter
C           - Eingabe eines Beschleunigungsspektrums m|glich
C
C INPUT PARAMETERS REQUIRED                    SIMQ 17
C                                             SIMQ 18
C IX--A STARTER FOR THE RANDOM NUMBER GENERATOR-IT MUST BE ODD SIMQ 19
C NPA---NUMBER OF DIFFERENT MOTIONS REQUIRED   SIMQ 20
C ICASE----=1 FOR STATIONARY CASE            SIMQ 21
C TL - THE LARGEST PERIOD VALUE FOR RESPONSE CALCULATIONS SIMQ 22
C TS - THE SMALLEST VALUE                    SIMQ 23
C TMIN,TMAX---OPTIONAL MINIMUM AND MAXIMUM PERIODS TO DETERMINE FREQUENSIMQ 24
C CONTENT OF THE MOTION. DEFAULT USES TS AND TL SIMQ 25
C NCYCLE---THE NUMBER OF ITERATIONS TO BE PERFORMED IS ONE LESS SIMQ 26
C THAN THIS NUMBER--IF NCYCLE = 1, NO ITERATION IS MADE SIMQ 27
C DELT -- TIME INTERVAL USED BETWEEN POINTS SIMQ 28
C NDAMP---NUMBER OF DIFFERENT DAMPINGS TO BE CONSIDERED SIMQ 29
C AMOR---ARRAY CONTAINING THE DAMPING VALUES SIMQ 30
C TRISE --- RISE TIME                        SIMQ 31
C TLVL --- INTERVAL AT THE HIGHEST AMPLITUDE SIMQ 32
C NGWK -- DEFINES TYPE OF SPECTRAL DENSITY FUNCTION USED SIMQ 33
C IF NGWK = 0 , THE PROGRAM GENERATES ITS OWN POWER SPECTRUM. SIMQ 34
C IF NGWK IS NOT = 0, THEN A PIECEWISE LINEAR POWER SPECTRUM SIMQ 35
C WILL BE PROVIDED BY USER AND NGWK = NUMBER OF POINTS THAT DEFINE IT. SIMQ 36
C IF NGWK IS NEGATIVE, THEN GWK WILL BE READ ALONG WITH PERIODS FOR SIMQ 37
C RESPONSE CALCULATIONS                      SIMQ 38
C ABS(NKK) = NUMBER OF POINTS FOR RESPONSE CALCULATIONS. SIMQ 39
C IF NKK IS POSITIVE, THE PROGRAM WILL GENERATE A STRING OF POINTS SIMQ 40
C ON A LOGARITHMIC SCALE FROM TS TO TL.      SIMQ 41
C IF NKK IS NEGATIVE, THE USER PROVIDES A LIST OF POINTS. SIMQ 42
C (TSV,SV0) - POINTS WHICH DEFINE DESIRED VELOCITY RESPONSE SPECTRUM SIMQ 43
C NRES---NUMBER OF POINTS WHICH DEFINE DESIRED VEL.RESPONSE SPECTRUM SIMQ 44
C IF NRES < 0, INPUT OF ACC. RESPONSE SPECTRUM
C IF NRES = 0, NO DATA NEED BE GIVEN(NO CYCLING ONLY). SIMQ 45
C (W0,GWK0) - POINTS THAT DEFINE POWER SPECTRUM IF NGWK IS NOT = 0. SIMQ 46
C TQ---OPTIONAL ARRAY OF PERIOD VALUES FOR RSPONSE CALCULATIONS. SIMQ 47
C AGMX --- MAX GROUND ACC INPUT UNIT IN M/S**2 SIMQ 48
C DUR --- DURATION                           SIMQ 49
C UNITS SECONDS,METER ---UNLESS SPECIFIED OTHERWISE SIMQ 50
C                                             SIMQ 51
C
C INTEGER*4 IX
C DIMENSION TQI(150)                          SIMQ 53
C DIMENSION RR(300)                            SIMQ 54
C DIMENSION YTITL(9),TITLO(9)                  SIMQ 55
C DIMENSION TIT(9),TIM(9),TIMX(9),TIMY(9),TIX(9),TITX(9),TITY(9) SIMQ 56
C DIMENSION ACCG(8001),WB(300),GWK(300),TIME(3001),FRQ(300), SIMQ 57
C 1 TQ(300),PLTVMX(10,300),AMOR(10),TITLE(20),IBUF(2000), SIMQ 58
C 2 FQ(1500),GWG(1500),PA(1500),DW(1500),TMD(10,300), SIMQ 59
C $ W0(300),GWK0(300),SV(300),TSV(1010),SV0(1010),SI(300) SIMQ 60
C * ,ANEWGK(300)                               SIMQ 61

```

```

DIMENSION PERCEN(300) SIMQ 62
-----
DIMENSION SAY(1010),VELROD(10)
CHARACTER*10 filename

EQUIVALENCE(TIME(1),FQ(1)),(TIME(1501),DW(1)),(GWG(1),PLTVMX(1)) SIMQ 63
DATA TIX/ 4H ,4H ,4HRESP,4HONSE,4H SPE,4HCTRU,4HM ,4H ,SIMQ 64
1 4H / SIMQ 65
DATA TIM/ 4H ,4H ,4HACCE,4HLERO,4HGRAM,4H ,4H ,4H ,SIMQ 66
1 4H / SIMQ 67
DATA BLANK / 4H / SIMQ 68
DATA TIT/ 4HRESP,4HONSE,4H SPE,4HCTRU,4HM D,4HAMPI,4HNG ,4H ,SIMQ 69
1 4H / SIMQ 70
DATA TITX/4H ,4H NA,4HTURA,4HL PE,4HRIOD,4H ,4H(SEC,4HONDS, SIMQ 71
1 4H) / SIMQ 72
DATA YTITL/ 4H ,4HG(W),4H - ,4H(M**,4H2/SE,4HC**3,4H) , SIMQ 73
1 4H ,4H / SIMQ 74
DATA TITLO/ 4HSPEC,4HTRAL,4H DEN,4HSITY,4H FUN,4HCTIO,4HN , SIMQ 75
1 4H ,4H / SIMQ 76
DATA TITY/4H ,4H ,4HMAXI,4HMUM ,4HVELO,4HCITY,4H (M,4H/SEC, SIMQ 77
1 4H) / SIMQ 78
DATA TIMX/4H ,4H ,4HTIME,4H (SE,4HCOND,4HS) ,4H ,4H ,SIMQ 79
1 4H / SIMQ 80
DATA TIMY/4H ,4HACCE,4HLERA,4HTION,4H ,4H G'S,4H ,4H ,SIMQ 81
1 4H / SIMQ 82
DATA BETAS,BETAL/0.005,0.2/,PI/3.14159/ SIMQ 83
ICONT=0 SIMQ 84
OPEN(UNIT =5,FILE='sim.inp',STATUS='OLD',FORM='FORMATTED')
OPEN(UNIT =6,FILE='SIM.OUT',status='unknown')
OPEN(UNIT=11,FILE='SIM.POW',status='unknown')
OPEN(UNIT=12,FILE='SIM.ACC',status='unknown')
OPEN(UNIT=13,FILE='SIM.RES',status='unknown')
C SIMQ 84
C REQUIRED INPUT PARAMETERS SIMQ 85
C SIMQ 86
9003 READ (5,1) TITLE SIMQ 87
C CALL STOIDV ('M5324-9950',9,0) SIMQ 88
-----
READ (5,9920) TS,TL,TMIN1,TMAX1,YMIN,YMAX,IUNIT SIMQ 89
IF(IUNIT.EQ.1) THEN
sclrod=9.81
ELSE
sclrod=386.4
ENDIF
C
READ (5,3020) ICASE,TRISE,TLVL,DUR,AO,ALFAO,BETAO,IPOW SIMQ 90
READ (5,129) DELT,AGMX,IIX,NDAMP,NCYCLE,NPA,NKK,NRES,NGWK,IPCH SIMQ 91
-----
AGMX=AGMX*sclrod
C
IF(IPCH.EQ.1)
*OPEN(UNIT=10,FILE='PUNCH',STATUS='UNKNOWN')
C SIMQ 93
C FIRST DAMPING VALUE MUST BE ONE WHICH IS CYCLED ON. SIMQ 94
C THE FIRST CURVE VALUE WILL BE PLOTTED (RESPONSE SPECTRUM) SIMQ 95
C SIMQ 96
C READ(5,7020) (AMOR(I),I=1,NDAMP) SIMQ 97
C WRITE (6,2) TITLE SIMQ 98
C WRITE(6,30) DELT SIMQ 99
C SIMQ 100
C IF (NKK.LE.0) GO TO 6301 SIMQ 101
C SIMQ 102
C OPTIONS 1 AND 2 SIMQ 103
C CALL PLTX2(TS,TL,TQ,NKK) SIMQ 104
C GO TO 3 SIMQ 105
C SIMQ 106

```

C	OPTION 3	SIMQ 107
	6301 NKK=-NKK	SIMQ 108
C		SIMQ 109
C	OPTIONAL INPUT PARAMETERS IF NKK IS NEGATIVE.	SIMQ 110
C	GWK IS REQUIRED ONLY IF NGWK IS NEGATIVE.	SIMQ 111
C		SIMQ 112
	READ (5,13) (TQ(I),I=1,NKK)	SIMQ 113
	READ (5,888) (GWK(NKK-I+1),I=1,NKK)	SIMQ 114
	READ (5,7020) N2,N3	SIMQ 115
14	READ (5,4262) TC,GWC	SIMQ 116
	IF (TC.GT.50.0) GO TO 5	SIMQ 117
	DO 9 I=1,NKK	SIMQ 118
	IF (ABS(TC-TQ(I)).LT.0.0002) GO TO 11	SIMQ 119
9	CONTINUE	SIMQ 120
	GO TO 14	SIMQ 121
11	GWK(NKK-I+1)=GWC	SIMQ 122
	GO TO 14	SIMQ 123
5	CONTINUE	SIMQ 124
	IF (N2.EQ.0) GO TO 3	SIMQ 125
	DO 10 I=1,N3	SIMQ 126
	READ (5,7020) TQ1,TQ2,RATIO	SIMQ 127
	DO 10 J=1,NKK	SIMQ 128
	IF (TQ(J).GT.TQ1.AND.TQ(J).LT.TQ2) GWK(NKK-J+1)=GWK(NKK-J+1)*RATIO	SIMQ 129
10	CONTINUE	SIMQ 130
3	DO 4325 I=1,NKK	SIMQ 131
	J=NKK-I+1	SIMQ 132
	FRQ(I)=1./TQ(I)	SIMQ 133
4325	WB(J)=6.2832/TQ(I)	SIMQ 134
	IF (TMIN1.EQ.0.) TMIN1=TS	SIMQ 135
	WL=6.2832/TMIN1	SIMQ 136
	IF (TMAX1.EQ.0.) TMAX1=TL	SIMQ 137
	WS=6.2832/TMAX1	SIMQ 138
C		SIMQ 139
C	WEND --- THE HIGHEST FREQUENCY FOR GROUND MOTION	SIMQ 140
C	WBEGIN --- THE LOWEST FREQUENCY FOR GROUND MOTION	SIMQ 141
C	THE FOLLOWING OPTIONS FOR COMPUTING WEND AND WBEGIN MAY BE	SIMQ 142
C	ELIMINATED SINCE BETAL AND BETAS HAVE BEEN DEFINED INTERNALLY BY	SIMQ 143
C	THE PROGRAM TO BE 0.2 AND 0.005 RESPECTIVELY	SIMQ 144
C		SIMQ 145
	WEND=2.0*WL	SIMQ 146
	IF ((5.0*BETAL).GE.1.0) WEND=WL*(1.+5.*BETAL)	SIMQ 147
	WBEGIN=WS*.5	SIMQ 148
	IF (BETAL.LT.0.05) WBEGIN=WS*(1.-10.*BETAL)	SIMQ 149
	IF (ICASE.GT.1) GO TO 42	SIMQ 150
C		SIMQ 151
C	NO INTENSITY ENVELOPE USED	SIMQ 152
	WRITE(6,134)	SIMQ 153
	GO TO 38	SIMQ 154
42	WRITE(6,135)	SIMQ 155
38	WRITE(6,106)AGMX	SIMQ 156
	IF (NRES.EQ.0) GO TO 6022	SIMQ 157
C	-----	
C		
C	IOP = 1 MEANS THE INPUT ARE DISPLACEMENT SPECTRUM	
C	IOP = 2 MEANS THE INPUT ARE VELOCITY SPECTRUM	
C	IOP = 3 MEANS THE INPUT ARE ACCELERATION SPECTRUM	
C	SAY(I) VALUE OF THE GIVEN SPECTRUM ( D or V or A)	
	READ(5,*) IOP	
	READ(5,*) (TSV(I),SAY(I),I=1,NRES)	
C		
C	-----	
	CALL CONVERT (TSV,SAY,NRES,IOP,SV0)	
	CALL POLATE(NRES,NKK,TSV,SV0,TQ,SV)	SIMQ 159
	WRITE(6,107) TRISE,TLVL,DUR	SIMQ 160
	WRITE(6,6016)	SIMQ 161
6022	IF (NGWK.EQ.0) GO TO 4260	SIMQ 162

```

          IF(NGWK.LT.0) GO TO 9703                                SIMQ 163
C
C   OPTIONAL INPUT OF ORIGINAL POWER SPECTRUM IF NGWK IS POSITIVE SIMQ 164
C   IF TQ WAS READ IN PREVIOUSY FOR NKK NEGATIVE, THIS OVERRIDES POWER SIMQ 165
C   SPECTRUM 'GWK' READ IN WITH 'TQ'.                          SIMQ 166
C                                                                SIMQ 167
C                                                                SIMQ 168
C                                                                SIMQ 169
C   OPTIONAL INPUT OF DESIRED RESPONSE VELOCITY                 SIMQ 170
C   SPECTRUM IF CYCLING IS USED.                                SIMQ 171
C                                                                SIMQ 172
          READ (5,4262) (W0(I),GWK0(I),I=1,NGWK)                SIMQ 173
          CALL POLATE(NGWK,NKK,W0,GWK0,WB,GWK)                   SIMQ 174
9703  DO 8011 I=1,NKK                                           SIMQ 175
          J=NKK+1-I                                             SIMQ 176
          GWK0(I)=GWK(I)                                         SIMQ 177
8011  WRITE(6,4340) TQ(I),FRQ(I),GWK(J)                        SIMQ 178
          GO TO 6007                                             SIMQ 179
4260  T=(DUR+TLVL)/2.                                          SIMQ 180
          BETA=AMOR(1)                                           SIMQ 181
          CALL SVGW(NKK,WB,GWK0,SV,T,BETA,16.0,0.6,0.368,GSUM,WCP,QP,RR) SIMQ 182
          INULL=0
          DO 6001 LLL=1,NKK                                       SIMQ 183
          LL1=NKK-LLL+1                                          SIMQ 184
          WRITE(11,889)FRQ(LL1),GWK0(LL1)
6001  WRITE(6,8901)TQ(LL1),FRQ(LL1),GWK0(LL1),RR(LL1)        SIMQ 185
          WRITE(11,27) INULL
          WRITE (6,8902) WCP,QP                                  SIMQ 186
C   SET THE MAXIMUM VALUE OF SPECTRAL DENSITY FUNCTION FOR PLOT SIMQ 187
          XMAX= 0.0                                             SIMQ 188
          DO 327 I12= 1,NKK                                       SIMQ 189
          IF (XMAX-GWK0(I12)) 326,327,327                       SIMQ 190
326  XMAX=GWK0(I12)                                             SIMQ 191
327  CONTINUE                                                  SIMQ 192
          IF (XMAX-70.0) 329,328,328                             SIMQ 193
328  XLAI=XMAX/100.                                            SIMQ 194
          NDUM=(IFIX(XLAI)+1)*100                                SIMQ 195
          XMAX=FLOAT(NDUM)                                       SIMQ 196
          GO TO 330                                              SIMQ 197
329  XMAX=70.0                                                 SIMQ 198
330  CONTINUE                                                  SIMQ 199
          CALL GWPLOT (NKK,0.01,4.0,0.0,XMAX,TQ,GWK0,TITX,TITLO,YTITL) SIMQ 200
          AREA=SQRT(GSUM)                                        SIMQ 201
          WRITE(6,6008) AREA                                     SIMQ 202
6007  ITOTAL=NDAMP*NKK                                         SIMQ 203
          IX=(IIX/2)*2+1                                         SIMQ 204
C-----                                                        SIMQ 205
C   LOOP OVER NPA, NUMBER OF ARTIFICIAL EARTHQUAKES DESIRED SIMQ 206
C-----
          DO 585 NTOTAL=1,NPA                                    SIMQ 207
C-----
C   Open output files for time-history and response spectras
          WRITE(filename,9901) NTOTAL+9,'h.hst'
          OPEN(UNIT=20,FILE=filename,STATUS='UNKNOWN')
          WRITE(filename,9901) NTOTAL+9,'d.spc'
          OPEN(UNIT=21,FILE=filename,STATUS='UNKNOWN')
          WRITE(filename,9901) NTOTAL+9,'v.spc'
          OPEN(UNIT=22,FILE=filename,STATUS='UNKNOWN')
          WRITE(filename,9901) NTOTAL+9,'a.spc'
          OPEN(UNIT=23,FILE=filename,STATUS='UNKNOWN')
9901  FORMAT('sim',I2,5A)

          WRITE(6,60) IX                                         SIMQ 208
          DO 8608 I=1,NKK                                         SIMQ 209
8608  GWK(I)=GWK0(I)                                           SIMQ 210
          MM=1                                                    SIMQ 211
          AREAG=0.                                               SIMQ 212

```

	SIGMS=0.	SIMQ 213
	NFQ=0	SIMQ 214
	W=WBEGIN	SIMQ 215
4080	DELW=BETAS*W	SIMQ 216
	W=W+DELW	SIMQ 217
	CALL DUMMY(W,FOUT,NKK,WB,GWK,MM)	SIMQ 218
	NFQ=NFQ+1	SIMQ 219
	GWG(NFQ)=FOUT	SIMQ 220
	FQ(NFQ)=W	SIMQ 221
	DW(NFQ)=DELW	SIMQ 222
	AREAG=AREAG+GWG(NFQ)*DELW	SIMQ 223
	SIGMS=SIGMS+GWG(NFQ)*DELW*W*W	SIMQ 224
	IF (W.LT.WEND) GO TO 4080	SIMQ 225
C		SIMQ 226
C	LOOP OVER NCYCLE, TO SMOOTHEN RESPONSE SPECTRUM FOR TARGET DAMPING	SIMQ 227
	DO 100 ICYCLE=1,NCYCLE	SIMQ 228
C		SIMQ 229
C	W IS LOWEST FREQUENCY REPRESENTED IN GROUND MOTION.	SIMQ 230
C		SIMQ 231
	IF (ICYCLE.LE.1) GO TO 1116	SIMQ 232
	AREAG=0.	SIMQ 233
	MM=1	SIMQ 234
	DO 6703 I=1,NFQ	SIMQ 235
	W=FQ(I)	SIMQ 236
	CALL DUMMX(W,FOUT,NKK,WB,GWK,MM)	SIMQ 237
	GWG(I)=FOUT	SIMQ 238
6703	AREAG=AREAG+DW(I)*GWG(I)	SIMQ 239
1116	DO 1117 IP=1,NFQ	SIMQ 240
1117	GWG(IP)=GWG(IP)*DW(IP)*2.	SIMQ 241
	IF(ICYCLE.GT.1) GO TO 8603	SIMQ 242
C		SIMQ 243
C	COMPUTE AVERAGE FREQUENCY AND PERIOD	SIMQ 244
C		SIMQ 245
	SIGMS=SIGMS/AREAG	SIMQ 246
	WA=SQRT(SIGMS)	SIMQ 247
	TA=6.2832/WA	SIMQ 248
C		SIMQ 249
C	DEFINE SLOPES OF ENVELOPE	SIMQ 250
C		SIMQ 251
	IF (ICASE.GT.2) GO TO 6	SIMQ 252
	IF(TRISE.GT..0) GO TO 33	SIMQ 253
	TRISE=0.25*DUR	SIMQ 254
	TLVL=0.	SIMQ 255
33	IF(ICASE.LE.1) GO TO 7	SIMQ 256
8	FTC1=1./TRISE	SIMQ 257
	FTC2=-1./(DUR-TRISE-TLVL)	SIMQ 258
	GO TO 6	SIMQ 259
7	FTC1=0.5	SIMQ 260
	FTC2=0.	SIMQ 261
	6 WRITE(6,114) WA,TA,NFQ,WBEGIN,WEND	SIMQ 262
C		SIMQ 263
C	COMPUTE RANDOM PHASE ANGLES	SIMQ 264
C		SIMQ 265
	DO 31 I=1,NFQ	SIMQ 266
C*IBM*YI=IX*65539		SIMQ 267
C	IY=IX*16777219	CDC ONLY
C	IF (IY.GE.0.) GO TO 32	SIMQ 268
C*IBM*YI=IY+2147483647+1		SIMQ 269
C	IY=IY+140737488355327+1	CDC ONLY
C	32 YFL=IY	SIMQ 270
C*IBM*YFL=YFL*.4656613E-9		SIMQ 271
C	YFL=YFL*.71054273576010E-14	CDC ONLY
cc	CALL RANDOM(YFL)	
	YFL=RAN(IX)	
	PA(I)=6.2832* YFL	SIMQ 272
C	31 IX=IY	SIMQ 273

31	CONTINUE	
C		SIMQ 274
C	ACCELERATION COMPUTATIONS	SIMQ 275
C		SIMQ 276
8603	NACCG=DUR/DELT+1.000001	SIMQ 277
	IF(NCYCLE.LE.ICYCLE) GO TO 9801	SIMQ 278
	WRITE(6,9008) ICYCLE,TQ(1)	SIMQ 279
	WRITE(6,9567)	SIMQ 280
9801	DO 1114 KK=1,NACCG	SIMQ 281
1114	ACCG(KK)=0.	SIMQ 282
	KCHEK=1000	SIMQ 283
	DO 12 LM=1,NFQ	SIMQ 284
	IF(GWG(LM).LT.0.0) WRITE(6,3000) GWG(LM),LM	SIMQ 285
	GWG(LM)=ABS(GWG(LM))	SIMQ 286
	AA=SQRT(GWG(LM))	SIMQ 287
	ALFA=FQ(LM)*DELT	SIMQ 288
	SINA=SIN(ALFA)	SIMQ 289
	COSA=COS(ALFA)	SIMQ 290
	SN=SIN(PA(LM))	SIMQ 291
	CN=COS(PA(LM))	SIMQ 292
	SNA=SINA*CN+COSA*SN	SIMQ 293
	CNA=COSA*CN-SINA*SN	SIMQ 294
	ACCG(2)=AA*SNA+ACCG(2)	SIMQ 295
	DO 12 KK=3,NACCG	SIMQ 296
	IF(KK.GE.KCHEK) GO TO 5012	SIMQ 297
	SNO=SNA	SIMQ 298
	SNA=SNA*COSA+CNA*SINA	SIMQ 299
	CNA=CNA*COSA-SNO*SINA	SIMQ 300
	GO TO 12	SIMQ 301
5012	KCHEK=KCHEK+1000	SIMQ 302
	SNA=SIN(PA(LM)+(KK-1)*ALFA)	SIMQ 303
	CNA=COS(PA(LM)+(KK-1)*ALFA)	SIMQ 304
12	ACCG(KK)=AA*SNA+ACCG(KK)	SIMQ 305
C		SIMQ 306
	GO TO (3003,3003,3004,3007),ICASE	SIMQ 307
C		SIMQ 308
C	TRAPEZOIDAL INTENSITY ENVELOPE	SIMQ 309
3003	IF(ICASE.LE.1) GO TO 18	SIMQ 310
	TX=TRISE	SIMQ 311
	GO TO 19	SIMQ 312
18	TX=2.	SIMQ 313
C		SIMQ 314
C	DEFINE MAXIMUM HEIGHTS IN TERMS OF SLOPES	SIMQ 315
C		SIMQ 316
19	DO 16 KK=2,NACCG	SIMQ 317
	TI=(KK-1)*DELT	SIMQ 318
	IF(TI.GT.TX) GO TO 15	SIMQ 319
	FT=FTC1*TI	SIMQ 320
	GO TO 16	SIMQ 321
15	IF(ICASE.LE.1) GO TO 28	SIMQ 322
	IF((TI-TX-TLVL).GT.0.) GO TO 29	SIMQ 323
28	FT=1.	SIMQ 324
	GO TO 16	SIMQ 325
29	FT=1.+(TI-TX-TLVL)*FTC2	SIMQ 326
C		SIMQ 327
C	COMPUTE ACCELERATION	SIMQ 328
C		SIMQ 329
16	ACCG(KK)=ACCG(KK)*FT	SIMQ 330
	GO TO 3011	SIMQ 331
C		SIMQ 332
C	EXPONENTIAL INTENSITY ENVELOPE	SIMQ 333
3004	DO 3006 KK=2,NACCG	SIMQ 334
	TI=(KK-1)*DELT	SIMQ 335
	FT=AO*(EXP(-ALFAO*TI)-EXP(-BETAO*TI))	SIMQ 336
3006	ACCG(KK)=ACCG(KK)*FT	SIMQ 337
	GO TO 3011	SIMQ 338



C		SIMQ 339
C	COMPOUND INTENSITY ENVELOPE	SIMQ 340
	3007 DO 3010 KK= 2,NACCG	SIMQ 341
	TI=(KK-1)*DELT	SIMQ 342
	IF(TI.GE.TRISE) GO TO 3008	SIMQ 343
	FT=(TI/TRISE)**IPOW	SIMQ 344
	GO TO 3010	SIMQ 345
C	3008 IF ((TI-TLVL-TRISE).LT.0.) GO TO 3009	SIMQ 346
	3008 IF (TI.LE.TLVL) GO TO 3009	
	FT=EXP(-ALFAO*(TI-TLVL))	SIMQ 347
	GO TO 3010	SIMQ 348
	3009 FT=1.0	SIMQ 349
	3010 ACCG(KK)=ACCG(KK)*FT	SIMQ 350
	3011 CONTINUE	SIMQ 351
C		SIMQ 352
C	COMPUTE MAX GROUND ACCELERATION BEFORE BASELINE CORRECTION	SIMQ 353
C		SIMQ 354
	20 AMAXIM=0.	SIMQ 355
	DO 5000 I=1,NACCG	SIMQ 356
	IF(ABS(ACCG(I)).LT.ABS(AMAXIM)) GO TO 5000	SIMQ 357
	AMAXIM=ACCG(I)	SIMQ 358
	TMAXIM=(I-1)*DELT	SIMQ 359
	5000 CONTINUE	SIMQ 360
	IF (NCYCLE.GT.ICYCLE) GO TO 8504	SIMQ 361
	WRITE(6,5200) AMAXIM,TMAXIM	SIMQ 362
	8504 T1=-DELT*0.5	SIMQ 363
C		SIMQ 364
C	JUSTIFY ACCG TO ZERO FINAL VELOCITY	SIMQ 365
C		SIMQ 366
	BETA1=0.	SIMQ 367
	BETA2=0.	SIMQ 368
	BETA3=0.	SIMQ 369
	VEL=0.	SIMQ 370
	DO 4300 IZ=1,NACCG	SIMQ 371
	VEL=VEL+ACCG(IZ)*DELT	SIMQ 372
	T1=T1+DELT	SIMQ 373
	BETA1=BETA1+VEL*T1	SIMQ 374
	BETA2=BETA2+VEL*T1*T1	SIMQ 375
	4300 BETA3=BETA3+VEL*T1*T1*T1	SIMQ 376
	BETA1=BETA1*DELT/(T1*T1*T1)	SIMQ 377
	BETA2=BETA2*DELT/(T1*T1*T1*T1)	SIMQ 378
	BETA3=BETA3*DELT/(T1*T1*T1*T1*T1)	SIMQ 379
	C1=300.*BETA1-900.*BETA2+630.*BETA3	SIMQ 380
	C2=(-1800.*BETA1+5760.*BETA2-4200.*BETA3)/T1	SIMQ 381
	C3=(1890.*BETA1-6300.*BETA2+4725.*BETA3)/(T1*T1)	SIMQ 382
	DO 4310 IZ=1,NACCG	SIMQ 383
	TI=(IZ-1)*DELT	SIMQ 384
	4310 ACCG(IZ)=ACCG(IZ)-C1-C2*TI-C3*TI*TI	SIMQ 385
C		SIMQ 386
C	GET MAXIMUM GROUND ACCELERATION	SIMQ 387
C		SIMQ 388
	GAMX=ACCG(1)	SIMQ 389
	VEL=0.	SIMQ 390
	VAMX=0.	SIMQ 391
	DISP=0.	SIMQ 392
	DMAX=0.	SIMQ 393
	LL1=0	SIMQ 394
	GAMX=ABS(GAMX)	SIMQ 395
	DO 59 LL=2,NACCG	SIMQ 396
	GAMY=ABS(ACCG(LL))	SIMQ 397
	VEL=VEL+ACCG(LL)*DELT	SIMQ 398
	DISP=DISP+VEL*DELT	SIMQ 399
	DAMY=ABS(DISP)	SIMQ 400
	VAMY=ABS(VEL)	SIMQ 401
	IF (DAMY.LE.DMAX) GO TO 52	SIMQ 402
	53 DMAX=DAMY	SIMQ 403

52	IF (VAMY.LE.VAMX) GO TO 56	SIMQ 404
	VAMX=VAMY	SIMQ 405
56	IF (GAMY.LE.GAMX) GO TO 59	SIMQ 406
58	GAMX=GAMY	SIMQ 407
	LL1=LL	SIMQ 408
59	CONTINUE	SIMQ 409
C		SIMQ 410
C	NO SCALING OF THE ENTIRE TIME HISTORY IS DONE BUT PEAKS ARE	SIMQ 411
C	ADJUSTED IN ORDER TO HAVE ONLY ONE PEAK EQUAL TO THE SPECIFIED	SIMQ 412
C	MAXIMUM GROUND ACCELERATION.	SIMQ 413
	TTT=ABS(GAMX/AGMX)	SIMQ 414
	IF(TTT.LE.1.) GO TO 1112	SIMQ 415
	DO 111 K1=1,NACCG	SIMQ 416
	DAR=ABS(ACCG(K1))-AGMX	SIMQ 417
	IF(DAR.LE.0.) GO TO 111	SIMQ 418
	ACCG(K1)=ACCG(K1)/TTT	SIMQ 419
111	CONTINUE	SIMQ 420
	GO TO 1113	SIMQ 421
1112	ACCG(LL1)=ACCG(LL1)/TTT	SIMQ 422
-----		
1113	GAMX=AGMX/sclrod	SIMQ 423
	LIM=NDAMP	SIMQ 424
	IF (ICYCLE.LT.NCYCLE) LIM=1	SIMQ 425
C		SIMQ 426
C	CHECK ACCG DIMENSIONS	SIMQ 427
C		SIMQ 428
	ICK=NACCG+2.*TQ(NKK)/DELT	SIMQ 429
	IF (ICK.GE.8000) WRITE (6,34) ICK	SIMQ 430
	IF (ICK.GE.8000) GO TO 9003	SIMQ 431
C		SIMQ 432
C	RESPONSE CALCULATION AND PLOTTING	SIMQ 433
C		SIMQ 434
	CALL SPECT(PLTVMX,TMD,ACCG,NACCG,DELT,TQ,NKK,AMOR,LIM)	SIMQ 435
	IF(IPCH.EQ.1) THEN	
	WRITE(10,27) ICYCLE	
	WRITE(10,13)(TQ(I),I=1,NKK)	
	WRITE(10,888)(GWK(NKK-I+1),I=1,NKK)	
	ENDIF	
	IF(NCYCLE.LE.ICYCLE) GO TO 44	SIMQ 440
C		SIMQ 441
C	CYCLING PROCEDURE WHICH MODIFIES G(W) TO SMOOTHEN THE CALCULATED	SIMQ 442
C	RESPONSE SPECTRUM	SIMQ 443
C		SIMQ 444
	SUMPOS = 0.	SIMQ 445
	SUMNEG = 0.	SIMQ 446
	DO 43 I=1,NKK	SIMQ 447
	AMULT=SV(I)/PLTVMX(1,I)	SIMQ 448
	RATIOS = ABS (1./AMULT)*100.	SIMQ 449
	PERCEN(I) = RATIOS - 100.	SIMQ 450
	WRITE(6,8901) TQ(I),FRQ(I),GWK(NKK-I+1),SV(I),PLTVMX(1,I),	SIMQ 451
	* PERCEN(I),TMD(1,I),I	SIMQ 452
	J=NKK-I+1	SIMQ 453
10002	ANEWGR(J) = GWK(J)*AMULT*AMULT	SIMQ 454
	AINCRM = ANEWGR(J)-GWK(J)	SIMQ 455
	IF (AINCRM.GE.0.) SUMPOS = SUMPOS+AINCRM	SIMQ 456
	IF (AINCRM.LT.0.) SUMNEG = SUMNEG-AINCRM	SIMQ 457
43	CONTINUE	SIMQ 458
	IF (SUMNEG.LE.1.E-8) GO TO 213	SIMQ 459
	FACTOR = SUMPOS/SUMNEG	SIMQ 460
	WRITE (6,10000) SUMPOS,SUMNEG,FACTOR	SIMQ 461
	DO 211 I=1,NKK	SIMQ 462
211	GWK(I) = ANEWGR(I)	SIMQ 463
	GO TO 100	SIMQ 464
C		SIMQ 465
C	OPTION THAT MAKES NO CHANGES IN POSITIVE INCREMENTS WHEN SUMNEG	SIMQ 466

```

C      IS LESS THAN 1.0E-8
C
213 DO 214 I=1,NKK
214 GWK(I) = ANEWGK(I)
      GO TO 100
C
C      WRITE MAXIMUM RESPONSE VALUE
C
44 CONTINUE
-----
      GAMXM=GAMX*sclrod

      WRITE(6,120)GAMXM,VAMX,DMAX
      DO 17 I=1,NACCG
17 ACCG(I)=ACCG(I)
      WRITE(6,5203) (ACCG(I),I=1,NACCG)
CRRR Output for the time history
      DO I=1,NACCG
cc      WRITE(12,4111) (I-1)*DELT,ACCG(I)
CRRR      WRITE(20,4111) (I-1)*DELT,ACCG(I)/9.81

      ENDDO
cc      WRITE(12,4112)DELT,DMAX,VAMX,GAMXM
-----
CRRR Changed by REV
CRRR Loop for the frequency
      DO N=1,NKK
          FREQ=FRQ(N)
          OM=2.0*PI*FREQ
          DO LL=1,NDAMP
              VELROD(LL)=ABS(PLTVMX(LL,N))
          ENDDO
          WRITE(21,9902) 1.0/FREQ,(VELROD(LL)/OM,LL=1,NDAMP)
          WRITE(22,9902) 1.0/FREQ,(VELROD(LL),LL=1,NDAMP)
          WRITE(23,9902) 1.0/FREQ,(VELROD(LL)*OM,LL=1,NDAMP)
9902 FORMAT(1X,F12.4,10E16.6)
      ENDDO
cc      DO 9012 LL=1,NDAMP
cc      WRITE(6,4535) AMOR(LL)
cc      CAM=AMOR(LL) * 100.
cc      DO 37 N=1,NKK
cc      FREQ=FRQ(N)
cc      OM=2.*PI*FREQ
cc      RVEL=ABS(PLTVMX(LL,N))
cc      RDIS=RVEL/OM
cc      RACC=RVEL*OM
cc 37 WRITE(13,889) FREQ,RDIS,RVEL,RACC
cc      WRITE(13,9016) CAM
cc 9012 WRITE(6,4340) (TQ(KK),FRQ(KK),PLTVMX(LL,KK),TMD(LL,KK),KK,
cc      $      kk=1,nkk)

      IF (NRES.EQ.0) GOTO 100
      WRITE(6,9567)
      DO 23 I=1,NKK
          AMULT=SV(I)/PLTVMX(1,I)
          RATIOS = ABS(1./AMULT)*100.
          PERCEN(I) = RATIOS - 100.
          WRITE(11,889)FRQ(NKK-I+1),GWK(I),SV(NKK-I+1),PLTVMX(1,NKK-I+1)
23 WRITE(6,8901) TQ(I),FRQ(I),GWK(NKK-I+1),SV(I),PLTVMX(1,I),
* PERCEN(I),TMD(1,I),I
          WRITE(11,27) ICYCLE
          DO 21 II=1,NDAMP
          DO 21 JJ=1,NKK
21 PLTVMX(II,JJ)=ABS(PLTVMX(II,JJ))
          NFC=2

```

```

DO 1000 II=1,NDAMP
DO 1001 J=1,NKK
1001 SI(J)=PLTVMX(II,J)
XAMOR=AMOR(II)
CALL DIB2 (NFC,4,1,0,NKK,TS,TL,YMIN,YMAX,1.,1.,0,0,0,0,-2,-2,
$TQ,SI,SV,TIX,TITX,TITY,36,36,36,0,0.,XAMOR)
1000 CONTINUE
100 CONTINUE
-----
CLOSE(20)
CLOSE(21)
CLOSE(22)
CLOSE(23)

585 CONTINUE
-----
C
C END OF LOOP OVER NPA (Number of artificial earthquakes)
C
-----
IF(NKK.GT.0)GOTO1100
1100 CALL PLTND(KIKI)
STOP
C
1 FORMAT (20A4)
2 FORMAT(1H1,/,2X,20A4)
13 FORMAT (10F8.4)
22 FORMAT (2I10)
27 FORMAT (1X,14HGWK FOR CYCLE ,I2)
30 FORMAT (/,7X,17H TIME INCREMENT = ,F8.6)
34 FORMAT (2X,55HACCG ARRAY NOT ENOUGH FOR NACCG+2*(LARGEST PERIOD)/DSIMQ
*T = ,I5)
60 FORMAT (/,10X,34HA NEW PHASE ANGLE SET WITH SEED = ,I10)
106 FORMAT (7X,30HEXPECTED MAXIMUM GROUND ACC = ,F7.2,' M/S**2')
107 FORMAT (7X,7HTRISE = ,F7.2,2X,8HTLEVEL = ,F7.2,2X,10HDURATION = ,F7.2SIMQ
*)
114 FORMAT (/,10X,29HCENTRAL CIRCULAR FREQUENCY = ,F10.4,13H RADIANS/SIMQ
*SEC.,/,10X,17HCENTRAL PERIOD = ,F8.4,8H SECONDS,/,10X,25HNUMBER SIMQ
*OF PHASE ANGLES = ,I5,/,10X,29HLOWEST FREQUENCY IN MOTION = ,F10.5SIMQ
*5,13H RADIANS/SEC.,/,10X,30HHIGHEST FREQUENCY IN MOTION = ,F10.5,SIMQ
*13H RADIANS/SEC.)
120 FORMAT (/,10X,30HMAXIMUM GROUND ACCELERATION = ,F6.3,' M/S**2'//,SIMQ
* 10X,26HMAXIMUM GROUND VELOCITY = ,F6.3,' M/S',// SIMQ
* 10X,30HMAXIMUM GROUND DISPLACEMENT = ,F6.3,' M',//, SIMQ
* 20X,29HSIMULATED GROUND ACCELERATION,//)
129 FORMAT (2F10.4,I10,8I5)
134 FORMAT(7X,15HSTATIONARY CASE)
135 FORMAT(7X,59HNON-STATIONARY IN INTENSITY BUT STATIONARY IN FREQ SPSIMQ
/ECTRUM)
301 FORMAT (8F9.5,I8)
888 FORMAT (6F13.3)
889 FORMAT (F15.5,3E15.5)
3000 FORMAT (1X,20HGWG NEGATIVE. EQUALS ,E10.3,2X,10HFOR LM OF ,I5)
3020 FORMAT (I5,6F10.4,I5)
4111 FORMAT(F12.4,4X,E15.7)
4112 FORMAT(2X,'DELT='F9.5', MAXD='E12.5', MAXV='E12.5', MAXA='E12.5)
4262 FORMAT (2F10.4)
4340 FORMAT (1X,4F14.4,I10)
4535 FORMAT (1H1,1X,10HDAMPING = ,F6.3,/,9X,6HPERIOD,6X,9HFREQUENCY,
* 7X,8HRESPONSE,6X,4H TIME,/)
5200 FORMAT (1H ,/,10X,29HMAX. ACCEL. BEFORE CORRECTION,F12.5,//
* 10X,7HAT TIME,F12.5,/)
5203 FORMAT (5H ,15F8.4)
6008 FORMAT (/,11X,31HSTANDARD DEVIATION OF PROCESS = ,F7.4,' M/S**2')
6016 FORMAT (/,11X,23HORIGIONAL POWER SPECTRUM,/,11X,6HPERIOD,8X,
* 9HFREQUENCY,7X,8HSPECTRUM,12X,1HR,/)
7020 FORMAT(8G10.0)
9920 FORMAT(6G10.0,I2)

```

```

8901 FORMAT (5(4X,E14.5),4X,F14.1,4H PCT,2X,F14.3,I10) SIMQ 575
8902 FORMAT (//,10X,24H CENTRAL FREQUENCY WC = ,F10.3,//,10X,26H DISPERSIMQ 576
*SION PARAMETER Q = ,F10.3,/) SIMQ 577
9008 FORMAT (1H1 ,30X,12HCYCLE NUMBER ,I2,20X,25HLOWEST MODIFIED PERIODSIMQ 578
* = ,F10.4,2X,7HSECONDS,/) SIMQ 579
9015 FORMAT(10F8.4) SIMQ 580
9016 FORMAT (1X,7HDAMPING,2X,F4.1,8H PERCENT) SIMQ 581
9102 FORMAT (F9.6,63X,I8) SIMQ 582
9567 FORMAT (///,9X,6HPERIOD,8X,9HFREQUENCY,4X,13HPOW.SPEC.DEN.,5X, SIMQ 583
* 12HDES.RESPONSE,4X,12HCAL.RESPONSE,7X,10HDIFFERENCE,9X,4HTIME,/)SIMQ 584
10000 FORMAT (//,10X,8HSUMPOS =,F12.3,10X,8HSUMNEG =,F12.3,10X,8HFACTOR SIMQ 585
* =,F12.3) SIMQ 586
C SIMQ 587
END SIMQ 588
-----
SUBROUTINE PLTX2(XMIN,XMAX,X,NPOINT) PLTX 1
-----
DIMENSION X(1) PLTX 2
POINT=NPOINT-1 PLTX 3
SPACE=ALOG10(XMAX/XMIN)/POINT PLTX 4
X(1)=XMIN PLTX 5
DO 1 I=2,NPOINT PLTX 6
AI=I-1 PLTX 7
EXPO=SPACE*AI PLTX 8
1 X(I)=XMIN*10.**EXPO PLTX 9
X(NPOINT)=XMAX PLTX 10
RETURN PLTX 11
END PLTX 12
-----
SUBROUTINE POLATE (N,M,XIN,YIN,XOUT,YOUT) POLA 1
-----
DIMENSION XIN(1),YIN(1),XOUT(1),YOUT(1) POLA 2
J=1 POLA 3
IF (XIN(1)-XOUT(1)) 2,2,100 POLA 4
2 IF (XIN(N)-XOUT(M)) 100,3,3 POLA 5
3 DO 30 I=1,M POLA 6
6 IF (XOUT(I)-XIN(J)) 5,40,4 POLA 7
4 J=J+1 POLA 8
GO TO 6 POLA 9
5 J=J-1 POLA 10
YTEST=(ALOG(YIN(J+1))-ALOG(YIN(J)))*(ALOG(XOUT(I))-ALOG(XIN(J)))/ POLA 11
1 (ALOG(XIN(J+1))-ALOG(XIN(J)))+ALOG(YIN(J)) POLA 12
YOUT(I)=EXP(YTEST) POLA 13
GO TO 30 POLA 14
40 YOUT(I)=YIN(J) POLA 15
30 CONTINUE POLA 16
RETURN POLA 17
100 WRITE (6,20) POLA 18
20 FORMAT (1H1,1X, 53HPROGRAM STOP. FUNCTION UNDEFINED IN DESIRED INTPOLA 19
1ERVAL ) POLA 20
STOP POLA 21
END POLA 22
-----
SUBROUTINE SVGW(NKK,W,GW,SV,S,B,WC,Q,P,XLAM0,WCP,QP,RR) SVGW 1
-----
DIMENSION GW(1),W(1),SV(1),RR(1) SVGW 2
PI=3.14159 SVGW 3
PI2=6.2831852 SVGW 4
GSUM=0. SVGW 5
DO 1000 I=1,NKK SVGW 6
NW=NKK-I+1 SVGW 7
POW=2.*B*W(I)*S SVGW 8
IF(POW.GT.50.0) GO TO 610 SVGW 9
TRANS=1.-EXP(-POW) SVGW 10
GO TO 611 SVGW 11
610 TRANS=1. SVGW 12

```

611	BS=B/TRANS	SVGW	13
	WCYS=W(I)	SVGW	14
	QYS=SQRT(4.0*BS/PI)	SVGW	15
	XSP=-WCYS*S/(PI2*ALOG(P))	SVGW	16
	RSTAR=SQRT(2.*ALOG(2.*XSP))	SVGW	17
	ET=-RSTAR*QYS*SQRT(PI/2)	SVGW	18
	ARG=2.*XSP*(1.-EXP(ET))	SVGW	19
	RSP=SQRT(2.*ALOG(ARG))	SVGW	20
	RR(I)=RSP	SVGW	21
	GW(I)=(4.*BS/(W(I)*PI))*((SV(NW)*W(I)/RSP)**2-GSUM)	SVGW	22
C	IF(GW(I).LE.0.01)GW(I)=0.01	SVGW	23
	IF(GW(I).LE.5.E-6)GW(I)=5.E-6	(M)	
	IF(I.GT.1)GO TO 140	SVGW	24
	GSUM=0.5*W(1)*GW(1)	SVGW	25
	GO TO 1000	SVGW	26
140	GSUM=GSUM+GW(I)*(W(I)-W(I-1))	SVGW	27
1000	CONTINUE	SVGW	28
	WCP=0.0	SVGW	29
	QP=0.0	SVGW	30
	XLAM0=0.	SVGW	31
	XLAM1=0.	SVGW	32
	XLAM2=0.	SVGW	33
	DO 5 I=2,NKK	SVGW	34
	DUMX=(GW(I)+GW(I-1))/2.	SVGW	35
	DUMY=W(I)-W(I-1)	SVGW	36
	IF(GW(I)-GW(I-1)) 10,15,15	SVGW	37
10	A=GW(I)	SVGW	38
	B=GW(I-1)	SVGW	39
	WBAR=DUMY*(2.*B+A)/(3.*(A+B))	SVGW	40
	WSTAR=W(I)-WBAR	SVGW	41
	GO TO 16	SVGW	42
15	A=GW(I-1)	SVGW	43
	B=GW(I)	SVGW	44
	WBAR=DUMY*(2.*B+A)/(3.*(A+B))	SVGW	45
	WSTAR=W(I-1)+WBAR	SVGW	46
16	AREA=DUMX*DUMY	SVGW	47
	XLAM0=XLAM0+AREA	SVGW	48
	XLAM1=XLAM1+WSTAR*AREA	SVGW	49
5	XLAM2=XLAM2+(WSTAR**2)*AREA	SVGW	50
	WCP=SQRT(XLAM2/XLAM0)	SVGW	51
	RATIO=(XLAM1**2)/(XLAM0*XLAM2)	SVGW	52
	QP=SQRT(1.-RATIO)	SVGW	53
	RETURN	SVGW	54
	END	SVGW	55
-----			
C	SUBROUTINE GWPLOT(NKK, TS, TL, GMIN, GMAX, TQ, GW, TITX, TITLO, YTITL)	GWPL	1
-----			
	DIMENSION TQ(1),GW(1),TITX(1),TITLO(1),YTITL(1)	GWPL	2
	IF (GMAX.LE.70.0) GO TO 3	GWPL	3
	IF (GMAX.LE.200.0) GO TO 2	GWPL	4
	DY=20.0	GWPL	5
	GO TO 4	GWPL	6
2	DY=10.0	GWPL	7
	GO TO 4	GWPL	8
3	DY=2.0	GWPL	9
4	CONTINUE	GWPL	10
C	ESTABLISH SEMILOG COORDINATES	GWPL	11
	CALL SMXYV(1,0)	GWPL	12
C	ESTABLISH MARGINS	GWPL	13
	CALL SETMIV(150,100,150,150)	GWPL	14
C	ESTABLISH GRID	GWPL	15
	CALL GRIDIV(1,TS,TL,GMIN,GMAX,1.0,DY,0,5,0,5,-2,-2)	GWPL	16
C	WRITE Y AXIS LABEL	GWPL	17
	CALL RITE2V(125,250,1000,90,2,28,1,YTITL,NLAST)	GWPL	18
C	WRITE X AXIS LABEL	GWPL	19
	CALL RITE2V(300,125,1000,0,2,36,1,TITX,NLAST)	GWPL	20

C	WRITE TITLE	GWPL	21
	CALL RITE2V(250,925,1000,0,2,28,1,TITLO,NLAST)	GWPL	22
C	JOIN POINTS WITH STRAIGHT LINES	GWPL	23
	NKKM1=NKK-1	GWPL	24
	DO 1 I=1,NKKM1	GWPL	25
	X1=TQ(I)	GWPL	26
	X2=TQ(I+1)	GWPL	27
	II=NKK+1-I	GWPL	28
	Y1=GW(II)	GWPL	29
	Y2=GW(NKK-I)	GWPL	30
C	IX1=NXV(X1)	GWPL	31
C	IY1=NYV(Y1)	GWPL	32
C	IX2=NXV(X2)	GWPL	33
C	IY2=NYV(Y2)	GWPL	34
C	CALL LINEV(IX1,IY1,IX2,IY2)	GWPL	35
1	CONTINUE	GWPL	36
	RETURN	GWPL	37
	END.	GWPL	38
-----			
C	SUBROUTINE DUMMY(W,FOUT,NKK,WB,GWK,MM)	DUMY	1
-----			
	DIMENSION WB(1),GWK(1)	DUMY	2
	JAY=MM	DUMY	3
1	IF(W-WB(JAY)) 5,4,2	DUMY	4
2	JAY=JAY+1	DUMY	5
	IF (JAY.LE.NKK) GO TO 1	DUMY	6
	FOUT=GWK(NKK)	DUMY	7
	GO TO 6	DUMY	8
4	FOUT=GWK(JAY)	DUMY	9
	MM=JAY	DUMY	10
	GO TO 6	DUMY	11
5	MM=JAY-1	DUMY	12
	IF (MM.LE.0) GO TO 4	DUMY	13
	SLOPE=(GWK(JAY)-GWK(JAY-1))/(WB(JAY)-WB(JAY-1))	DUMY	14
	FOUT=GWK(JAY-1)+SLOPE*(W-WB(JAY-1))	DUMY	15
6	CONTINUE	DUMY	16
	RETURN	DUMY	17
	END	DUMY	18
-----			
C	SUBROUTINE DUMMX(W,FOUT,NKK,WB,GWK,MM)	DUMX	1
-----			
	DIMENSION WB(1),GWK(1)	DUMX	2
	JAY=MM	DUMX	3
1	IF(W-WB(JAY)) 5,4,2	DUMX	4
2	JAY=JAY+1	DUMX	5
	IF (JAY.LE.NKK) GO TO 1	DUMX	6
	FOUT=GWK(NKK)	DUMX	7
	GO TO 6	DUMX	8
4	FOUT=GWK(JAY)	DUMX	9
	MM=JAY	DUMX	10
	GO TO 6	DUMX	11
5	MM=JAY-1	DUMX	12
	IF (MM.LE.0) GO TO 4	DUMX	13
	X=(WB(JAY)+WB(JAY-1))/2.	DUMX	14
	IF(W-X) 7,7,8	DUMX	15
7	FOUT=GWK(JAY-1)	DUMX	16
	GO TO 6	DUMX	17
8	FOUT=GWK(JAY)	DUMX	18
6	CONTINUE	DUMX	19
	RETURN	DUMX	20
	END	DUMX	21
-----			
C	SUBROUTINE SPECT (VMAX,TA,GA,N,DEL,PD,IP,DMP,ID)	SPEC	1
-----			
C		SPEC	2
C	SUBROUTINE FOR COMPUTATION OF SPECTRA FROM EARTHQUAKE RECORD	SPEC	3

C	DIGITIZED AT EQUAL TIME INTERVALS	SPEC 4
C		SPEC 5
	DIMENSION VMAX(10,300),TA(10,300),GA(6001),PD(300),DMP(10),	SPEC 6
1	A(2,2),B(2,2),TY(3),X(3),G(2)	SPEC 7
	DO 6 J=1, ID	SPEC 8
	D=DMP(J)	SPEC 9
	DO 6 K=1, IP	SPEC 10
	P=PD(K)	SPEC 11
	IF (P.LT.0.001) P=0.001	SPEC 12
	W=6.2831854/P	SPEC 13
C		SPEC 14
C	CHOICE OF INTERVAL OF INTEGRATION	SPEC 15
C		SPEC 16
	DELP=P/10.	SPEC 17
	L=DEL/DELP+1.-1.E-5	SPEC 18
	DELT=DEL/L	SPEC 19
C		SPEC 20
C	COMPUTATION OF MATRICES A AND B	SPEC 21
C		SPEC 22
	CALL PCN04(D,W,DELT,A,B)	SPEC 23
C		SPEC 24
C	INITIATION	SPEC 25
C		SPEC 26
	X(1)=0.	SPEC 27
	X(2)=0.	SPEC 28
	DMAX=0.	SPEC 29
	I=1	SPEC 30
	DW=2.*W*D	SPEC 31
	W2=W**2	SPEC 32
	IA=2.*P/DELT+1.E-05	SPEC 33
C		SPEC 34
C	COMPUTATION OF RESPONSE	SPEC 35
C		SPEC 36
	L1=0	SPEC 37
1	SL=(GA(I+1)-GA(I))/ L	SPEC 38
	DO 5 M=1,L	SPEC 39
	G(1)= GA(I)+SL*(M-1)	SPEC 40
	G(2)= GA(I)+SL*M	SPEC 41
	TY(1)=A(1,1)*X(1)+A(1,2)*X(2)-B(1,1)*G(1)-B(1,2)*G(2)	SPEC 42
	TY(2)=A(2,1)*X(1)+A(2,2)*X(2)-B(2,1)*G(1)-B(2,2)*G(2)	SPEC 43
	L1=L1+1	SPEC 44
	TIME=(L1-1)*DELT	SPEC 45
C		SPEC 46
C	MONITORING THE MAX. VALUES	SPEC 47
C		SPEC 48
	IF (ABS(TY(1)).LE.ABS(DMAX)) GO TO 2	SPEC 49
	DMAX=TY(1)	SPEC 50
	TD=TIME	SPEC 51
2	X(1)=TY(1)	SPEC 52
5	X(2)=TY(2)	SPEC 53
C		SPEC 54
C	TEST FOR END OF INTEGRATION	SPEC 55
C		SPEC 56
	I=I+1	SPEC 57
	IF (I.EQ.N) GO TO 7	SPEC 58
	GO TO 8	SPEC 59
7	VEND=X(2)	SPEC 60
8	IF (I.EQ.(N+IA)) GO TO 10	SPEC 61
	IF (I.GE.N) GO TO 9	SPEC 62
	GO TO 1	SPEC 63
9	GA(I+1)=0.	SPEC 64
	GO TO 1	SPEC 65
10	CONTINUE	SPEC 66
	VMAX(J,K)=W*DMAX	SPEC 67
	TA(J,K)=TD	SPEC 68
6	CONTINUE	SPEC 69



RETURN	SPEC	70
END	SPEC	71
-----		
SUBROUTINE PCN04 (D,W,DELT,A,B)	PCNO	1
-----		
C	PCNO	2
C SUBROUTINE FOR COMPUTATION OF MATRICES A AND B	PCNO	3
C	PCNO	4
DIMENSION A(2,2),B(2,2)	PCNO	5
DW=D*W	PCNO	6
D2=D**2	PCNO	7
A0=EXP(-DW*DELT)	PCNO	8
A1=W*SQRT(1.-D2)	PCNO	9
AD1=A1*DELT	PCNO	10
A2=SIN(AD1)	PCNO	11
A3=COS(AD1)	PCNO	12
W2=W**2	PCNO	13
A4=(2.*D2-1.)/W2	PCNO	14
A5=D/W	PCNO	15
A6=2.*A5/W2	PCNO	16
A7=1./W2	PCNO	17
A8=(A1*A3-DW*A2)*A0	PCNO	18
A9=- (A1*A2+DW*A3)*A0	PCNO	19
A10=A8/A1	PCNO	20
A11=A0/A1	PCNO	21
A12=A11*A2	PCNO	22
A13=A0*A3	PCNO	23
A14=A10*A4	PCNO	24
A15=A12*A4	PCNO	25
A16=A6*A13	PCNO	26
A17=A9*A6	PCNO	27
A(1,1)=A0*(DW*A2/A1+A3)	PCNO	28
A(1,2)=A12	PCNO	29
A(2,1)=A10*DW+A9	PCNO	30
A(2,2)=A10	PCNO	31
B(1,1)=(-A15-A16+A6)/DELT-A12*A5-A7*A13	PCNO	32
B(1,2)=(A15+A16-A6)/DELT+A7	PCNO	33
B(2,1)=(-A14-A17-A7)/DELT-A10*A5-A9*A7	PCNO	34
B(2,2)=(A14+A17+A7)/DELT	PCNO	35
RETURN	PCNO	36
END	PCNO	37
-----		
SUBROUTINE DIB2 (NFC,IND,NGRAPH,NGD,NPOINT,XL,XR,YB,YT,DX,DY, \$N,M,I,J,NX,NY,X,Y,Z,TIT,TITX,TITY,NT,NTX,NTY,NPT,PTMRK,XAMOR)	DIB2	1
	DIB2	2
-----		
DIMENSION X(1),Y(1),Z(1),TIT(1),TITX(1),TITY(1),PTMRK(1)	DIB2	3
INDA=0	DIB2	4
GO TO (1,2,3,4),IND	DIB2	5
1 CALL SMXYV(0,0)	DIB2	6
GO TO 5	DIB2	7
2 CALL SMXYV(0,1)	DIB2	8
GO TO 5	DIB2	9
3 CALL SMXYV(1,0)	DIB2	10
GO TO 5	DIB2	11
4 CALL SMXYV(1,1)	DIB2	12
5 CONTINUE	DIB2	13
CALL SETMIV(150,100,150,150)	DIB2	14
IF(NFC-1) 11,10,20	DIB2	15
10 NFA=2	DIB2	16
GO TO 30	DIB2	17
20 NFA=4	DIB2	18
30 CALL GRID1V(NFA,XL,XR,YB,YT,DX,DY,N,M,I,J,NX,NY)	DIB2	19
CALL RITE2V(125,250,1000,90,2,NTY,1,TITY,NLAST)	DIB2	20
CALL RITE2V(300,125,1000,0,2,NTX,1,TITX,NLAST)	DIB2	21
CALL RITE2V(250,925,1000,0,2,NT,1,TIT,NLAST)	DIB2	22
CALL LABLV (XAMOR,750,880,6,1,1)	DIB2	23

11	CALL INCRV(8,4)	DIB2	24
	NAU=NGRAPH+NGD	DIB2	25
	IF(NAU) 401,401,400	DIB2	26
400	DO 7 II=1,NAU	DIB2	27
	NAUX=NPOINT-1	DIB2	28
	DO 8 K=1,NAUX	DIB2	29
	IAUX=(II-1)*NPOINT+K	DIB2	30
	X1=X(K)	DIB2	31
	Z1=Z(K)	DIB2	32
	X2=X(K+1)	DIB2	33
	Z2=Z(K+1)	DIB2	34
	Y1=Y(IAUX)	DIB2	35
	Y2=Y(IAUX+1)	DIB2	36
	IF(Y1-YT) 100,100,101	DIB2	37
100	IF(Y2-YT) 110,110,103	DIB2	38
103	X2=(X2-X1)*(YT-Y1)/(Y2-Y1)+X1	DIB2	39
	Y2=YT	DIB2	40
	GO TO 110	DIB2	41
101	IF(Y2-YT) 104,104,105	DIB2	42
104	X1=(X2-X1)*(YT-Y1)/(Y2-Y1)+X1	DIB2	43
	Y1=YT	DIB2	44
	GO TO 110	DIB2	45
105	INDA=1	DIB2	46
110	CONTINUE	DIB2	47
	IF(Y1-YB) 200,201,201	DIB2	48
200	IF(Y2-YB) 205,203,203	DIB2	49
205	INDA=1	DIB2	50
	GO TO 210	DIB2	51
203	X1=(X2-X1)*(YB-Y1)/(Y2-Y1)+X1	DIB2	52
	Y1=YB	DIB2	53
	GO TO 210	DIB2	54
201	IF(Y2-YB) 204,210,210	DIB2	55
204	X2=(X2-X1)*(YB-Y1)/(Y2-Y1)+X1	DIB2	56
	Y2=YB	DIB2	57
210	CONTINUE	DIB2	58
	IF(INDA) 303,303,302	DIB2	59
303	IF(II-NGRAPH) 300,300,301	DIB2	60
300	CALL LINEV(NX,NY,NX,NY)	DIB2	61
	CALL LINEV(NX,NY,NX,NY)	DIB2	62
	CALL DOTLNV(NX,NY,NX,NY)	DIB2	63
	GO TO 302	DIB2	64
301	CALL DOTLNV(NX,NY,NX,NY)	DIB2	65
	CALL DOTLNV(NX,NY,NX,NY)	DIB2	66
302	INDA=0	DIB2	67
	8 CONTINUE	DIB2	68
	7 CONTINUE	DIB2	69
401	IF(NPT) 402,402,403	DIB2	70
403	LL=NPOINT*NPT	DIB2	71
	DO 500 I=1,NPOINT	DIB2	72
	CALL APLOTV(LL,X(I),Y(I),0,NPOINT,NPT,PTMRK,IERR)	DIB2	73
500	CALL APLOTV(LL,X(I),Y(I),0,NPOINT,NPT,PTMRK,IERR)	DIB2	74
402	RETURN	DIB2	75
	END	DIB2	76
-----			
	SUBROUTINE PLTND (KIKI)	PLTN	1
-----			
C	DUMMY PLOT SUBROUTINE	PLTN	2
	RETURN	PLTN	3
	END	PLTN	4
	SUBROUTINE SMXYV (I,J)	SMXY	1
C	DUMMY PLOT SUBROUTINE	SMXY	2
	RETURN	SMXY	3
	END	SMXY	4
	SUBROUTINE SETMIV (J,K,L,M)	SETM	1
C	DUMMY PLOT SUBROUTINE	SETM	2
	RETURN	SETM	3

	END	SETM	4
	SUBROUTINE GRID1V (NFA,XL,XR,YB,YT,DX,DY,N,M,I,J,NX,NY)	GRID	1
C	DUMMY PLOT SUBROUTINE	GRID	2
	RETURN	GRID	3
	END	GRID	4
	SUBROUTINE RITE2V (II,JJ,KK,I,J,K,IJ,IK,IL)	RITE	1
C	DUMMY PLOT SUBROUTINE	RITE	2
	RETURN	RITE	3
	END	RITE	4
	SUBROUTINE LABLV (XAMOR,X,Y,Z,I,J)	LABL	1
C	DUMMY PLOT SUBROUTINE	LABL	2
	RETURN	LABL	3
	END	LABL	4
	SUBROUTINE INCRV (I,J)	INCR	1
C	DUMMY PLOT SUBROUTINE	INCR	2
	RETURN	INCR	3
	END	INCR	4
	SUBROUTINE LINEV (N1,N2,N3,N4)	LINE	1
C	DUMMY PLOT SUBROUTINE	LINE	2
	RETURN	LINE	3
	END	LINE	4
	SUBROUTINE DOTLV (N1,N2,N3,N4)	DOTL	1
C	DUMMY PLOT SUBROUTINE	DOTL	2
	RETURN	DOTL	3
	END	DOTL	4
	SUBROUTINE APLOTV (LL,X,Y,I,N,NPT,P,IERR)	APLO	1
C	DUMMY PLOT SUBROUTINE	APLO	2
	RETURN	APLO	3
	END	APLO	4
-----			
C	SUBROUTINE CONVERT(TSV,SAY,NRES,IOP,SV0)		
-----			
C	DIMENSION TSV(1010),SV0(1010),SAY(1010)		
C	THIS SUBROUTINE CONVERT THE INPUT DATA FROM ACCELERATION AND		
C	RESPONSE SPECTRA TO VELOCITY RESPONSE SPECTRA		
-----			
C	TSV = PERIOD INPUT		
C	SAY = THE INPUT ORDINATE OF THE RESPONSE SPECT IT CAN (A OR V OR D)		
C	NRES = NUMBER OF DATA TO BE ENTERED		
C	SV0 = THE CONVERTED VELOCITY SPECTRUM		
C			
C	SPEC = D MEANS DISPLACEMENT SPECTRUM AS INPUT		
C	SPEC = V MEANS VELOCITY SPECTRUM AS INPUT		
C	SPEC = A MEANS ACCELERATION SPECTRUM AS INPUT		
C	IOP = A NUMBER WHICH STAND FOR D V OR A		
C	IOP = 1 DISP SPECT		
C	IOP = 2 VELOCITY SPECT		
C	IOP = 3 ACCELE SPECT		
C			
C	IF(SPEC .EQ. 'D') IOP=1		
C	IF(SPEC .EQ. 'V') IOP=2		
C	IF(SPEC .EQ. 'A') IOP=3		
-----			
	OPEN(UNIT=25,FILE='target.spc',status='unknown')		
	DO 62 I=1,NRES		
	IF(TSV(I) .LE. 0.) TSV(I)=0.01		
	W=2.*3.14159/TSV(I)		
	GO TO (71,72,73) , IOP		
71	SAY(I)=W*SAY(I)		
	GO TO 72		
73	SAY(I)=SAY(I)/W		
72	SV0(I)=SAY(I)		
-----			
	WRITE(25,1000) TSV(i),SV0(i)/W,SV0(i),SV0(i)*W		
1000	FORMAT(1X,F10.4,3F14.4)		

62 CONTINUE

C-----

CLOSE(25)

C

RETURN

END

## APPENDIX C    TABLE FOR STATIC & DYNAMIC FRICTION COEFFICIENTS

Table C1 Coefficients of Friction for Selected Engineering Materials

	Static $\mu_s$	Kinetic $\mu$
Oil-lubricated Contacts (excluding hydrodynamic lubrication):		
Hardened Steel on Same	0.06	0.01–0.03
Soft Steel on Same	0.10	0.01–0.05
Cast Iron on Same	0.05–0.15	0.05–0.015
Cast Iron on Hardened Steel	0.08	0.01–0.05
Steel on Bronze	0.1	0.06
Leather on Metal	0.15	0.15
Ball Bearings	0.0010–0.0024	
Roller Bearings	0.0010–0.0040	
Rollers of Radius $R$	$0.5/R$ ( $R$ in mm)	
Dry Contacts:		
Steel on Steel	0.11–0.33	0.10–0.11
Cast Iron on Cast Iron	0.20–0.25	0.12–0.25
Cast Iron on Hardened Steel	0.18–0.20	0.16–0.20
Steel on Bronze	0.20	0.18
Leather on Metal	0.6	0.48
Rubber on Asphalt (tires)	0.5–0.8	
PTFE (Teflon) on steel	0.05	
Polyester on Steel	0.12	
Polycarbonate on Steel	0.39	



MULTIDISCIPLINARY CENTER FOR EARTHQUAKE ENGINEERING RESEARCH

*A National Center of Excellence in Advanced Technology Applications*

University at Buffalo, State University of New York  
Red Jacket Quadrangle ■ Buffalo, New York 14261-0025  
Phone: 716/645-3391 ■ Fax: 716/645-3399  
E-mail: [mceer@acsu.buffalo.edu](mailto:mceer@acsu.buffalo.edu) ■ WWW Site: <http://mceer.buffalo.edu>



University at Buffalo *The State University of New York*

ISSN 1520-295X